

# Designing a Concussion-Reducing Football Helmet



A Major Qualifying Project Report  
Submitted to the Faculty of  
WORCESTER POLYTECHNIC INSTITUTE  
In partial fulfillment of the requirements for the  
Degree of Bachelor of Science  
In Mechanical Engineering

**Submitted by:**

Kelly Beisswanger

Danielle Haley

Glen Morgan

Vincent Tavernelli

**Project Advisor:**

Professor Brian Savilonis

Project Number: CR15

3/25/2016

## Abstract

The goal of this project was to reduce the likelihood of concussions for football players by designing a helmet that decreased linear acceleration of the head. The design incorporated shock-absorbent protective padding. A testing assembly was created to simulate an impact force while measuring x and z accelerations experienced in the head. Recorded accelerations were used in equations to calculate the Head Injury Criteria (HIC) and Gadd Severity Index (SI) parameters, which are commonly used to measure the probability of a head injury. Results obtained from the helmet with shock-absorbent material were compared to results obtained from the helmet in its original condition. Analysis of the results demonstrated that exterior shock-absorbent protective padding was effective at reducing the likelihood of a concussion by reducing the linear acceleration of the head when comparing parameters such as acceleration, HIC, and GSI.

*Key Words: concussion, traumatic brain injury (TBI), linear acceleration, shock absorbent, HIC, GSI*

## **Acknowledgements**

Kelly, Danielle, Glen, and Vinny would like to acknowledge the individuals who contributed to the success of this project. First, we would like to thank Peter Hefti, Professor John Hall, Professor Cosme Furlong, Jim Monaco, and Dr. Adriana Hera for their expertise, advice, and support. Special thanks goes to WPI Facilities Manager Shawn McAvey, as well as Rogers Corporation and Sorbothane for the donated materials. We would also like to acknowledge the support of other MQP teams with who we shared equipment and materials; thank you to the Bone MQP group as well as the Sea Turtle MQP group.

Finally, we would like to thank our advisor, Professor Brian Savilonis, for his support and guidance. This project would not have been possible without your insight, enthusiasm, and interest in sports as well as engineering.

## Table of Contents

Abstract .....	i
Acknowledgements .....	ii
Table of Contents .....	iii
List of Figures .....	vii
List of Tables .....	viii
1.0 Introduction .....	1
2.0 Background .....	3
2.1 Traumatic Brain Injuries .....	3
2.1.1 Causes and Examples of TBI's .....	3
2.1.2 Concussions .....	4
2.1.3 Grading a Concussion and Effects .....	4
2.1.4 Incidence .....	5
2.2 Athletics and Concussions .....	5
2.2.1 Football and Concussions .....	6
2.2.2 NFL Attention to Concussions.....	7
2.3 NFL Rule Changes.....	8
2.3.1 Kickoff .....	8
2.3.2 Defenseless Player .....	9
2.4 Concussion Regulations and Programs .....	9
2.4.1 NFL Concussion Protocol.....	10
2.4.2 NFL Research into Concussions .....	10
2.4.3 Concussion Reductions in the NFL .....	11
2.5 Evolution of the Football Helmet.....	11
2.5.1 First Helmets .....	11
2.5.2 Standards.....	12
2.5.3 Current Helmets .....	12
2.6 Technology and Analysis for Testing Head Impacts .....	15
2.6.1 Testing Methods.....	15
2.6.2 Linear and Rotational Acceleration .....	17
2.6.3 Common Concussion Inducing Hits .....	17
2.6.4 Algorithms and Testing Methods.....	19
2.6.5 Assessing the Injury: HIC, GSI.....	20
2.7 Materials .....	21
2.7.1 Sorbothane® .....	21

2.7.2 PORON Medical® Urethane-Firm-Energy Absorbing ..... 22

2.7.3 Neoprene Commercial Grade..... 22

3.0 Methodology ..... 23

3.1 Design Specifications..... 24

3.2 Preliminary Design ..... 24

3.3 Design Materials ..... 25

3.4 Preliminary Force Plate Tests ..... 26

3.5 Final Design..... 28

3.6 Test Rig..... 32

3.6.1 Accelerometer ..... 32

3.6.2 Neck, Head, and Helmet ..... 32

3.6.3 Air Cylinder ..... 34

3.7 Force Impact Test ..... 35

3.8 Acceleration Tests..... 36

3.9 Calculating HIC and GSI..... 37

3.10 System Model ..... 41

3.10.1 Calculating K and D for Pads ..... 44

3.10.2 Determining Velocity and Displacement ..... 46

4.0 Results and Analysis ..... 48

4.1 Preliminary Force Plate Tests ..... 48

4.2 Force Sensor..... 48

4.3 Acceleration Tests..... 49

4.3.1 Accelerations..... 51

4.3.2 HIC and GSI ..... 52

4.3.3 Model Analysis ..... 53

5.0 Conclusion and Future Recommendations ..... 55

6.0 References..... 58

7.0 Appendices..... 62

Appendix A- Hanging String Method for Determining the Head’s Center of Mass ..... 62

Appendix B – Determining the Bending Stiffness of the Neck ..... 62

Appendix C Pendulum Calculations ..... 64

Length of Pendulum..... 64

Load supported by pendulum..... 64

Appendix D..... 65

Air Cylinder Calculations ..... 65

Appendix E Force Sensor Calibration and LabVIEW ..... 67

    Force Sensor Calibration..... 67

    LabVIEW for Force Sensor ..... 68

Appendix F LabVIEW for Acceleration Testing ..... 70

Appendix G- System Model ..... 70

Appendix H – Preliminary Force Plate Test Results ..... 72

Appendix I – Impacts to Front of Helmet ..... 76

    Control ..... 76

    Interior Front and Top Padding: 9 lbs/ft<sup>3</sup>..... 77

    Interior Front and Top Padding: 12 lbs/ft<sup>3</sup>..... 78

    Interior Front and Top Padding: 15 lbs/ft<sup>3</sup>..... 79

    Interior Front and Top Padding: 20 lbs/ft<sup>3</sup>..... 80

    Interior Back Padding: 9 lbs/ft<sup>3</sup> ..... 81

    Interior Back Padding: 12 lbs/ft<sup>3</sup> ..... 82

    Interior Back Padding: 15 lbs/ft<sup>3</sup> ..... 83

    Interior Back Padding: 20 lbs/ft<sup>3</sup> ..... 84

    Exterior Padding: 9 lbs/ft<sup>3</sup> ..... 85

    Exterior Padding: 12 lbs/ft<sup>3</sup> ..... 86

    Exterior Padding: 15 lbs/ft<sup>3</sup> ..... 87

    Exterior Padding: 20 lbs/ft<sup>3</sup> ..... 88

Appendix J – Impacts to Facemask..... 89

    Control ..... 89

    Interior Front and Top Padding: 9 lbs/ft<sup>3</sup>..... 90

    Interior Front and Top Padding: 12 lbs/ft<sup>3</sup>..... 91

    Interior Front and Top Padding: 15 lbs/ft<sup>3</sup>..... 92

    Interior Front and Top Padding: 20 lbs/ft<sup>3</sup>..... 93

    Interior Back Padding: 9 lbs/ft<sup>3</sup> ..... 94

    Interior Back Padding: 12 lbs/ft<sup>3</sup> ..... 95

    Interior Back Padding: 15 lbs/ft<sup>3</sup> ..... 96

    Interior Back Padding: 20 lbs/ft<sup>3</sup> ..... 97

    Exterior Padding: 9 lbs/ft<sup>3</sup> ..... 98

    Exterior Padding: 12 lbs/ft<sup>3</sup> ..... 99

    Exterior Padding: 15 lbs/ft<sup>3</sup> ..... 100

    Exterior Padding: 20 lbs/ft<sup>3</sup> ..... 101

    Exterior Padding: 9 and 12 lbs/ft<sup>3</sup> ..... 102

Appendix K – Impacts to Side of Helmet ..... 103

    Control ..... 103

    Interior Padding: 9 lbs/ft<sup>3</sup> ..... 104

    Interior Padding: 12 lbs/ft<sup>3</sup> ..... 105

    Interior Padding: 15 lbs/ft<sup>3</sup> ..... 106

    Interior Padding: 20 lbs/ft<sup>3</sup> ..... 107

    Exterior Padding: 9 lbs/ft<sup>3</sup> ..... 108

    Exterior Padding: 12 lbs/ft<sup>3</sup> ..... 109

    Exterior Padding: 15 lbs/ft<sup>3</sup> ..... 110

    Exterior Padding: 20 lbs/ft<sup>3</sup> ..... 111

Appendix L- MATLAB Code Example: ..... 112

## List of Figures

FIGURE 1 TOP FIVE SPORTS WITH THE HIGHEST RATE OF CONCUSSIONS.....	6
FIGURE 2 NFL KICKOFF DATA.....	9
FIGURE 3 ONE EXAMPLE OF EARLY FOOTBALL DESIGNS.....	12
FIGURE 4 RIDDELL HELMET.....	13
FIGURE 5 SCHUTT VENGEANCE VTDII HELMET.....	14
FIGURE 6 XENITH X2E HELMET.....	14
FIGURE 7 RAWLINGS HELMET.....	15
FIGURE 8 HORIZONTAL PNEUMATIC IMPACTOR.....	16
FIGURE 9 HORIZONTAL IMPACT TESTS.....	16
FIGURE 10 DISTRIBUTION OF IMPACT LOCATIONS.....	18
FIGURE 11 HIGH-G IMEMS ACCELEROMETERS.....	19
FIGURE 12 COMPARISON BETWEEN 6DOF AND PREVIOUS HITS DATA.....	20
FIGURE 13 SORBOTHANE® MATERIAL.....	22
FIGURE 14 PORON® SAMPLES.....	22
FIGURE 15 NEOPRENE SAMPLES.....	23
FIGURE 16 SHOCK ABSORBING MATERIAL WITHIN THE HELMET.....	25
FIGURE 17 SHOCK ABSORBING MATERIAL ON THE OUTSIDE OF THE HELMET.....	25
FIGURE 18 SHORE SCALE COMPARISON CHART.....	26
FIGURE 19 PRELIMINARY FORCE PLATE TESTS WITH MATERIALS.....	27
FIGURE 20: PORON® PADDING.....	28
FIGURE 21: CONTROL CONFIGURATION.....	29
FIGURE 22: FRONT AND TOP CONFIGURATION.....	29
FIGURE 23: BACK AND SIDES CONFIGURATION.....	30
FIGURE 24: EXTERIOR FOREHEAD CONFIGURATION.....	30
FIGURE 25: EXTERIOR FACEMASK CONFIGURATION.....	31
FIGURE 26: EXTERIOR SIDE CONFIGURATION.....	31
FIGURE 27 HEAD WITH PLASTER AND ACCELEROMETER.....	32
FIGURE 28: MODEL NECK AND STEEL BASE.....	33
FIGURE 29: CROSS-SECTION OF SCHUTT DNA FOOTBALL HELMET [41].....	33
FIGURE 30 METAL FRAME CONSTRUCTED FOR AIR CYLINDER.....	35
FIGURE 31 FORCE SENSOR HYSTERESIS CHECK.....	36
FIGURE 32 FRONT IMPACT ACCELERATION GRAPHS.....	38
FIGURE 33 FRONT IMPACT CONTROL HIT.....	38
FIGURE 34 X-AXIS ACCELERATION.....	39
FIGURE 35 Z-AXIS ACCELERATION.....	39
FIGURE 36 X AXIS ACCELERATION PEAK INTERVAL WITH TRENDLINE.....	40
FIGURE 37 Z-AXIS ACCELERATION INTERVAL WITH TRENDLINE.....	40
FIGURE 38: HORIZONTAL SYSTEM DIAGRAM.....	41
FIGURE 39: MODEL HEAD FREE BODY DIAGRAM.....	42
FIGURE 40: CAUSAL BOND GRAPH WITH ASSIGNED STATE VARIABLES.....	43
FIGURE 41 IMAGES FROM HIGH-SPEED DATA ANALYSIS.....	47
FIGURE 42: FORCE SENSOR IMPACT READINGS GRAPH.....	49
FIGURE 43 METHOD TO FIND THE CENTER OF MASS.....	62
FIGURE 44 DETERMINING BASELINE POSITION FOR NECK.....	63



FIGURE 45 POSITION AFTER WEIGHT APPLIED TO NECK. ....63

FIGURE 46 FORCE SENSOR CALIBRATION GRAPH. ....68

FIGURE 47 FORCE SENSOR LABVIEW PROGRAM BLOCK DIAGRAM. ....69

FIGURE 48 LABVIEW ACCELEROMETER PROGRAM BLOCK DIAGRAM. ....70

FIGURE 49 SORBOTHANE© SAMPLE 2 1569 N AVERAGE (17% IMPROVEMENT).....72

FIGURE 50 SAMPLE 1 SORBOTHANE© 1637 N AVERAGE (13% IMPROVEMENT).....73

FIGURE 51 PORON© SAMPLE A 1508 N AVERAGE (20%). ....73

FIGURE 52 PORON© SAMPLE B 1350 N AVERAGE (29% IMPROVEMENT). ....74

FIGURE 53 PORON© SAMPLE C 1402 N AVERAGE (26% IMPROVEMENT). ....74

FIGURE 54 PORON© SAMPLE D 1594 N AVERAGE (16% IMPROVEMENT). ....75

FIGURE 55 NEOPRENE 1664 N AVERAGE (12% IMPROVEMENT). ....75

**List of Tables**

TABLE 1 FREQUENCY OF IMPACTS ABOVE SPECIFIED RESULTANT ACCELERATION THRESHOLDS.  
.....18

TABLE 2: TESTING CONFIGURATIONS.....29

TABLE 3: STIFFNESS DATA FOR 9LB/FT3 DENSITY PAD.....45

TABLE 4: STIFFNESS AND DAMPING COEFFICIENTS .....46

TABLE 5: PRELIMINARY FORCE PLATE TEST RESULTS .....48

TABLE 6: ACCELERATION TEST DATA .....50

TABLE 7: MEASURED VS CALCULATED ACCELERATIONS .....53

TABLE 8 VARIABLES USED IN DETERMINING IMPACT FORCE AND AIR CYLINDER REQUIREMENTS  
.....65

TABLE 9 VARIABLES USED IN DETERMINING NECK MOTION AND ROTATION .....67

## 1.0 Introduction

In 2012, an estimated 3.8 million concussions were reported [1]. This number is more staggering when the number of unreported concussions are considered. An estimated 26 out of 27 concussions go unreported by college football players, according to a Harvard University and Boston University study [2].

A concussion is a traumatic brain injury (TBI) which is defined as a blow or jolt to the head, or a penetrating head injury, which disrupts the normal functioning of the brain [3]. TBIs are often caused when the head suddenly hits or receives a hit by another object and when the body rapidly accelerates [1]. High impact forces move the brain within the skull, potentially causing brain injury. The rapid acceleration of the body itself will create a whiplash effect of the head and neck, causing effects similar to a direct hit to the skull and a hit that shakes the brain within the skull [4].

TBI's are classified into three main categories: mild, moderate, and severe. During a mild TBI, there is only a brief change in the player's mental state or consciousness. During a severe TBI, there are extended periods of unconsciousness that can lead to coma or death. The most common forms of reported concussions while playing sports are moderate TBIs; however, severe TBIs also occur [3].

A concussion is a common TBI that is defined as a complex pathophysiological process that affects the brain and is commonly induced by a pathological injury. Concussions can occur from any blow to the body that causes an impulsive force to be transmitted to the head. A concussion is categorized as a mild TBI [3].

Football is one of the leading sources of head and neck injuries in sports. This particular sport accounts for roughly 48,000 of the 450,000 total injuries (~ 10.67%) [3]. In 2015, the NFL

received court approval to pay \$765 million to settle concussion-related lawsuits after more than 4,500 ex-players sued the league in 2013, claiming that the NFL failed to protect them adequately against concussions and head injuries [5]. Football players of all ages are in desperate need for adequate preventive equipment to reduce head injuries and to prevent the onset of severe neurological conditions linked to head trauma, such as ALS and Alzheimer's Disease.

Current helmets aim to prevent skull fractures, but neglect emphasis on concussion reduction. Since acceleration experienced by the head is a chief cause of concussions in football, a helmet design that focuses on reducing linear acceleration is the focus of this Major Qualifying Project.

## 2.0 Background

### 2.1 Traumatic Brain Injuries

In most sport contests, there are high levels of physical contact between players and their surroundings. In fact, sports are responsible for more than 20% of all brain injuries in children and adolescents. These injuries are commonly called traumatic brain injuries (TBI) [1]. A TBI is a blow or jolt to the head, or a penetrating head injury, which disrupts the normal functioning of the brain. A TBI is also defined by the American Association of Neurological Surgeons as a sports related head injury [3].

#### 2.1.1 Causes and Examples of TBI's

A TBI is commonly caused by the head's sudden contact with another object. The high impact forces experienced make the brain move within the skull, potentially causing brain injury. Another cause of TBI is the rapid acceleration of the body itself. This will create a whiplash effect on the head and neck, which causes the brain to move around within the skull. This whiplash has similar effects on the brain as a direct hit to the head. A rare TBI is one caused by an object piercing the skull and brain tissue [3].

There are three main categories of TBI's. The first is mild, which results in a brief change in the players' mental state or consciousness. These symptoms may pass quickly and not greatly affect the player. The second is severe, which results in extended periods of unconsciousness that can lead to coma or death. A severe TBI is an extremely dangerous situation and occurs occasionally in sports. The most common form of concussions sustained during sports is categorized as moderate. The severity of moderate TBIs falls between the mild and severe categories [3].

### 2.1.2 Concussions

Concussions are a mild-moderate form of TBI. A concussion is defined as a complex pathophysiological process that affects the brain. These are commonly induced by pathological injury. Concussions usually occur in low velocity situations. The subsequent shaking of the brain within the skull will cause clinical symptoms that are not necessarily related to a pathological injury. Some symptoms experienced may include confusion, headache, dizziness, nausea, visual disturbances, vertigo, or memory loss [3].

Concussions can be caused by a direct blow to the head, face, neck, or anywhere else on the body that causes an impulsive force to be transmitted to the head. Usually the effects of a concussion occur quickly and neurologic function is impaired immediately. In some cases, however, the effects are not evident for a few minutes or hours after the injury occurs. A concussion can cause neuropathic changes but does not largely affect the structures within the brain [3]. This causes the observation of the effects on a neuroimaging study to be nearly impossible.

### 2.1.3 Grading a Concussion and Effects

Determining the severity of a concussion is an important factor regarding the well-being of the person hit. The process of treating the concussion depends on its severity. The first factor that doctors and trainers consider is the person's state of consciousness. The second factor to observe is the duration of time for which the person lost consciousness. The greater this duration is, the more severe the concussion.

In sports, a player who has suffered a concussion but returns to play too early due to misdiagnosis may experience devastating repercussions. The most frequent consequence is Second Impact Syndrome (SIS). SIS is a potentially fatal brain swelling that occurs when a

person sustains a second concussion before fully recovering from a previous concussion. SIS causes vascular congestion and increased intracranial pressure that is nearly impossible to control [6].

#### **2.1.4 Incidence**

In order to study concussions, it is important to record all related head injuries that occur in sports. The US Consumer Product Safety commission tracks a large number of sports-related injuries through National Electronic Injury Surveillance System (NEISS). In 2009, estimates show more than 400,000 high school sports related head injuries were treated at hospital emergency rooms [7]. This estimate accounts only for documented head injuries and does not include concussions that were not reported by athletes. In football, there were close to 50,000 concussions in 2009 [3].

Concussions are mainly caused by plays that involve tackling. In the past 40 years, tackling was responsible for 67% of all TBIs [3]. More specifically, the majority of concussions in football are associated with the defensive position players who frequently participate in tackling.

## **2.2 Athletics and Concussions**

The first major change regarding concussion awareness in sports occurred at the high school level. In 2010, the National Federation of State High School (NFSHS) Football ruled that “Any player who shows signs, symptoms, or behaviors associated with a concussion must be removed from the game and shall not return to play until cleared by an appropriate health-care professional”[3]. This rule was implemented into all high school sports.

The National Collegiate Athletics Association (NCAA) was responsible for further meaningful concussion prevention policies in sports. In 2013, a rule was established which made

it illegal for a player to lead with a down-facing helmet when hitting another player [3]. Also, the NCAA implemented a similar policy to the NFSHF Football's rule concerning clearance to return to play.

### 2.2.1 Football and Concussions

In any given football game, over 100 "big hits" can occur. A "big hit" is commonly defined by sports doctors as a contact that causes the helmet of a player to experience forces upward of 100 g's for a short period of time (concussions may occur at this number) [8].

Despite the tendency to cause injury, these "big hits" are viewed as integral to football. Football currently has the highest rate of concussions in games [9]. Recently, a study to determine the amount of concussions in various sports (Figure 1) demonstrated that football has more concussions than any other sport.

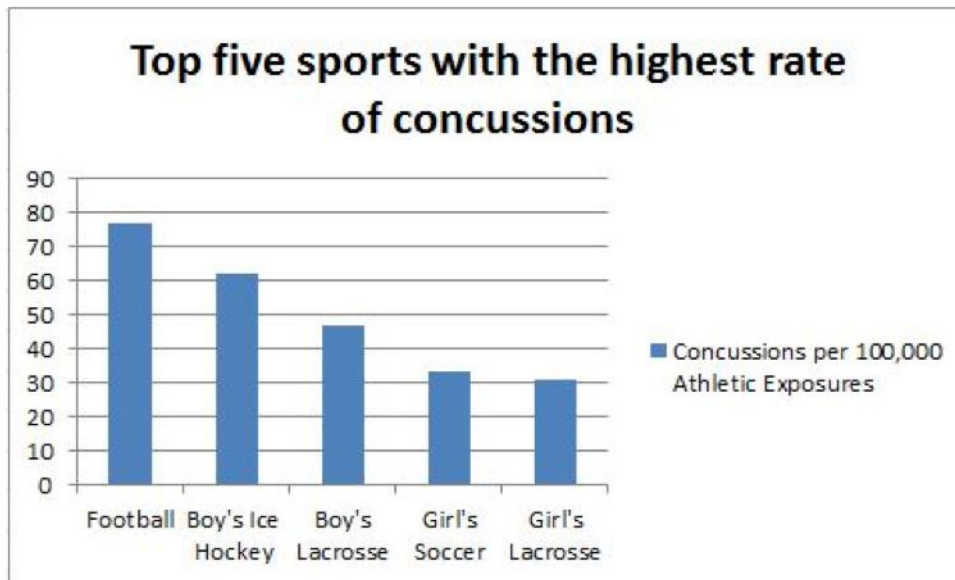


*Figure 1 Top Five Sports with the Highest Rate of Concussions.*

Most children begin to participate in the game of football between the ages of 5 and 7. At this age, children are weaker and smaller in size and weight. Children's decreased strength and mass lessen their ability to cause a "big hit," which is one reason beginners have the lowest rate

of concussions in football (1 in 30 players per year). As a player moves into the high school level (ages 15 to 18) the concussion rate is greater than double the rate of concussions for beginners at 1 in 14 per year. In high school football, players are still learning and improving skills and proper techniques but now they are larger and capable of administering concussion-inducing hits [11].

Similar to the contrast between elementary and high school level players, athletes at the collegiate level also differ. Despite the higher collision force, college players are more knowledgeable and experienced in enduring "big hits." The brains of players below the age of 21 are still developing. During brain development, the brain is more vulnerable to injury and takes longer to recover from injury. College players possess brains that are developmentally more mature, especially in the frontal lobe region [42]. This region affects judgment and voluntary movement, which are both imperative in one's ability to avoid concussion-inducing hits. The concussion rate in college football is lower than in high school football (1 in 20 per year) [11].

### **2.2.2 NFL Attention to Concussions**

In the past 15 years, studies showing troubling results associating concussions and long-term health issues have stimulated attention from many sports associations, especially the National Football League (NFL). Dr. Gerard Gioria has spent the past twenty years researching concussions in youth sports. Over the recent years, he has noticed major advancements in concussion prevention. He cites the NFL's focus on these injuries as being one of the main reasons, stating:

What is amazing about this is how, over the last year, with the attention that's been brought to the issue by the NFL, the whole field has just vaulted forward. In 2003, I had to convince families that this injury was something they needed to be concerned about.



Now I have families coming to me, asking mostly the right questions and prepared to deal with the issue in ways so much ahead of where we were [12].

As previously discussed, concussions are a serious problem in non-professional football; however, concussions remain a dilemma at the professional level as well. Due to the size and strength of professional football players, injuries and concussions in the NFL are commonplace. The NFL has reported that an average of 1 to 2 concussions occur per game. This does not take into account the minor concussions frequently unreported [12]. The NFL has taken some preventative measures on this “concussion epidemic.”

## **2.3 NFL Rule Changes**

### **2.3.1 Kickoff**

The play in a football game that experiences the highest rate of concussions is the kickoff. In order to lower the risk of injury during this play, the NFL moved the starting point of the play 5 yards forward in 2011. This change had two beneficial results. First, players have less time to reach full speed, resulting in less powerful hits. Second, many more kickoffs now result in touchbacks, meaning that the play is in fact immediately called dead, thus removing the possibility for a concussion altogether. In the first year this change was implemented (2011) there were fifteen less kickoff concussions than in the previous season (Figure 2) [13].

<b>NFL Kickoff Data: Touchbacks (TB) &amp; Concussions (MTBIs)</b>							
<b>Year</b>	<b>Kickoffs</b>	<b>Returns</b>	<b>Pct.</b>	<b>TB</b>	<b>Pct.</b>	<b>MTBIs</b>	<b>Pct.</b>
<b>2004</b>	2,453	2,155	87.9%	208	8.5%	30	1.39%
<b>2005</b>	2,439	2,137	87.6%	218	8.9%	36	1.68%
<b>2006</b>	2,427	2,037	83.9%	316	13.0%	27	1.33%
<b>2007</b>	2,515	2,074	82.5%	311	12.4%	34	1.64%
<b>2008</b>	2,576	2,114	82.1%	371	14.4%	34	1.61%
<b>2009</b>	2,484	2,004	80.7%	401	16.1%	30	1.50%
<b>2010</b>	2,539	2,033	80.1%	416	16.4%	35	1.72%
<b>2011</b>	2,572	1,375	53.5%	1,120	43.5%	20	1.45%
<b>2012</b>	2,620	1,395	53.2%	1,156	44.1%	26	1.86%

*Figure 2 NFL Kickoff Data.*

### 2.3.2 Defenseless Player

In 2010, a rule regarding defenseless players was established in an effort to reduce concussions. The rule made it illegal to initiate any unnecessary contact against a player in a defenseless posture. There are now numerous rules in the NFL focused on reducing big, unnecessary hits in football [14].

## 2.4 Concussion Regulations and Programs

In 2014, the NFL agreed to pay over 5000 NFL players a lawsuit settlement concerning the concussions they had experienced while playing for the league; the settlement totaled \$765 million. The players sued because they claimed they were not adequately informed of the dangers of their concussions. Since this lawsuit, the NFL has come up with a more intensive protocol for dealing with concussions. All players who have a concussion, and players suspected of having a concussion, must go through a very strict protocol system. The NFL reports that the system works well in the evaluation of concussions, although it is not foolproof [15].

### 2.4.1 NFL Concussion Protocol

The first step of this protocol takes place before training camps begin. The trainers have the players perform tests to assess critical functioning skills affected by concussions. This establishes a baseline to compare to throughout the season [16].

The next part of the protocol occurs on the field. An athletic trainer sits in the stadium box to review all hits on players throughout the game. If he observes a hit that he believes may have caused a concussion, he directs the trainers on the field to check on the players involved. The trainers give the player the same test administered to him at the beginning of the season, using his previous results as the baseline for normal behavior. This test, which takes about 10 minutes, indicates whether the player needs further attention [16].

The final protocol step occurs during the days after a game in which a player is suspected to have sustained a concussion. Trainers and doctors monitor the player and as his symptoms start to improve he is be allowed to take part in more activities. Once all symptoms have subsided and the player has passed his baseline tests, he is able to return to play [16].

### 2.4.2 NFL Research into Concussions

Due to the increased awareness of concussions, the NFL has offered contracts for concussion research and development. In 2013, General Electric began a \$60 million project with the NFL focusing on improving concussion-detecting imaging technology over a four-year period. As part of this investment, \$20 million will be spent on an open innovation program called the "Head Health Challenge" to generate ideas for new and improved safety equipment. This is a project open to the public to participate in [17].

The "Head Health Challenge" is divided into two main categories. The first component focuses on increased understanding of the relationships between physiological biomarkers and

mechanical causes of brain injuries, as well as improved knowledge of advanced brain imaging. These advancements could potentially improve the prevention of brain injury and diagnosis. The second part of the challenge is to develop new ways to reduce impact forces to the head, potentially through new materials and protective devices. GE and the NFL will pursue the best developments and research to further develop and potentially introduce to the football helmet market [17].

### **2.4.3 Concussion Reductions in the NFL**

Research indicates that concussion rates have decreased. In regular season games, concussions have reduced by 35%. Hits against defenseless players have decreased by 68%. In addition, head to head hit concussions have decreased by 43% [18].

The NFL offers many types of screening events for former NFL players. Tests conducted on former players are incorporated into future research. The NFL fully covers costs for a program for Neurological Care offered in five areas in the U.S. to assist players with any mental issues [18].

## **2.5 Evolution of the Football Helmet**

### **2.5.1 First Helmets**

The first documented football helmet was used in 1893. It was a basic leather cap that was used until the 1950s when more advanced materials, such as polymers, were developed. Helmets were made mandatory for NCAA football games in 1939 and in the NFL in 1940. These helmets were designed to protect a player's head from skull fractures, but were not designed to prevent concussions [19].



*Figure 3 One example of early football designs.*

### **2.5.2 Standards**

A steady increase in the number of head injuries over many years caused the NFL and NCAA to begin collecting injury data in 1967. Soon after, the National Operating Committee on Standards for Athletic Equipment (NOSCAE) was founded in 1969.

This committee initiated research efforts for head protection and implemented the first safety standards for football helmets in 1973. Due to these research efforts, many changes occurred in the early 1970s, such as the design of the outer shell currently seen in the modern football helmet. NOSCAE stated that the outer shell of the helmet should be constructed to cover the fragile areas of the cranium, which may fracture, or to cover specific portions of the intracranial contents, which are most frequently vulnerable to head injuries and may result in concussion. The helmet design and standards have not changed much since the 1970's other than the materials used and slight modifications to the helmet itself [20].

### **2.5.3 Current Helmets**

The Riddell Speedflex Helmet (Figure 4) is a popular new design, incorporating some features which help prevent concussions. This design incorporates new technologies that have

been shown to reduce concussions, such as a moving facemask. The facemask is attached by hinge clips that allow the mask to move, reducing the impact on the athlete. A flexible plastic piece located on the forehead of the helmet deforms during a hit. Similar to the deformation of a car's bumper during a crash, the deformation of this plastic plate helps mitigate the forces applied to the head. Finally, it incorporates side impact protection that provides extra padding. For safety only, the facemask has a quick release system to remove the facemask quickly in case of serious injury [21].



*Figure 4 Riddell Helmet.*

Another new, innovative football helmet is the Schutt Vengeance VTDII (Figure 5). This helmet is known for using thermoplastic polyurethane (TPU) as its interior padding. The single layers provide better absorption impact and lower overall weight. Dual layer TPU is used in the helmet's front. These layers are mechanically secured and cannot move. The helmet features a two piece facemask and a soft foam system that fits the head snugly and comfortably. The back of the helmet has a patented system called a Flexural Resistance Back Sheif Design, which increases strength and absorption in the back of the helmet [22].



*Figure 5 Schutt Vengeance VTDII Helmet.*

Another popular product is the Xenith X2E Helmet (Figure 6). This helmet focuses on fit, comfort, and protection. The outer shell is an extremely tough polycarbonate shell. It has a Fit Seeker system which “adapts to the head.” There are no pumps needed and the Fit Seeker helps keep the helmet secure during impact. When the chinstraps are pulled, the “Shock Bonnet” liner conforms around the head for a custom instant fit. The pads used on the inside of the helmet are durable, and are also resistant to all bacterial growth due to its chemical properties. The Aware Flow X2E shock absorber technology “adapts to the hit.” The Shock Bonnet system acts as a suspension system allowing the helmet and shell to move independently which deflects rotational forces. The shock absorbers collapse venting air, providing optimal response to a wide range of hits [23].



*Figure 6 Xenith X2E Helmet.*

The Rawlings NRG Tachyon is another popular, new helmet (Figure 7). The purpose of this helmet is to be as lightweight as possible. It utilizes Rawlings AC2 Technology – a system

of easily deforming pads which help guarantee a secure fit on a player's head. This technology uses Active Compression cores for comprehensive, lightweight coverage that is integrated with the foam to protect against diverse impact levels and temperatures. The helmet also uses a heat reduction system called Rawlings Heat Exchange. The padding system is designed for temperature control using strategically placed top vents that move hot air away from the head. Back and side vents circulate cooler air into the helmet [24].



*Figure 7 Rawlings Helmet.*

## 2.6 Technology and Analysis for Testing Head Impacts

### 2.6.1 Testing Methods

A vertical drop test is used to test most football helmets. The standards for this test were set by the NOCSAE: the "test standard involves mounting a football helmet on a synthetic head model and dropping it a total of 16 times onto a firm rubber pad" [25]. However, as one study points out, this test is not effective at determining a helmet's ability to prevent concussions because it does not take into account the linear and horizontal accelerations of the head within the helmet. A test which better simulates these accelerations is one where a football helmet is mounted on an upright synthetic head attached to a model neck which accurately mimics the movements of a human neck. The helmet is then struck by horizontal force great enough to cause a concussion (usually at a speed of 7.4 - 9.3 m/s). This force is commonly simulated using a



linear pneumatic impactor. Accelerometers are placed on the helmet and synthetic head in order to measure the accelerations generated by the test. The horizontal impact method is shown in Figures 8 and 9 [26].

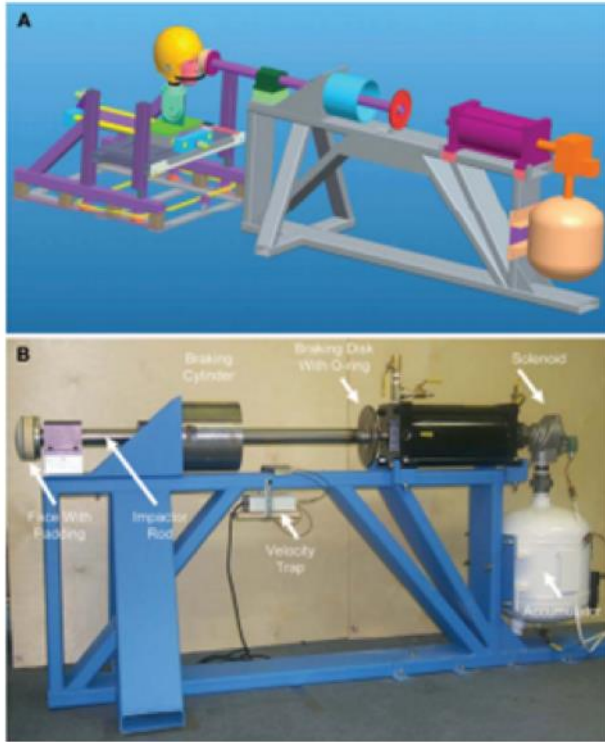


Figure 8 Horizontal pneumatic impactor.

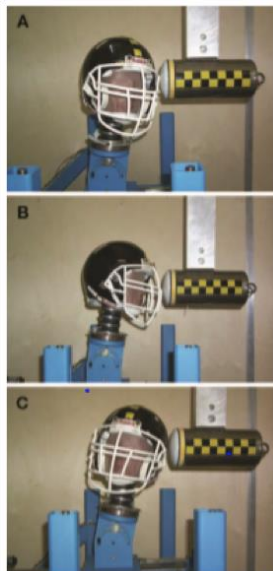


Figure 9 Horizontal Impact Tests.

### 2.6.2 Linear and Rotational Acceleration

In any hit experienced by the head, there are two forms of acceleration. The first, linear acceleration, usually occurs when the head is hit straight on, generating an acceleration in a linear direction for a short period of time. There is an axis of rotation for the head because the head is attached to the neck securely. When a direct hit is made to a head the linear acceleration is forced around the axis of the head and neck, generating a rotational acceleration. Each hit to the head can cause these two accelerations, putting the brain at risk in both situations [27].

On average, the linear acceleration for a concussed player is roughly  $94 \pm 27$  g's. Non-concussed players experience about half of that acceleration, generally  $55 \pm 21$  g's. When the neck was considered in the calculations, the axis of rotation was also included. This created the rotational accelerations, which for a concussed player can reach  $6398 \pm 1978$  rad/s<sup>2</sup>. Once again, a non-concussed player typically sustains approximately half as much rotational acceleration reaching  $3938 \pm 1406$  rad/s<sup>2</sup>. To find rotational acceleration, linear acceleration vectors and an assumed point of rotation were obtained. Angular acceleration was then estimated. The brain motion in linear acceleration was limited to  $\pm 1$  mm and the rotational acceleration motion was limited to  $\pm 5$  mm [27].

### 2.6.3 Common Concussion Inducing Hits

In one study with Virginia Tech Football, the frequency of impacts (Table 1) and impact locations of hits to the head were measured (Figure 10). Most impacts occurred at less than 40 g's.

Table 1 Frequency of impacts above specified resultant acceleration thresholds.

Linear acceleration (g)	Number of impacts	Angular acceleration (rad/s <sup>2</sup> )	Number of impacts
>0	1712	>0	1712
>20	684	>1000	875
>40	172	>2000	339
>60	52	>3000	143
>80	11	>4000	57
>100	3	>5000	23
>120	1	>6000	12
>140	0	>7000	5
>160	0	>8000	4
>180	0	>9000	1

In most sports, concussions occur in similar ways. The most common impact location is from the front. Hits to the sides of the head cause a whiplash effect, also producing a concussion. Beyond the initial impact, players often experience subsequent impacts, typically with the ground [28].

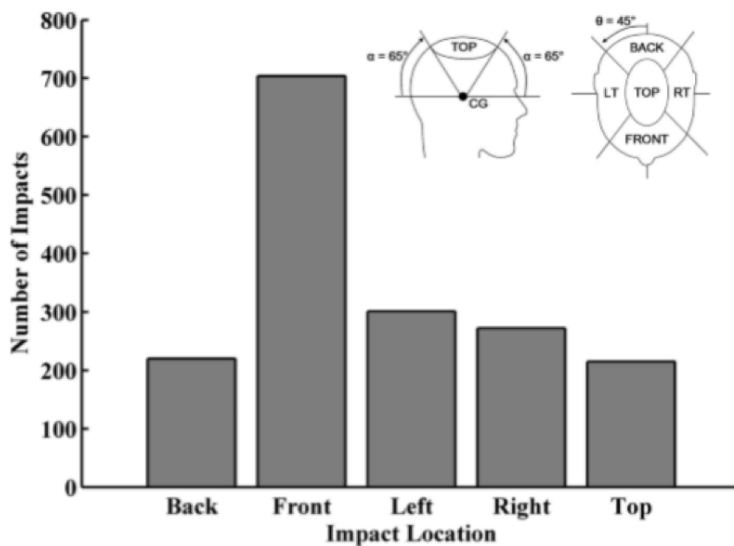


Figure 10 Distribution of impact locations.

## 2.6.4 Algorithms and Testing Methods

### *Head Impact Telemetry (HIT) System*

The HIT system is a testing method which has been shown to accurately estimate the cranial center of mass acceleration. HIT can also evaluate all impacts in a system, even if the hit is not in the correct field of view. The HIT system does this through several main steps. A helmet is fitted with 6 single axis accelerometers. Each one is angled differently and transmits wirelessly to a computing system. Once the data has been transferred, the linear acceleration can be determined. From this value, the angular or rotational acceleration can be estimated [31].

### *6DOF Measurement Device*

This device was developed to measure linear and angular accelerations of each axis of the head. It is composed of 12 single axis high-g iMEMs accelerometers. They are placed in orthogonal positions at 6 different locations in the helmet. During the game these accelerometers send information wirelessly to the computers on the sideline which collect the data. These measuring devices cannot be used in real time but can be assessed after the game [28].



*Figure 11 High-g iMEMs accelerometers.*

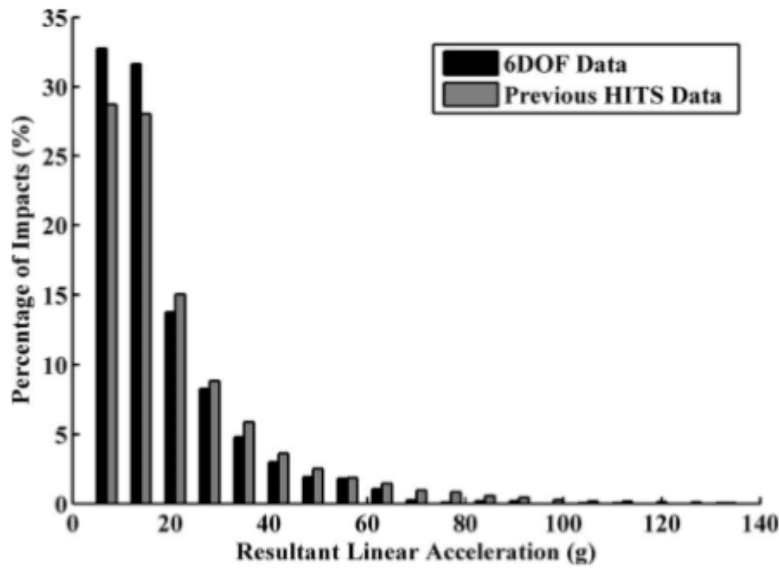


Figure 12 Comparison between 6DOF and Previous HITS Data.

### 2.6.5 Assessing the Injury: HIC, GSI

The two most widely used metrics for assessing head impacts are the Head Injury Criteria (HIC) and Gadd Severity Index (GSI). Each is used to predict when a single, linear acceleration of the head may lead to brain injury. They are mathematically defined as:

$$HIC = \left\{ (t_2 - t_1) \left[ \frac{1}{t_2 - t_1} \int_0^T a(t) dt \right]^{5/2} \right\}_{max}$$

$$GSI = \int_0^T a(t)^{5/2} dt$$

where T is the duration of acceleration during head trauma,  $t_1$  and  $t_2$  are the time bounds (in seconds) of the interval during which the HIC is at its maximum, and  $a$  is the acceleration of the head's center of gravity (in units of "g") [39]. HIC is a measure of the likelihood of head injury that consists of the integral of the acceleration over a certain amount of time. The period of time is the difference of the initial and final times of the interval during which HIC attained a

maximum value. This time is between 3 and 36 milliseconds but is typically 15 milliseconds.

The acceleration is measured in g's (standard gravity acceleration). HIC is significant because it not only includes the effects of head acceleration but it also considers the duration of the head acceleration.

Both formulas were designed to indicate a fatal injury at a value of 1000, and are used to measure the likelihood and severity of head injury arising from an impact. The tolerance for NFL concussions is believed to be a GSI of 300 and HIC 250. The NOCSAE uses HIC as a measure of helmet acceptability. Head rotation is a second type of biomechanical response that influences head injury; however, there is no concurrence on tolerance limits [40].

## 2.7 Materials

### 2.7.1 Sorbothane®

Sorbothane® is a proprietary, visco-elastic polymer. It has a very high damping coefficient, reducing impact forces by up to 80%, and has an extremely low transmissibility, which helps to reduce vibration and damage to sensitive components nearby. Sorbothane® has an operating range of temperatures superior to other elastomers, ranging from -20 degrees F to 160 degrees F [32].

Unlike fluid-based shock absorbers or foam products, Sorbothane® absorbs shocks efficiently for millions of cycles and eliminates the need for metal springs to return the system to its equilibrium position after absorbing a shock [32]. Sorbothane® works by deforming and turning mechanical energy to heat. This heat is translated perpendicularly away from its origin [32].



*Figure 13 Sorbothane® material.*

### **2.7.2 PORON Medical® Urethane-Firm-Energy Absorbing**

Rogers Corporation manufactures PORON® Medical Urethanes available in multiple density/thickness combinations that offer high-energy return and excellent impact absorption. Furthermore, this urethane combines comfort, elasticity, breathability, and fungal resistance. It can be abraded as well [33].

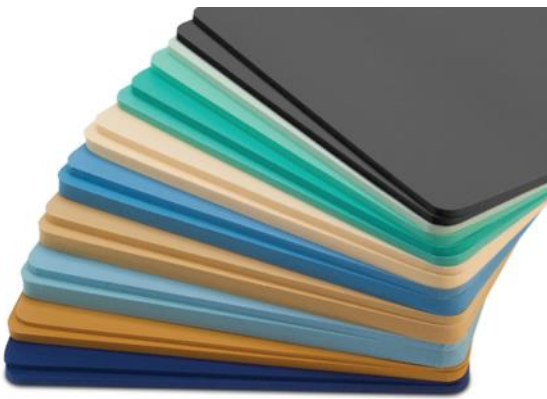


*Figure 14 PORON® samples.*

### **2.7.3 Neoprene Commercial Grade**

The Neoprene sample tested was a compound of 10% neoprene base and a blend of Styrene Butadiene Rubber and neoprene. Neoprene is a group of synthetic rubbers that are produced by polymerization of chloroprene. This sample is resistant to moderate oil, petroleum, ozone, and weathering. Neoprene is used in a variety of applications because it maintains

flexibility over a wide temperature range (-20°F to 212°F) and exhibits good chemical stability. Neoprene is often used as a protective garment in various sports and activities to protect the user's skin and body.

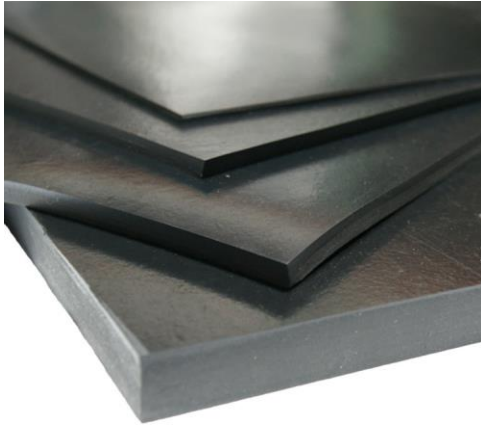


*Figure 15 Neoprene samples.*

### **3.0 Methodology**

With the objective of designing a helmet that was more effective at preventing concussions, a number of steps were required. First, preliminary designs were drafted with a series of design specifications. Next, materials for constructing the design needed to be tested in order to determine which would be most effective. Upon completion of this step, a final design was chosen and then assembled. Next, each piece of the rig on which the design was to be tested needed to be constructed. Then, tests were necessary to determine the impact forces the rig was capable of delivering. Finally, the accelerations of the head during impacts were measured, recorded, and analyzed. Evaluation of the results supported the development of future recommendations for a more effective design.



### 3.1 Design Specifications

Certain requirements were considered for decreasing concussion risk in football helmets in order for the helmets to be considered viable options. The conditions used to guide and evaluate potential design ideas were:

- Non-restrictive (allows for same range of motion as unmodified helmet)
- Comfortable (no more uncomfortable to wear than unmodified helmet)
- Lightweight (less than 3 kilograms)
- Sweat-proof/resistant
- Effective at reducing head acceleration/absorbing shock and isolating vibration from impact. Goal is to decrease HIC and GSI baseline values by at least 25%. Findings indicate that linear acceleration of 98g was most directly related to concussion with a mean threshold for injury, and corresponds to a 75% HIC [43].

### 3.2 Preliminary Design

Shock absorbing material was used within the helmet and on the outside of the helmet. The pads were placed within a typical football helmet and served as more effective shock absorbers than the typical pads found within a football helmet. The outside pads were positioned to cover areas of the helmet that most commonly experience concussion-inducing hits (Figure 16). The inside pads replaced any padding already placed within the helmet (Figure 17). The damping element of these pads should absorb more of the energy from the impact, thus decreasing the acceleration of the head.

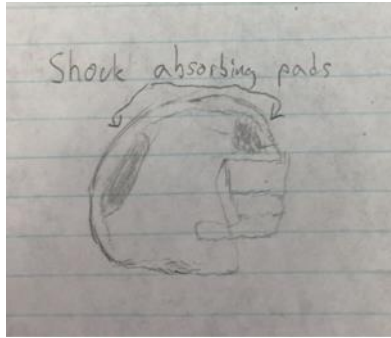


*Figure 16 Shock absorbing material within the helmet.*

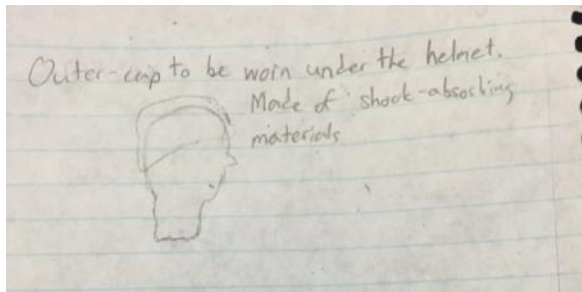


*Figure 17 Shock absorbing material on the outside of the helmet.*

### 3.3 Design Materials

Materials evaluated for the design were Sorbothane® Isolation Pads, Energy Absorbing PORON Medical® Urethane (Firm) and Neoprene sheets.

Three different samples of Sorbothane® Isolation Pads of varying size and durometer were evaluated. The first sample was 12.5 by 12.5 centimeters with a durometer of 70. The second sample was also 12.5 by 12.5 centimeters but had a durometer of 50. The third sample was 10 by 10 centimeters and had a durometer of 50. All samples had a thickness of 1.25 centimeters. The durometers of all three samples were measured on a Shore Scale of OO.

Four different samples of Energy Absorbing PORON Medical® Urethane (Firm) materials of varying densities were evaluated. All samples were 22 by 28 centimeters with a thickness of 6 millimeters. The first sample (09236) had a density of 144 kilograms per cubic meter (9 pounds per cubic foot) with a durometer of 10 (Sample A). The second (12236) had a density of 192

kilograms per cubic meter (12 pounds per cubic foot) with a durometer of 19 (Sample B). The third (15236) had a density of 240 kilograms per cubic meter (15 pounds per cubic foot) with a durometer of 32 (Sample C). The fourth (20236) had a density of 320 kilograms per cubic meter (20 pounds per cubic foot) with a durometer that was still being tested by the company (Sample D). The durometers of these PORON® materials were measured on a Shore Scale of O.

The sample of Neoprene was 22 by 28 centimeters with a thickness of 3.175 millimeters. Multiple layers were cut to layer the sheets in order to test the material at 6 millimeters thickness and 12 millimeters thickness as the others were. The durometer of the Neoprene was 60 on a Shore Scale of A.

The varying durometers of the different materials were compared using the chart in Figure 18.

<b>Comparison Chart</b>		<i>This chart is for comparison purposes only. This is <b>not</b> and <b>cannot</b> be used as a conversion chart.</i>														
<b>A</b>		10	20	30	40	50	60	70	80	90	100					
<b>B</b>			10	20	30	40	50	60	70	80	90	100				
<b>C</b>				10	20	30	40	50	60	70	80	90	100			
<b>D</b>					10	20	30	40	50	60	70	80	90	100		
<b>DO</b>						10	20	30	40	50	60	70	80	90	100	
<b>O</b>							10	20	30	40	50	60	70	80	90	100
<b>OO</b>		10	20	30	40	50	60	70	80	90	100					
<b>M</b>																

Figure 18 Shore Scale Comparison Chart.

### 3.4 Preliminary Force Plate Tests

In order to determine the comparative effectiveness of each material's ability to absorb energy from an impact, preliminary force tests were conducted. These tests were conducted by dropping a 5-kilogram weight from a height of 0.5 meters onto a Vernier force plate. The Vernier

force plate was connected to a laptop computer and data recorded to a LoggerLite file for analysis. The goal was to determine which material would dissipate force most effectively. Due to the simplicity of the Vernier force plate, these tests were only used to compare peak forces experienced by the system. A chute approximately 0.5 meters tall was constructed out of cardboard and used to guide the head in order to ensure it landed on the same spot on the force plate each run.



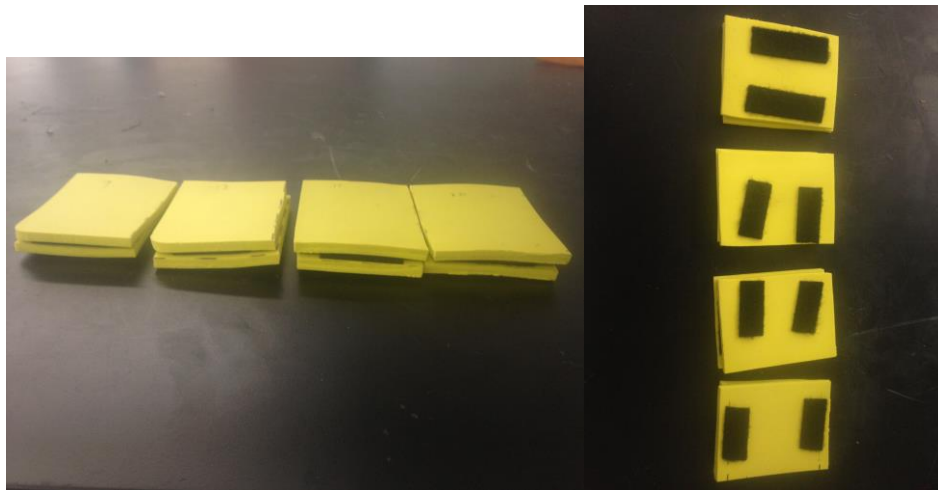
*Figure 19 Preliminary Force Plate Tests with Materials*

First, ten control tests were completed without any materials on the force plate in order to obtain an average, baseline impact force. Next, tests were performed for each sample of the Sorbothane® and PORON®. Each test consisted of placing a material sample at the center of the force plate and placing the cardboard chute directly over the sample and dropping the head from the top of the chute (Figure ). In order to obtain an average impact force, the test would be performed on each individual sample ten times. The average impact force of each sample could then be compared in order to obtain a preliminary idea of which sample was most effective.

### 3.5 Final Design

Ultimately, the Sorbothane® and Neoprene materials were abandoned and PORON® was chosen for the final design. The decision to disregard Sorbothane® was due to the limited amount of material in possession and the inability to acquire more due to budget constraints. The Neoprene was abandoned due to its poor performance in the preliminary force plate testing (Table 5).

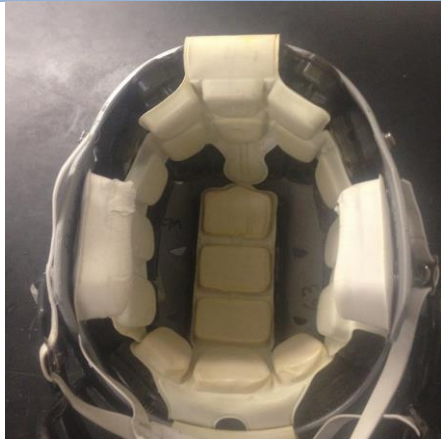
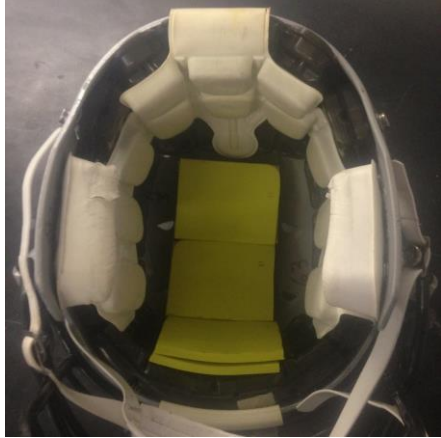
The 22 by 28 centimeter sheets of PORON® were cut into nine 5.5 by 7.0 cm pieces. Each piece was paired with an identical piece using Velcro, resulting in 5.5 by 7.0 cm pads with a thickness of 12.0 mm. Some of these pads were shown in Figure 20.



*Figure 20: PORON® Padding*

These pads were placed on the inside and/or outside of the helmet in various configurations and used during the simulation of three different hit impacts- top front of helmet, face mask, and middle side of helmet. Table 2 demonstrates an explanation of each padding configuration and the impact locations.

Table 2: Testing Configurations

Padding Configuration	Visual	Impact Locations Tested
<p><b>Control</b> – all original pads only</p>	 <p><i>Figure 21: Control Configuration</i></p>	<p>All</p>
<p><b>Front and Top Interior</b> – double-layered PORON® pads of same density in front and top, original padding in back</p>	 <p><i>Figure 22: Front and Top Configuration</i></p>	<p>Top front, Face mask</p>

<p><b>Back and Sides Interior</b> – double-layered PORON® of same density in back and sides of helmet, original padding in front and top</p>	 <p><i>Figure 23: Back and Sides Configuration</i></p>	<p>All</p>
<p><b>Exterior</b> – double-layered PORON® pad of same density on outside of helmet at impact location, all original pads in helmet interior</p>	 <p><i>Figure 24: Exterior Forehead Configuration</i></p>	<p>All</p>





*Figure 25: Exterior Facemask Configuration*



*Figure 26: Exterior Side Configuration*

Figure 22 and Figure 23 demonstrate the helmet with PORON® on the inside of the helmet at the front and back respectively. Figure 24 demonstrates the helmet with PORON® padding on the exterior, placed on the forehead. Figure 25 demonstrates the padding on the facemask. Figure 26 shows PORON® padding on the exterior side of the helmet. Due to a limited amount of material, a variation of the helmet with PORON® padding at each location was not possible.



## 3.6 Test Rig

### 3.6.1 Accelerometer

In order to measure accelerations during testing, a two-axis accelerometer with a range of approximately  $\pm 35$  g's was used. In order to measure accelerations experienced by a model football player's brain, this accelerometer was placed at the center of mass of the model head.

### 3.6.2 Neck, Head, and Helmet

A CPR manikin head was used for the model head for the test rig. Appendix A explains the procedure for locating the head's center of mass. In order to make testing scenarios more realistic, the hollow head was cut open along one of the planes of its center of mass with a band saw. The two halves of the head were filled with plaster to increase the weight. The total final weight was 5.5 kg. A small cavity was carved in the plaster at the head's center of mass. The accelerometer was glued in place inside this cavity before the halves of the head were taped back together.



*Figure 27 Head with plaster and accelerometer.*

The model head was mounted on a model neck. This neck, used in previous MQPs, was made of  $\frac{1}{4}$ " aluminum vertebrae disks, a combination of  $\frac{3}{4}$ " 50 durometer Neoprene rubber

sections, and a  $\frac{1}{2}$ " diameter 6-ply steel cable for tensioning. The neck was found to have a bending stiffness of roughly 5500 N/m (see Appendix B for the procedure and calculations). The head and neck combination was placed on a steel base in order to make it the proper height (Figure 28).



*Figure 28: Model Neck and Steel Base*

This entire component was secured to a wooden platform. The test helmet was fastened to the model head. The test helmet was borrowed from the WPI equipment room and had previously been used by the varsity football team. It was a Schutt DNA model, in size large, with SKYDEX™ Cushioning Components and a SUREFIT™ Air Liner system. A cross-section of this model type is shown in Figure 29.



*Figure 29: Cross-section of Schutt DNA football helmet [41]*

The helmet was also fitted with an RJOP-DW (reinforced jaw, oral protection, double wire) type face mask and an Adams 4-Point High Hook Up vinyl chinstrap.

### 3.6.3 Air Cylinder

In order to generate a force comparable to one that causes concussions, the team had to decide between two systems; a pendulum or a pneumatic air cylinder. A pendulum system could not be used due to constraints of testing areas; see Appendix B for calculations and more detailed reasoning. Thus, the team used a pneumatic cylinder system. To generate the necessary force, a 100 mm bore air cylinder with a 250 mm stroke was chosen (see Appendix D for calculations).

A solenoid valve was used in combination with the air cylinder to release the air from an air tank once it had reached the desired pressure.  $\frac{3}{4}$ " tubing connected the air tank to the solenoid and then to the input port of the air cylinder using adjustable fittings for easy disassembly. The air cylinder had to be mounted in such a way that it could hit the helmet at certain positions and speeds.

A frame was constructed using slotted aluminum angle pieces so it would be sturdy enough to withstand the recoil force while also allowing for easy height adjustments of the air cylinder (Figure 30). Once mounted at each of the three different heights (corresponding to different impact positions on the helmet), the air cylinder was extended to its full stroke length and arranged on the wooden platform at the correct distance away from the helmet component. Three sets of holes (one for each impact position) were marked and drilled out so that the frame could be mounted on the platform. The cylinder was placed so that any contact between the cylinder rod's impact cap and the helmet would last around 15 milliseconds (see Appendix D for calculations).

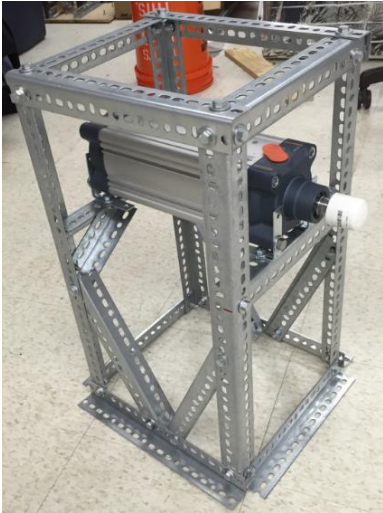


*Figure 30 Metal frame constructed for air cylinder.*

### **3.7 Force Impact Test**

The team decided to use a force of 2000 Newtons to generate a simulated concussion-inducing hit (reasoning and calculations shown in Appendix D). In order to ensure that the cylinder was truly generating this magnitude of force, a force impact test was designed that utilized a force sensor acquired from another MQP team. The force sensor was calibrated before it was used to measure forces (Appendix E). Calibration showed no hysteresis (Figure 31). The equation from calibration was used in the LabVIEW for the slope and intercept used for testing (Appendix E). The force sensor was attached to the impact site in order to measure the forces of the impacts. The force sensor was thin, flexible, and had stable output with respect to load area.

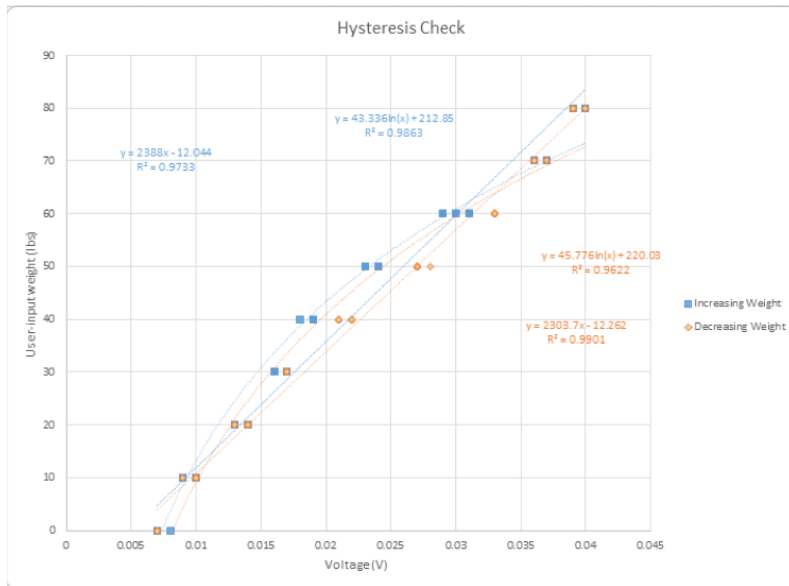


Figure 31 Force Sensor Hysteresis Check

### 3.8 Acceleration Tests

The main focus of this study was to determine how different padding materials and configurations in the helmet influence the resulting head acceleration after a collision. Three different hit impacts were simulated – top front of helmet, facemask, and middle side of helmet. For each impact location, a variety of padding configurations were tested, as explained and illustrated in Table 2.

For each testing scenario, the air tank was filled to a pressure of 40 psi before air was manually released to the cylinder by pressing and holding a button on the solenoid. After the cylinder fired and impact occurred, everything was reset and repeated until a total of ten hits were obtained for each impact location, padding configuration, and PORON® density (aside from the controls). Data for each hit was recorded using a LabVIEW program constructed to change the voltages read from the accelerometers to x-axis and z-axis acceleration values (Appendix F). In order to collect enough data points to thoroughly capture and analyze the hits,

data was collected at a rate of 3000 samples per second. The minimum and maximum z- and x-axis acceleration values of each hit were averaged, along with the time interval of the initial impact (taken as the length of the first x-axis acceleration).

The average x-axis and z-axis peak accelerations, and calculated HIC and GSI values of the different padding configurations were all evaluated against the control to assess the performance of the PORON® materials.

### **3.9 Calculating HIC and GSI**

Calculating the HIC and GSI values involves the average value of the acceleration over the most critical part of the impact. The time interval for the critical impact period was determined by picking an impact that resembled the average impact over the same series the closest. The x-axis accelerations were used as a basis for the critical time intervals because they were of a much higher magnitude than the z-axis accelerations, thus contributed more to the overall resultant acceleration of the head.

The first step in calculating HIC and GSI was to use the full acceleration graphs generated by a series of impacts. Figure 32 Front Impact Acceleration Graphs shows both the X and Z acceleration graphs of the front impact control hit. The X acceleration max average was 10.58 g's and the Z acceleration max average was 4.88 g's.

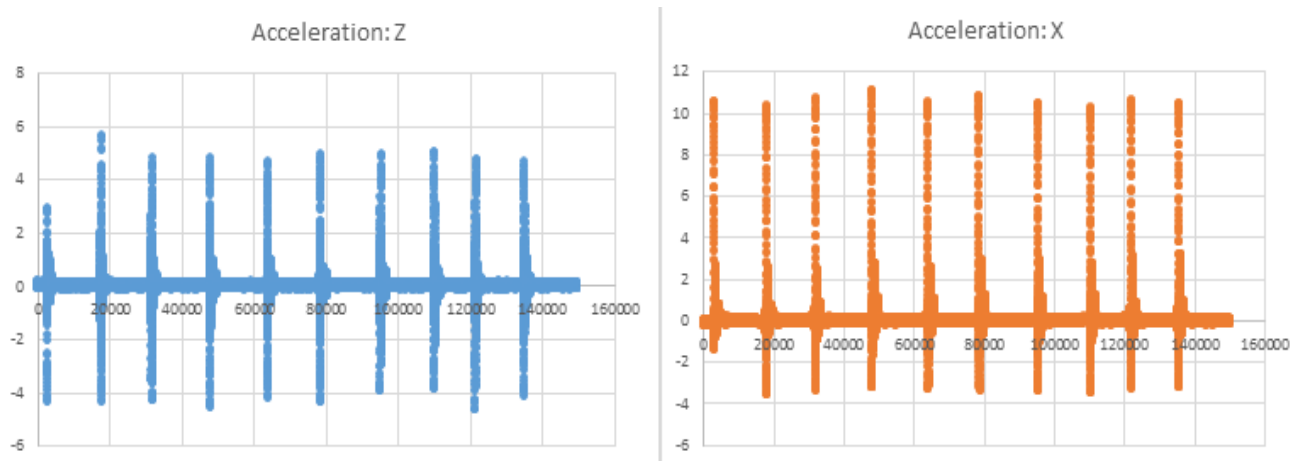


Figure 32 Front Impact Acceleration Graphs

The next step was to pick an impact that fits the average of the series done in this test.

Figure 33 shows a zoomed in front impact control hit, with a maximum x-axis acceleration value of 10.61 g's, which was closest to the average impact series of 10.58 g's.

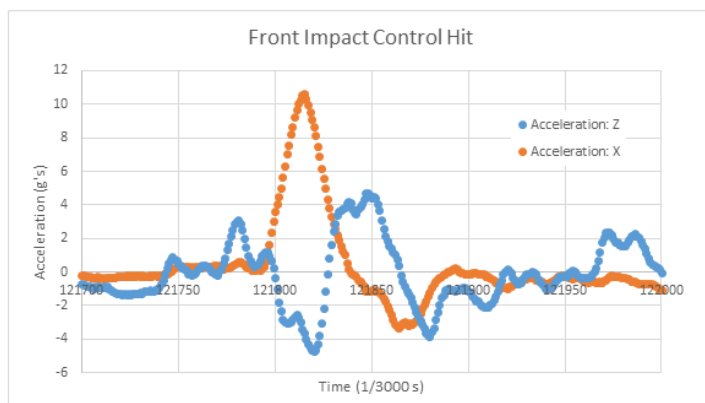


Figure 33 Front Impact Control Hit.

The next step was to select the correct portion of the impact, which represents an acceleration curve under the critical time-period. Figure 34 shows a zoomed-in section of the impact from when the x-axis acceleration first starts to spike until it becomes negative.

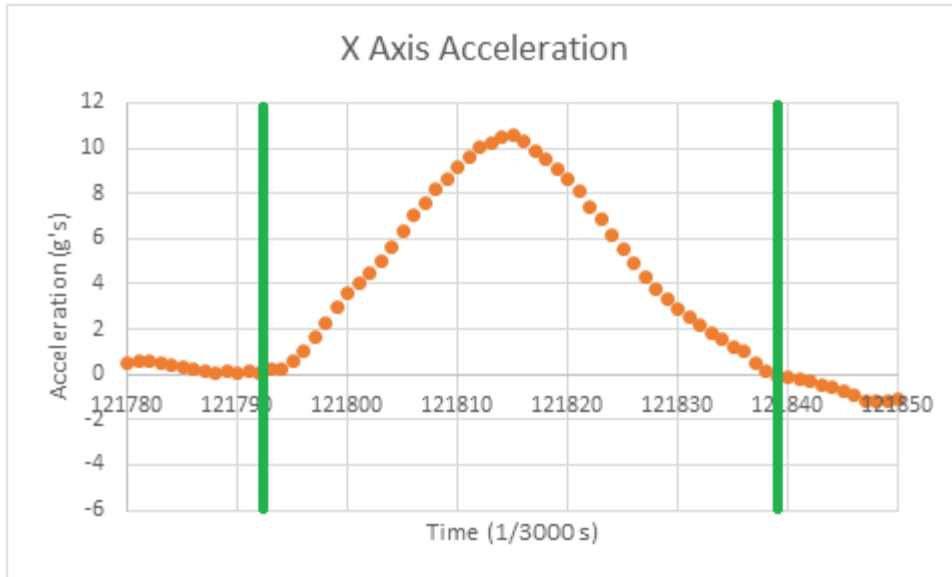


Figure 34 X-Axis Acceleration.

Figure 34 Figure 35 shows the same time interval for the z-axis acceleration.

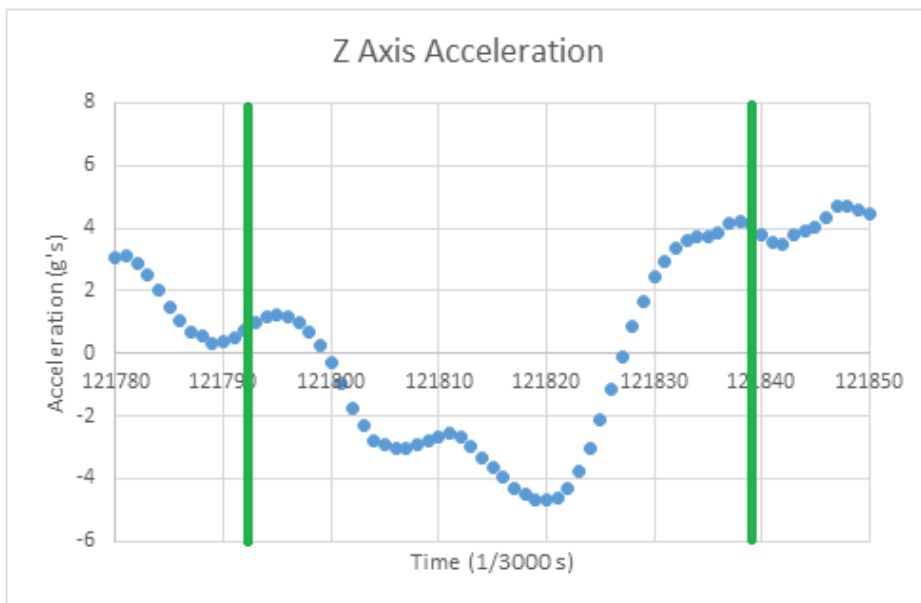


Figure 35 Z-Axis Acceleration.

The data points in this critical time period were plotted individually and fitted with sixth-order polynomials. The modeled curves are shown in Figure 36 and Figure 37.



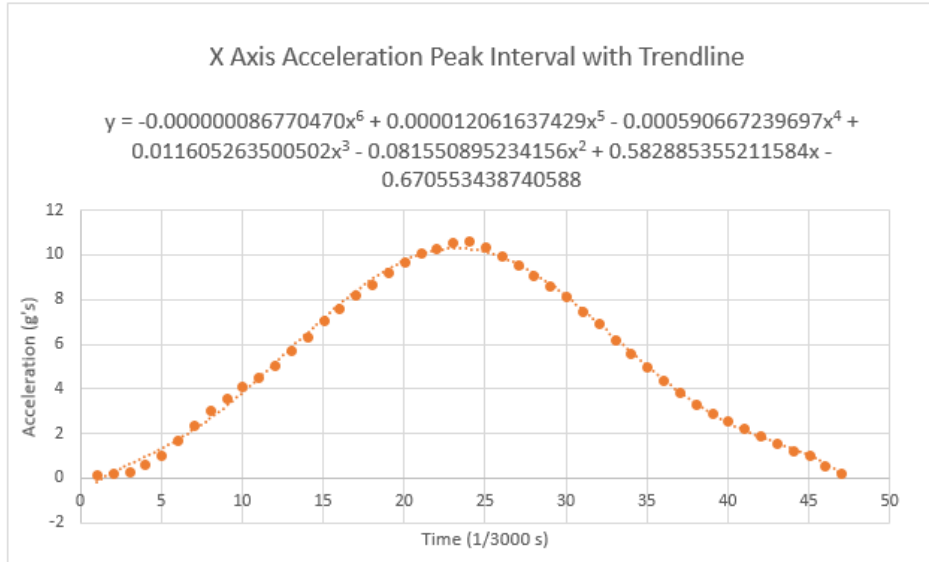


Figure 36 X Axis Acceleration Peak Interval with Trendline.

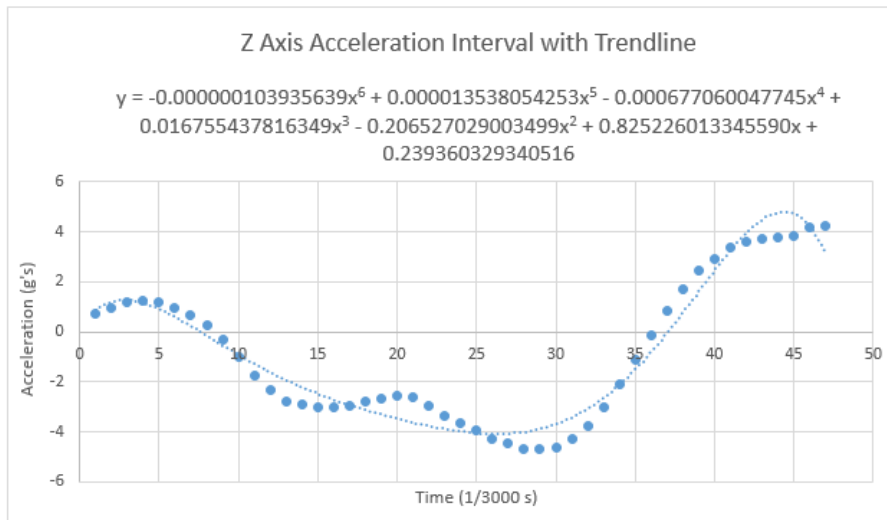


Figure 37 Z-Axis Acceleration Interval with Trendline.

These equations generated by the best-fit line were combined to produce an overall resultant acceleration equation by using the formula:  $a(t) = \sqrt{[a_x(t)^2 + a_z(t)^2]}$ . Both the X and Z accelerations were evaluated in the corresponding critical time interval to find HIC and GSI using the following equations:

$$HIC = \left\{ (t_2 - t_1) \left[ \frac{1}{t_2 - t_1} \int_0^T a(t) dt \right]^{5/2} \right\}_{max}$$

$$GSI = \int_0^T a(t)^{5/2} dt$$

HIC and GSI values were calculated using MATLAB and Excel. The results of the HIC and GSI calculations are in Table 6. Appendix L shows an example of the MATLAB code created to calculate the resultant acceleration and integral value.

### 3.10 System Model

This model analysis focused on the horizontal forces and accelerations of the system. The simplified version of the horizontal system diagram is represented below in Figure 38.

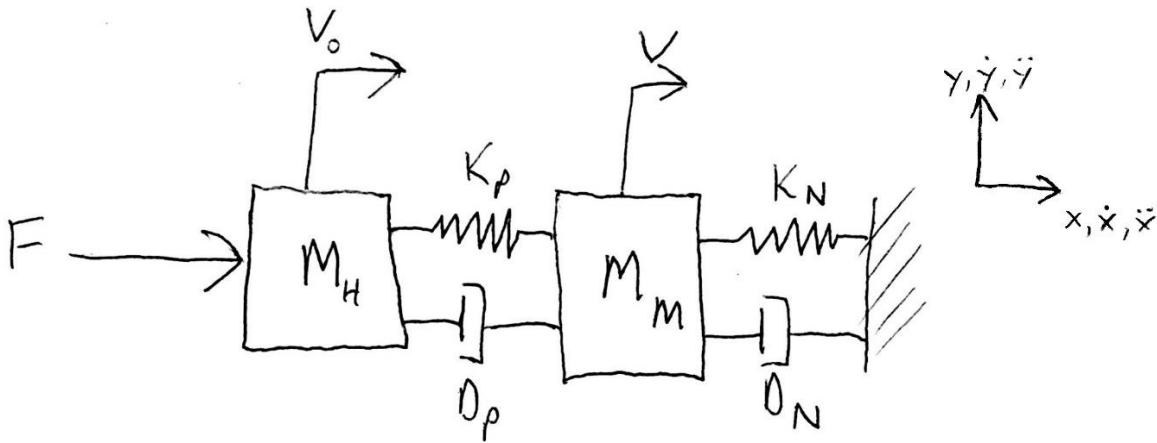


Figure 38: Horizontal System Diagram

For Figure 38, the nomenclature was as follows:

- $F$  = Force being applied by the pneumatic cylinder.
- $v_0$  = Velocity of the helmet.
- $M_h$  = Mass of the helmet.

- $K_p$  = Stiffness coefficient of shock-absorbing pad.
- $D_p$  = Damping coefficient of shock-absorbing pad.
- $v$  = Velocity of the model head within the helmet.
- $M_m$  = Mass of the model head.
- $K_n$  = Stiffness coefficient of model neck.
- $D_n$  = Damping coefficient of model neck.

Figure 38 represented the system when shock-absorbing pads are used within the interior of the helmet, applied directly to the head. The spring and damping coefficients of the neck were depicted as horizontal to better illustrate the translational effects of their forces.

The diagram illustrated that when an initial force was applied to the helmet it created a velocity which was slowed down by compression of the pad which in turn exerted a reaction force (consisting of a damping force and a spring force) onto the model head. This reaction force resulted in a velocity of the model head which was slowed down by the spring and damping forces of the model neck. The forces acting on the model head are illustrated in the free body diagram, Figure 39. This project's goal was to minimize the acceleration of the model head caused by the initial force.

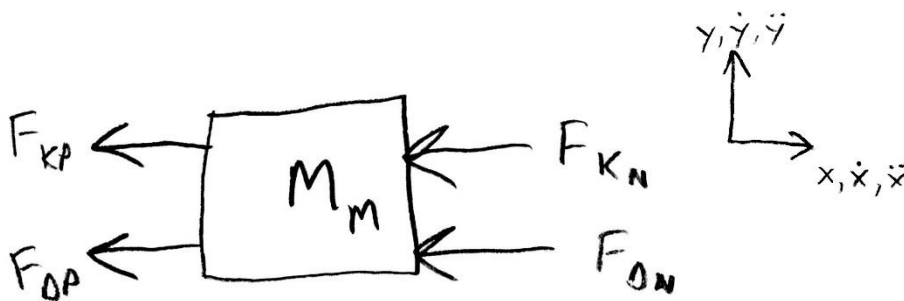


Figure 39: Model Head Free Body Diagram

Gravity was neglected in this model.

From Figure 38, a bond graph was created. The system's causal bond graph and state variables were shown in Figure 40.

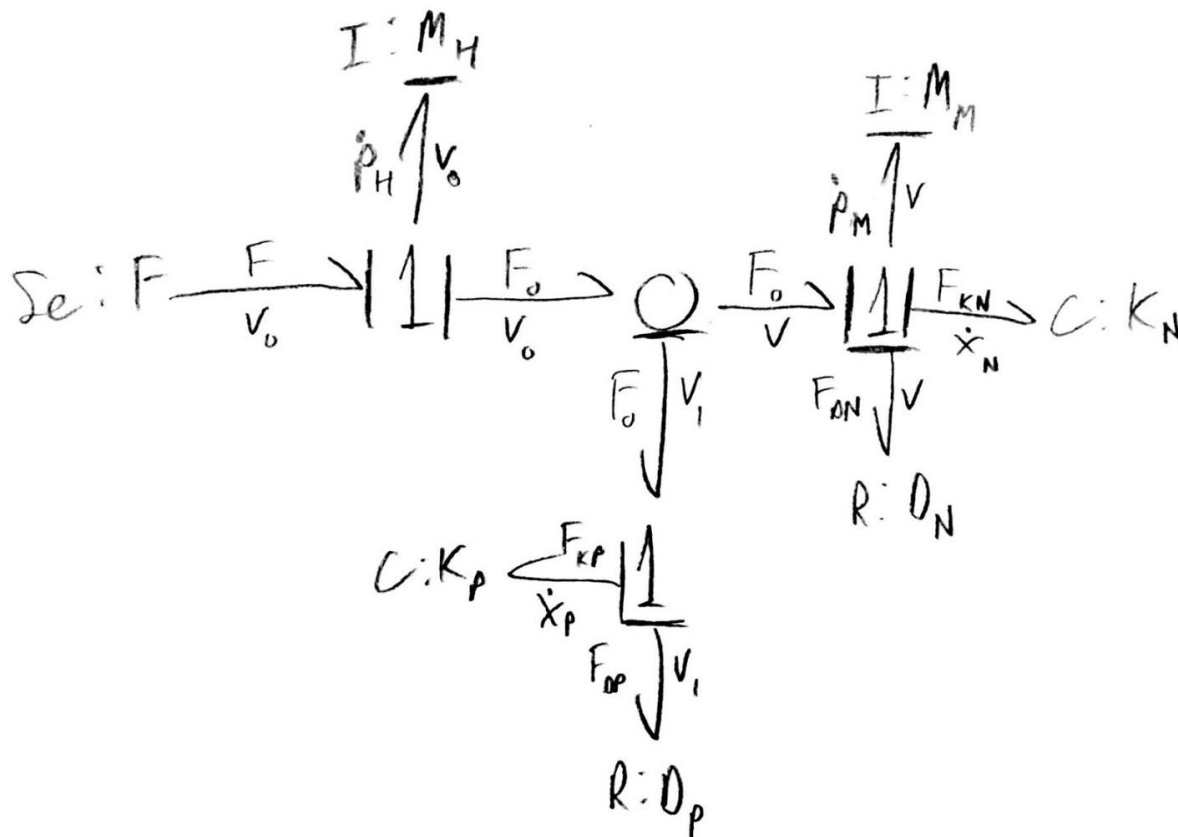


Figure 40: Causal Bond Graph with Assigned State Variables

As illustrated, this system's state variables were  $p_h$ ,  $p_m$ ,  $x_p$ , and  $x_n$ . Each of these state variables were functions of the source of effort (in this case, F) and the derivative of each state variable.

These functions are in Appendix G. From the equations in Appendix G, the equation for determining the peak x acceleration for the system was:

$$a_m = \{ [K_p * x_p + D_p * (v_0 - v)] - K_n * x_n - D_n * v \} / (9.8 * M_m) \quad (1)$$

Equation (1) solved for the peak acceleration of the model head where  $a_m$  was measured in g's. In order to calculate this acceleration the values for  $K_p$ ,  $x_p$ ,  $D_p$ ,  $v_0$ ,  $v$ ,  $K_n$ ,  $x_n$ , and  $D_n$  must be known.

### 3.10.1 Calculating K and D for Pads

#### *Stiffness*

In order to determine values for the stiffness coefficients for the varying types of PORON® padding, a test was developed. The steps for this test were:

1. Place pad on rigid surface
2. Place lightweight aluminum plate on top of pad to ensure that applied weight was distributed equally across surface area of pad.
3. Measure thickness of pad.
4. Record thickness in excel.
5. Apply 10 pound weight to aluminum plate.
6. Repeat steps 3-5 until thickness of pad with 100 pounds of weight applied was measured.

This procedure was performed for each of the 4 types of PORON® foams used by the team.

Using the equation:

$$F = K * x$$

where  $x$  is displacement, the excel sheet calculated values for the stiffness coefficients which varied depending on the applied force. As an example, the data from the excel sheet for the 9 lb/ft<sup>3</sup> density pad was shown in **Error! Reference source not found..**

Table 3: Stiffness Data for 9lb/ft<sup>3</sup> Density Pad.

Force (lbs)	Force (N)	Height (mm)	Height (m)	Stiffness (N/m)	Displacement (m)
0.01	0	11.9	0.0119	0	0
10	44.4822	11	0.011	49424.66667	0.0009
20	88.9644	10	0.01	46823.36842	0.0019
30	133.4466	8.5	0.0085	39249	0.0034
40	177.9288	7	0.007	36312	0.0049
50	222.411	6	0.006	37696.77966	0.0059
60	266.8932	5.6	0.0056	42364	0.0063
70	311.3754	5.1	0.0051	45790.5	0.0068
75	333.6165	4.9	0.0049	47659.5	0.007
80	355.8576	4.7	0.0047	49424.66667	0.0072
100	444.822	4	0.004	56306.58228	0.0079

These stiffness values were averaged to obtain a single stiffness coefficient for the pad.

### Damping

A different test was developed to find the damping coefficient of each PORON® sample. Using a high-speed camera, the team filmed the drop of a lacrosse ball from a measured height. Five different drops were recorded: one where the ball was dropped onto the rigid floor and the other four where the ball was dropped onto each sample of PORON® padding. The height of the ball's bounce for each test through analysis of the videos. The values for these heights were inserted into the equations below:

$$M \cdot g \cdot h_0 = \frac{1}{2} \cdot M \cdot v_0^2$$

$$M \cdot g \cdot h_f = \frac{1}{2} \cdot M \cdot v_f^2$$

$$e = v_f / v_0$$

$$C = (-\ln(e)/\pi) * [1 + (\ln(e)/\pi)^2]^{-1/2}$$

$$D = 2C * (K \cdot M)^{1/2}$$

With nomenclature as follows:

M = mass of the ball

g = gravity

h<sub>0</sub> = height from where the ball was dropped

h<sub>f</sub> = height that the ball bounced

v<sub>0</sub> = velocity of ball immediately before impact

$v_f$  = velocity of ball immediately after impact

$K$  = stiffness coefficient of material

$D$  = damping coefficient of material

Through these equations, the damping coefficient of each PORON® sample was calculated. The calculated stiffness and damping coefficients for each sample of PORON® are in Table 4.

*Table 4: Stiffness and Damping Coefficients*

<b>PORON® Sample Density</b>	<b>Stiffness (kN/m)</b>	<b>Damping (N/ms)</b>
9 lb/ft <sup>3</sup>	45.11	86.64
12 lb/ft <sup>3</sup>	50.24	74.33
15 lb/ft <sup>3</sup>	101.79	89.65
20 lb/ft <sup>3</sup>	222.76	108.21

### 3.10.2 Determining Velocity and Displacement

In order to determine the velocities and displacements experienced by the system, this group used the same high-speed camera from the damping tests to capture the impacts on video and analyze the data frame by frame. By placing a marked board behind the system, the starting position of the system and the point at which it reached its full displacement were determined.

Images from the video are shown in Figure 41.

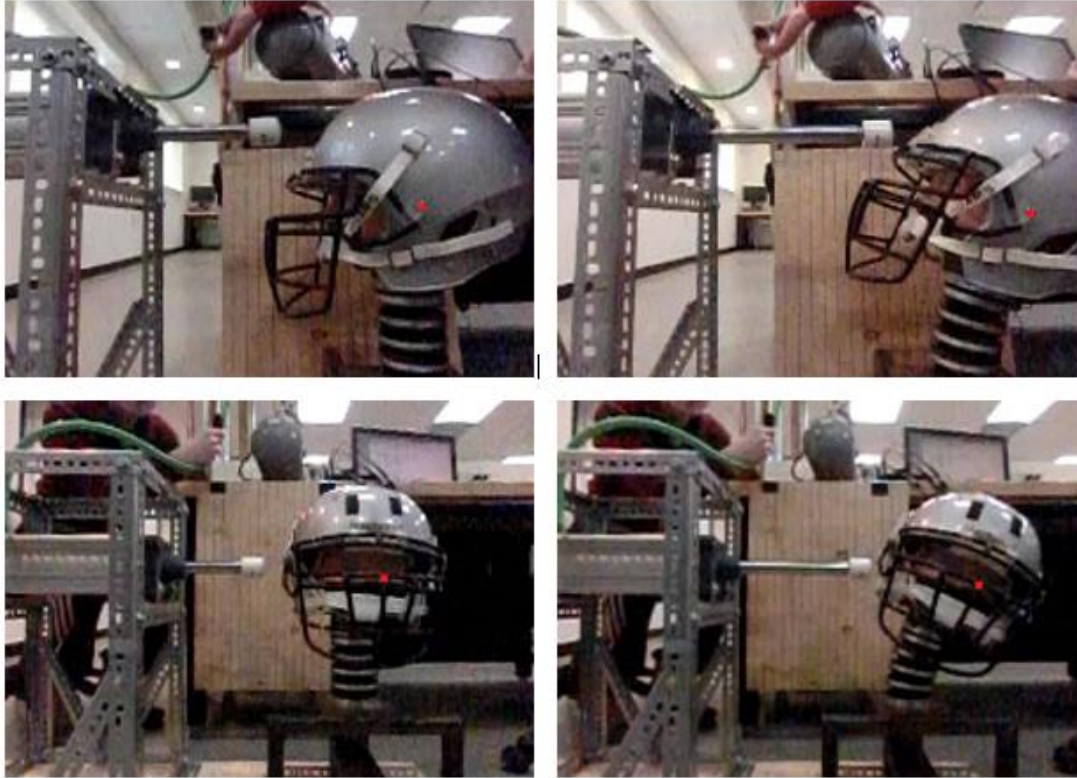


*Figure 41 Images from High-Speed Data Analysis.*

From this procedure, the maximum displacement experienced by the model from a frontwards-facing hit was 12.37 cm, which corresponds to 0.14 seconds of movement for the model in the positive x direction. From this data, the average velocity of the system was calculated to be roughly 0.9 m/s. However, this displacement and time do not correspond to the system at peak acceleration. The following equation was used to calculate for the velocity at peak acceleration (constant acceleration was assumed due to the short period of time for which the impact occurs):

$$v = x / t$$

Where x was the displacement of the head at peak velocity and t was the time. The team used 0.025 meters for x (calculations in Appendix C) and estimated 15 milliseconds for t. The velocity was calculated as 1.67 m/s.



## 4.0 Results and Analysis

### 4.1 Preliminary Force Plate Tests

The results from the preliminary force plate tests are in Table 5.

*Table 5: Preliminary Force Plate Test Results*

Sample	Thickness (mm)	Average Impact Force (N)	% Improvement from Control Test
No material (Control)		1890 +/- 100	NA
Sorbothane® 70 Durometer	12.5	1637 +/- 246	-13%
Sorbothane® 50 Durometer	12.5	1569 +/- 227	-17%
PORON® 9 lb/ft <sup>3</sup> Density	6.0	1508 +/- 213	-20%
PORON® 12 lb/ft <sup>3</sup> Density	6.0	1350 +/- 153	-29%
PORON® 15 lb/ft <sup>3</sup> Density	6.0	1402 +/- 210	-26%
PORON® 20 lb/ft <sup>3</sup> Density	6.0	1594 +/- 182	-16%
Neoprene	6.0	1664	-12%

For all materials tested, the standard deviation for average impact force was between 10-15%. This was likely due to the force plate's data collection speed, which was sometimes too slow to record the rapid impacts produced by the tests.

PORON® performed the best despite the fact that each sample was less than half the thickness of the Sorbothane® samples. The 12 lb/ft<sup>3</sup> PORON® sample showed the most potential with a 29% reduction in force measured by the force plate.

### 4.2 Force Sensor

Figure 42 shows data collected from the force sensor test.

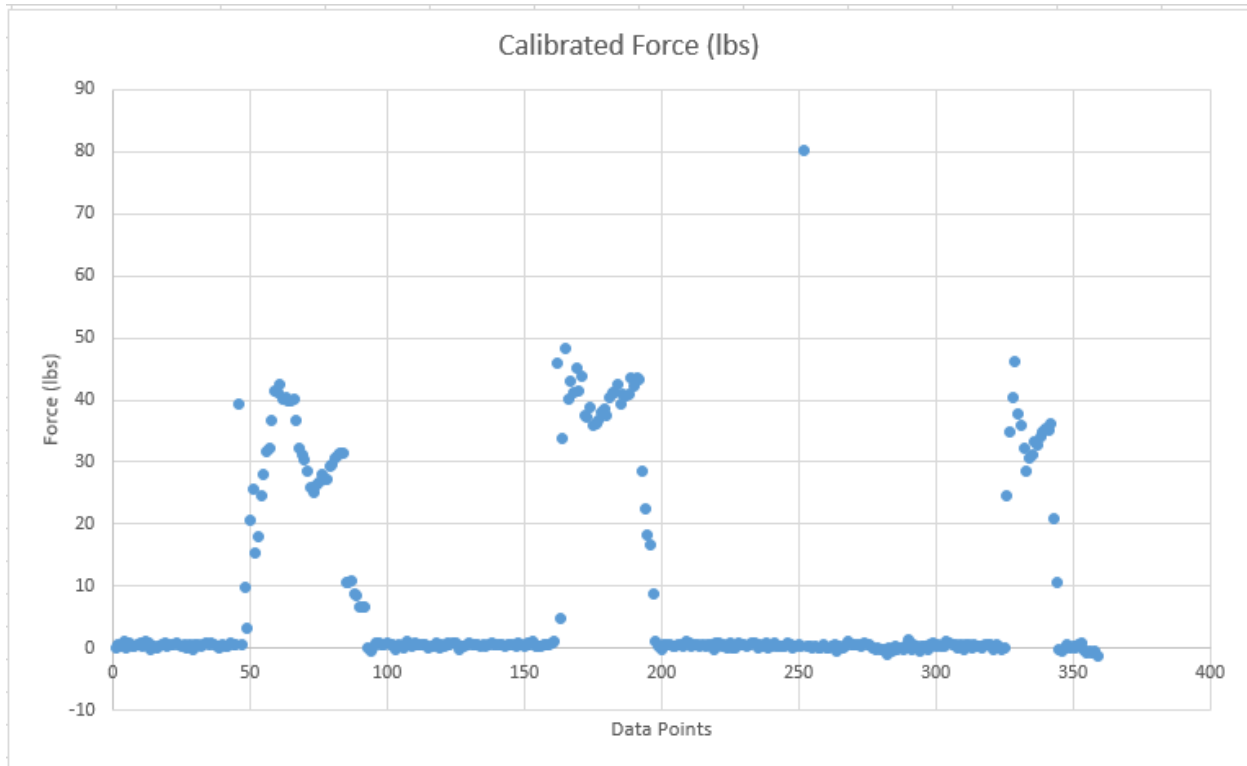


Figure 42: Force Sensor Impact Readings Graph

The force impact generated by the air cylinder on the helmet was, on average, 40-50 lbs (175-225 Newtons). This impact force was much lower than the predicted force of 2000 N (defined in Appendix D). This was most likely due to the damping effects within the air cylinder itself.

These lower force impacts resulted in head accelerations that were far less than anticipated. Therefore, the accelerations measured by this project were not comparable to accelerations experienced by football players during a concussion inducing impact. However, despite these weaker hits, this team still compared the effectiveness of the different PORON® materials and configurations with that of the control (original Schutt padding, Figure 21) to determine which was more efficient at reducing accelerations.

### 4.3 Acceleration Tests

Table 6 displays the acceleration test results.

Table 6: Acceleration Test Data

Location of Impact	Pad Orientation	Pad Density (lb/ft <sup>3</sup> )	Avg. Max X-Accel (g)	Accel % Change from Control	Avg. Max Z-Accel (g)	Accel % change from control	Time of Impact (s)	HIC	HIC % change from control	SI	SI % change from control	
Front of Helmet	Control	NA	10.58 +/- 0.24	NA	4.89 +/- 0.3	NA	0.015	1.40	NA	2.16	NA	
	Pads in Interior, Front and Top	9	12.45 +/- 0.24	17.7%	5.30 +/- 0.32	8.5%	0.013	1.74	24.4%	2.78	29.0%	
		12	13.50 +/- 0.42	27.6%	5.65 +/- 0.11	15.6%	0.013	2.02	44.1%	3.31	53.4%	
		15	12.91 +/- 0.26	21.9%	5.62 +/- 0.25	15.0%	0.012	1.89	35.0%	2.98	38.0%	
		20	13.32 +/- 0.43	25.9%	5.48 +/- 0.64	12.2%	0.012	2.04	45.5%	3.30	53.2%	
	Pads in Interior, Back Only	9	10.23 +/- 0.30	-3.4%	4.93 +/- 0.58	0.9%	0.017	1.37	-2.1%	2.17	0.4%	
		12	10.45 +/- 0.31	-1.2%	5.30 +/- 0.49	8.4%	0.016	1.40	-0.1%	2.14	-0.7%	
		15	10.38 +/- 0.42	-1.9%	5.95 +/- 0.57	21.8%	0.015	1.36	-2.9%	2.10	-2.7%	
		20	10.87 +/- 0.44	2.7%	5.12 +/- 0.55	4.8%	0.014	1.58	12.5%	2.41	11.7%	
	Pads on Exterior of Helmet	9	7.63 +/- 0.61	-27.9%	4.49 +/- 0.52	-8.0%	0.018	0.64	-54.2%	0.98	-54.6%	
		12	7.94 +/- 0.22	-25.0%	3.97 +/- 0.21	-18.7%	0.017	0.69	-51.1%	1.11	-48.6%	
		15	7.64 +/- 0.20	-27.8%	4.26 +/- 0.14	-12.8%	0.017	0.63	-55.3%	1.04	-51.7%	
		20	8.99 +/- 0.35	-15.0%	3.83 +/- 0.22	-21.6%	0.015	0.89	-36.1%	1.46	-32.1%	
	Face-mask	Control	NA	9.26 +/- 0.27	NA	2.36 +/- 0.16	NA	0.018	0.88	NA	1.46	NA
		Pads in Interior, Front Only	9	10.81 +/- 0.43	16.7%	4.88 +/- 0.50	106.4%	0.015	1.39	57.5%	2.18	49.1%
			12	11.22 +/- 0.25	21.1%	4.61 +/- 0.85	95.0%	0.014	1.40	58.8%	1.98	35.3%
15			10.76 +/- 0.85	16.2%	4.32 +/- 0.25	82.8%	0.015	1.44	63.1%	1.98	35.1%	
20			11.07 +/- 0.57	19.6%	4.37 +/- 0.44	84.7%	0.015	1.16	31.5%	1.80	22.6%	
Pads in Interior, Back Only		9	8.01 +/- 0.40	-13.5%	3.26 +/- 0.41	37.8%	0.021	0.79	-10.2%	1.22	-16.4%	
		12	9.00 +/- 0.79	-2.8%	3.87 +/- 0.52	63.8%	0.018	1.18	33.4%	1.70	16.4%	
		15	8.96 +/- 0.68	-3.2%	5.08 +/- 0.69	114.9%	0.021	1.12	26.8%	1.65	12.3%	
	20	8.63 +/- 0.49	-6.8%	3.94 +/- 0.42	66.5%	0.019	1.02	15.3%	1.51	3.4%		

	Pads on Exterior of Facemask	9	8.04 +/- 0.45	-13.1%	2.46 +/- 0.45	4.1%	0.016	0.68	-23.5%	1.09	-25.7%
		12	7.66 +/- 0.23	-17.2%	1.90 +/- 0.32	-19.5%	0.016	0.61	-30.5%	0.98	-33.1%
		15	8.28 +/- 0.55	-10.6%	2.69 +/- 0.56	14.0%	0.016	0.75	-14.6%	1.19	-18.9%
		20	8.76 +/- 0.39	-5.4%	2.95 +/- 0.42	24.8%	0.015	0.92	4.4%	1.41	-3.5%
Side	Control	NA	13.05 +/- 0.22	NA	3.23 +/- 0.64	NA	0.012	1.89	NA	3.13	NA
	Pads in Interior	9	16.15 +/- 0.16	23.8%	5.07 +/- 0.28	57.0%	0.010	3.03	60.7%	4.52	44.2%
		12	16.66 +/- 0.36	27.7%	2.72 +/- 0.25	-15.7%	0.010	3.31	75.4%	4.94	57.7%
		15	17.06 +/- 0.50	30.7%	2.92 +/- 0.20	-9.5%	0.010	3.79	101.0%	5.35	70.9%
		20	17.69 +/- 0.36	35.6%	3.06 +/- 0.46	-5.1%	0.009	3.30	74.9%	5.23	67.0%
	Pads on Exterior	9	10.12 +/- 0.09	-22.5%	3.93 +/- 0.20	21.7%	0.013	1.19	-37.1%	1.68	-46.4%
		12	10.17 +/- 0.29	-22.1%	3.65 +/- 0.14	13.0%	0.014	1.06	-44.0%	1.69	-45.9%
		15	10.96 +/- 0.19	-16.0%	2.99 +/- 0.18	-7.3%	0.013	1.21	-35.9%	2.00	-36.0%
		20	12.88 +/- 0.35	-1.3%	4.38 +/- 0.55	35.6%	0.013	1.80	-4.4%	2.90	-7.4%

Appendices I-K show graphs from all tests.

### 4.3.1 Accelerations

In each impact-testing scenario, both X and Z accelerations were affected by the placement of the PORON® pads. In most of the tests, adding pads to the interior of the helmet did not make any difference or produced worse results. In some tests, the impacts increased by over 20% when interior PORON® pads were used. When adding pads to the outside of the helmet, the accelerations were reduced considerably. Adding exterior padding to the helmet was capable of decreasing the resulting accelerations of the head up to 28%.

When looking at the acceleration curves over time, some of the Z acceleration curves were inconsistent. The Z accelerations were difficult to determine because the data produced had large oscillations and noise. This may have been caused from the way the helmet was impacted. On impact, a slight upward or downward movement (Upwards for facemask impact, downward

for front and side impacts) of the head was generated. Some of the Z acceleration curves did not match up well over time when compared to the X accelerations. However, some of these impacts were matched over time with the X accelerations. Evaluation of the accelerations in both the X and Z directions described each hit more thoroughly but the angular acceleration could still not be determined.

Impact testing on the facemask was highly inconsistent. The impact sight on the facemask was a small vertical bar, making it difficult to produce a flush impact. Despite adding flat plates to the facemask and air cylinder to create a planar impact site, the helmet ricocheted in various directions over the course of many hits. This produced varied accelerations in all directions, making the results inconsistent.

Overall, the lower density pads (densities 9 and 12 lb/ft<sup>3</sup>) performed better than the higher density pads (densities 15 and 20 lb/ft<sup>3</sup>). However, almost all of the PORON® pads tested in the interior of the helmet performed worse than the control pads. The major finding of this project's testing was that padding added to the exterior of the helmet was most effective in reducing the acceleration of the head during a hit in football

#### **4.3.2 HIC and GSI**

From the HIC and GSI values, a different intensity was observed for different pad samples. As the pad density increased, the resultant HIC and GSI values increased as well (Table 6). The higher density PORON® made for higher HIC and GSI values, indicating greater risk of injury.

The HIC and GSI values calculated were lower than anticipated. This was due to the low-impact forces discussed in Section 4.2.

The main observation was the effect that exterior pads caused on the HIC and GSI values. In each of the three main impact tests, padding attached to the outside of the helmet greatly decreased the HIC and GSI values (Table 6). Padding added to the front interior of the helmet proved to make the intensity of impacts worse. In each front interior padding test, the HIC and GSI increased. Adding padding to the back of the helmet did not make much of a difference. Only slight changes were observed.

### 4.3.3 Model Analysis

The following equation was found in Section 3.10 to calculate the peak acceleration of the head during an impact with PORON® padding in the front interior of the helmet:

$$a_m = \{ [K_p * x_p + D_p * (v_0 - v)] - K_n * x_n - D_n * v \} / (9.8 * M_m)$$

Using this equation, a peak acceleration for a 400 N impact was calculated for each sample of the PORON® padding. These values were compared to the corresponding measured accelerations from Table 6. These comparisons were shown in Table 7.

*Table 7: Measured vs Calculated Accelerations*

<b>PORON® Sample Density</b>	Measured Acceleration (m/s <sup>2</sup> )	Calculated Acceleration (m/s <sup>2</sup> )	% Error
9 lb/ft <sup>3</sup>	12.45	6.95	44%
12 lb/ft <sup>3</sup>	13.50	7.08	48%
15 lb/ft <sup>3</sup>	12.91	10.56	18%
20 lb/ft <sup>3</sup>	13.32	8.34	37%

Unfortunately, the calculated values varied greatly from the actual measured accelerations. This variation was expected and was most likely due to the System Model from Section 3.10 that drastically simplified the far more intricate system that this project tested. Despite the variation, the calculated accelerations from the System Model support the trend

observed in the acceleration testing (Table 6) that indicated 9 lb/ft<sup>3</sup> and 12 lb/ft<sup>3</sup> density pads were more effective at reducing acceleration.

## 5.0 Conclusion and Future Recommendations

The goal of this MQP was to reduce the likelihood of concussions for football players by designing a helmet that reduced the linear acceleration of the head.

Testing indicated that lower density PORON® samples demonstrated higher effectiveness at decreasing accelerations. The two samples with densities of 9 lb/ft<sup>3</sup> and 12 lb/ft<sup>3</sup> had lower stiffness coefficients, thus making them less resistant to deformation than the 15 lb/ft<sup>3</sup> and 20 lb/ft<sup>3</sup> density pads. Better damping effects were due to the lower density materials' ability to deform more upon impact before transferring the force to the helmet and head as demonstrated in Section 3.10. The other two samples, with densities of 15 lb/ft<sup>3</sup> and 20 lb/ft<sup>3</sup> were too stiff. The high stiffness prevented the pads from deforming as much as the lower density pads within the time of impact (15 milliseconds), thus reducing their ability to dissipate energy through damping.

While the lower density samples performed better during testing with relatively low impact forces, if they were exposed to greater forces (more typical of those experienced in football games) results might be different. The impacts generated by the air cylinder were around 200 N with a maximum of 400 N. A concussion-inducing impact in football is generally around 3000 N. Therefore, it can be assumed that the 15 lb/ft<sup>3</sup> and 20 lb/ft<sup>3</sup> density pads would be more effective at reducing accelerations during a 3000 N impact than the 9 lb/ft<sup>3</sup> and 12 lb/ft<sup>3</sup> density pads. A 3000 N impact may compress the lower density pads too quickly; therefore, the pads would reach their max displacement before the impact was over. Since the pads can only dissipate the force of the impact while they are being deformed, the lower density pads would only be effective during the first few milliseconds of a 3000 N impact and provide no dissipation for the remainder of the impact. Conversely, the higher stiffness of the higher density pads would



allow the PORON® padding to deform throughout a 3000 N impact. Because of this, the pads would dissipate the force of the hit for the full time of impact as opposed to just a portion of the time.

Another key finding was that exterior padding was far more effective at reducing accelerations than interior padding. It was predicted that the PORON® padding deformed more when the impact was applied to it directly as opposed to when the impact was applied to the helmet, which in turn transmitted the force to the interior PORON® pads. This greater deformation allowed the PORON® pads to dissipate more of the impact energy when placed on the exterior of the helmet. In addition, when testing PORON® pads in the interior of the helmet, the PORON® pads were tested as a substitute for the Schutt pads, because the original Schutt pads within the helmet were removed and replaced with the PORON®. It could be concluded that PORON® on the interior of the helmet might be slightly less effective at reducing the acceleration than the Schutt pads. One explanation may be that the Schutt Pads offered more consistent coverage of the interior of the helmet than the PORON® pads. The Schutt pads were better arranged to accommodate the head than the square pieces of PORON® pads that were not fitted for the inner sphere of a helmet. However, when testing PORON® pads on the exterior of the helmet, the PORON® pads were tested as additional protection with the original Schutt pads unaltered. Because of this, a greater reduction in acceleration was expected when testing the PORON® on the exterior of the helmet.

For future projects, this team recommends producing a means to generate a force closer to a concussion-inducing impact of 3000 N. Using a larger air cylinder or a different test method discussed in Section 2.6.1 could achieve this. A greater force would allow future projects to observe the effectiveness of concussion-reducing materials in a more accurate depiction of a

football impact by producing more realistic HIC and GSI values. In addition, a recommendation is to develop a more consistent testing procedure capable of generating highly repeatable impact forces. Finally, this team recommends that future projects attempt to evaluate the relationship between concussions and angular acceleration.

## 6.0 References

- [1] Harmon, Kimberly G., Jonathan A. Drezner, Matthew Gammons, Kevin M. Guskiewicz, Mark Halstead, Stanley A. Herring, Jeffrey S. Kutcher, Andrea Pana, Margot Putukian, and William O. Roberts. "American Medical Society for Sports Medicine position statement: concussion in sport." *Journal of Sport and Exercise Medicine* 47, no. 3 (January 2013): 15-26. Accessed October 9, 2015.  
[http://LabVIEW.amssm.org/Content/pdf%20files/2012\\_ConcussionPositionStmt.pdf](http://LabVIEW.amssm.org/Content/pdf%20files/2012_ConcussionPositionStmt.pdf).
- [2] Lindskog, Chad. "Concussions Problematic at Collegiate Level." *The Post* (Athens, OH), October 8, 2014. Accessed October 5, 2015.  
[http://LabVIEW.thepostathens.com/culture/concussions-problematic-at-collegiate-level/article\\_ce0fa5aa-4f47-11e4-a5f5-0017a43b2370.html](http://LabVIEW.thepostathens.com/culture/concussions-problematic-at-collegiate-level/article_ce0fa5aa-4f47-11e4-a5f5-0017a43b2370.html).
- [3] "Sports-related Head Injury." American Association of Neurological Surgeons. Last modified August 2014. Accessed October 15, 2015.  
<http://LabVIEW.aans.org/patient%20information/conditions%20and%20treatments/sports-related%20head%20injury.aspx>.
- [4] NNA. "Brain Injury Program: The Neuroscience Center at NNA." Neurology & Neuroscience Associates, Inc. Accessed October 3, 2015.  
[http://LabVIEW.nnadoc.com/html/brain\\_injury\\_program.html](http://LabVIEW.nnadoc.com/html/brain_injury_program.html).
- [5] McCormick, Rich. "Judge approves NFL's \$765 million concussion settlement." *The Verge* (New York, NY), April 23, 2015. Accessed October 7, 2015.  
<http://LabVIEW.theverge.com/2015/4/23/8476807/nfl-765-million-concussion-settlement-approved>.
- [6] Giza, Christopher, and David Hovda. "The Neurometabolic Cascade of Concussion." *Journal of Athletic Training*, 3rd ser., 36 (2001): 228-35. Accessed October 10, 2015.  
<http://LabVIEW.ncbi.nlm.nih.gov/pmc/articles/PMC155411/>.
- [7] *The Impact of Concussions on High School Athletes: Hearings Before the Committee on Education and Labor*, 111th Cong., 2d Sess. (2010). Accessed October 10, 2015.  
<http://LabVIEW.gpo.gov/fdsys/pkg/CHRG-111hhr56354/html/CHRG-111hhr56354.htm>.
- [8] Higgins, Matt. "Football Physics: The Anatomy of a Hit." *Popular Mechanics*. December 18, 2009. Accessed October 16, 2015.  
<http://LabVIEW.popularmechanics.com/adventure/sports/a2954/4212171/>.
- [9] Rowson, Steven, Stefan M. Duma, Jonathan G. Beckwith, Jeffrey J. Chu, Richard M. Greenwald, Joseph J. Crisco, P. Gunnar Broolinson, Ann-Christine Duhaim, Thomas LABVIEW. Mcallister, and Arthur C. Maerlender. "Rotational Head Kinematics in Football Impacts: An Injury Risk Function for Concussion." *Annals of Biomedical Engineering Ann Biomed Eng*, 2011, 1-13.
- [10] Mendelson, Will, and Katie Dzwierzynski. "Young Athletes Risk a Lasting Blow from Concussions." *Young Athletes Risk a Lasting Blow from Concussions*. May 31, 2012. Accessed September 16, 2015. <http://newsarchive.medill.northwestern.edu/chicago/news-206365.html>.
- [11] Nordrom, Amy. "Football Concussions: Head Injuries Not Confined To NFL; Youth, High School, College Players At Risk." *International Business Times*. May 4, 2015. Accessed September 20, 2015. <http://LabVIEW.ibtimes.com/football-concussions-head-injuries-not-confined-nfl-youth-high-school-college-players-1907108>.

- [12] "Focus on NFL Concussions Brings Attention to Kids, Doctor Says." NFL.com. July 26, 2012. Accessed September 18, 2015.  
<http://LabVIEW.nfl.com/news/story/09000d5d81cb6930/article/focus-on-nfl-concussions-brings-attention-to-kids-doctor-says>.
- [13] Kacsmar, Scott. "Football Outsiders." Football Outsiders Everything. August 16, 2013. Accessed September 16, 2015. <http://LabVIEW.footballoutsiders.com/stat-analysis/2013/nfls-battle-concussions-and-severe-injuries>.
- [14] "2015 NFL Rulebook." 2015 NFL Rulebook. Accessed October 16, 2015.  
<http://operations.nfl.com/the-rules/2015-nfl-rulebook>.
- [15] Pennington, Bill. "Concussions, by the New Book." The New York Times. November 29, 2014. Accessed September 23, 2015.  
[http://LabVIEW.nytimes.com/2014/11/30/sports/football/nfl-teams-now-operate-under-a-concussion-management-protocol.html?\\_r=0](http://LabVIEW.nytimes.com/2014/11/30/sports/football/nfl-teams-now-operate-under-a-concussion-management-protocol.html?_r=0).
- [16] Bradley, Bill. "NFL's 2013 Protocol for Players with Concussions." NFL's 2013 Protocol for Players with Concussions. August 22, 2014. Accessed September 17, 2015.  
<http://LabVIEW.nfl.com/news/story/0ap2000000253716/printable/nfls-2013-protocol-for-players-with-concussions>.
- [17] "GE Teams up with NFL to Accelerate Concussion Research, Diagnosis, and Treatment." GE Healthcare The Pulse. March 11, 2013. Accessed October 16, 2015.  
<http://newsroom.gehealthcare.com/ge-nfl-concussion-research/>.
- [18] "2015 NFL Health and Safety Report." NFL. 2015. Accessed September 27, 2015.  
<http://static.nfl.com/static/content/public/photo/2015/08/05/0ap3000000506671.pdf>.
- [19] Levy, Michael, Burak Ozgur, Cherisse Berry, Henry Aryan, and Michael Apuzzo. "Birth and Evolution of the Football Helmet." ResearchGate. October 6, 2000. Accessed October 16, 2015.  
[http://LabVIEW.researchgate.net/publication/8377825\\_Birth\\_and\\_Evolution\\_of\\_the\\_Football\\_Helmet](http://LabVIEW.researchgate.net/publication/8377825_Birth_and_Evolution_of_the_Football_Helmet).
- [20] Doherty, John. "John Doherty: Chemistry Commands Concussion Comeback." NWtimes. October 2, 201. \* [http://LabVIEW.nwitimes.com/sports/high-school/football/john-doherty-chemistry-commands-concussion-comeback/article\\_92a262bf-6b4d-5d29-9e59-615af03e1c48.html](http://LabVIEW.nwitimes.com/sports/high-school/football/john-doherty-chemistry-commands-concussion-comeback/article_92a262bf-6b4d-5d29-9e59-615af03e1c48.html).
- [21] "Riddell SpeedFlex Helmet - Helmets - On-Field Equipment - Shop." Shop Riddell. Accessed September 16, 2015. <http://LabVIEW.riddell.com/shop/on-field-equipment/helmets/riddell-speedflex-helmet.html#details-tab>.
- [22] "Schutt Sports: Helmets - Vengeance VTD II." Schutt Sports: Helmets - Vengeance VTD II. Accessed September 16, 2015.  
<http://LabVIEW.schuttsports.com/aspx/Sport/ProductCatalog.aspx?id=1702>.
- [23] "Varsity Football Helmet | X2E." Xenith. Accessed September 16, 2015.  
<http://shop.xenith.com/pages/x2e-varsity-football-helmet>.
- [24] "Rawlings Football Helmets | Rawlings NRG Tachyon." Rawlings Football Helmets | Rawlings NRG Tachyon. Accessed September 16, 2015.  
<http://LabVIEW.rawlingsfootball.com/products/helmets/tachyon.aspx#.Ve41cDZRGUc>.
- [25] "FAQs | NOCSAE." NOCSAE FAQs Comments. Accessed September 16, 2015.  
<http://nocsae.org/about-nocsae/faqs/#seven>.
- [26] Pellman,, Elliot, David Viano, Chris Withnall, Nick Shewchenko, Cynthia Bir, and David Halstead. "CONCUSSION IN PROFESSIONAL FOOTBALL: HELMET."

- Neurosurgery. April 8, 2005. Accessed September 16, 2015.  
[http://orzo.union.edu/~curreyj/BNG-202\\_files/Helmet\\_Testing\\_to\\_Assess\\_Impact\\_Performance\\_11.pdf](http://orzo.union.edu/~curreyj/BNG-202_files/Helmet_Testing_to_Assess_Impact_Performance_11.pdf).
- [27] King, Albert, King Yang, Liying Zhang, and Warren Hardy. "Is Head Injury Caused by Linear or Angular Acceleration?" ResearchGate. October 16, 2015. Accessed September 16, 2015.  
[http://LabVIEW.researchgate.net/publication/242211067\\_Is\\_Head\\_Injury\\_Caused\\_by\\_Linear\\_or\\_Angular\\_Acceleration](http://LabVIEW.researchgate.net/publication/242211067_Is_Head_Injury_Caused_by_Linear_or_Angular_Acceleration).
- [28] Rowson, Steven, and Gunnar Broolinson. "Linear and Angular Head Acceleration Measurements in Collegiate Football." June 1, 2009. Accessed September 16, 2015.  
[http://LabVIEW.brainsentry.com/assets/pdf/Helmet\\_Accelerations\\_Review.pdf](http://LabVIEW.brainsentry.com/assets/pdf/Helmet_Accelerations_Review.pdf).
- [29] Funk, J., S. Duma, S. Manoogian, and S. Rowson. "Biomechanical Risk Estimates for Mild Traumatic Brain Injury." Annual Proceedings / Association for the Advancement of Automotive Medicine. 2007. Accessed September 16, 2015.  
<http://LabVIEW.ncbi.nlm.nih.gov/pmc/articles/PMC3217524/>.
- [30] Funk, J., S. Duma, S. Manoogian, and S. Rowson. "Biomechanical Risk Estimates for Mild Traumatic Brain Injury." Annual Proceedings / Association for the Advancement of Automotive Medicine. 2007. Accessed September 16, 2015.  
<http://LabVIEW.ncbi.nlm.nih.gov/pmc/articles/PMC3217524/>.
- [31] "High School and Collegiate Football Athlete Concussions: A Biomechanical Review." National Center for Biotechnology Information. January 12, 2012. Accessed September 16, 2015. <http://LabVIEW.ncbi.nlm.nih.gov/pubmed/21994058>.
- [32] "Innovative Shock and Vibration Solutions | Sorbothane." Innovative Shock and Vibration Solutions | Sorbothane. Accessed September 16, 2015. <http://LabVIEW.sorbothane.com/>.
- [33] "PORON Microcellular Urethanes for Gasketing and Sealing." PORON® Microcellular Urethanes for Gasketing and Sealing. Accessed September 16, 2015.  
<http://LabVIEW.rogerscorp.com/ems/poron/industrial/index.aspx>.
- [34] "Impact Protection D3O." D3O Lab. Accessed September 16, 2015.  
<http://LabVIEW.d3o.com/>.
- [35] Pellman, Elliot J., David C. Viano, Andrew M. Tucker, and Ira R. Casson. "Concussion in Professional Football: Location and Direction of Helmet Impacts -- Part 2." *Neurosurgery* 53, no. 6 (December 2003): 1328-41.
- [36] Pellman, Elliot J., David C. Viano, Andrew M. Tucker, Ira R. Casson, and Joe F. Waeckerle. "Concussion in Professional Football: Reconstruction of Game Impacts and Injuries." *Neurosurgery* 53, no. 4 (October 2003): 779-814.  
doi:10.1227/01.NEU.0000083559.68424.3F.
- [37] Barth, Jeffrey T., Jason R. Freeman, Donna K. Broshek, and Robert N. Varney. "Acceleration-Deceleration Sport-Related Concussion: The Gravity of It All." *Journal of Athletic Training* 36, no. 3 (July/August 2001): 253-56.  
<http://LabVIEW.ncbi.nlm.nih.gov/pmc/articles/PMC155415/>.
- [38] Broglio, Steven P., Tyler Surma, and James A. Ashton-Miller. "High School and Collegiate Athlete Concussions: A Biomechanical Review." *Annals of Biomedical Engineering* 40, no. 1 (January 2012): 37-46. DOI:10.1007/s10439-011-0396-0.
- [39] Naunheim, Rosanne S., Philip V. Bayly, John Standeven, Jeremy S. Neubauer, Larry M. Lewis, and Guy M. Genin. "Linear and Angular Head Accelerations during Heading of a Soccer Ball." *Medicine & Science in Sports & Exercise* 35, no. 8 (2003): 1406-12.

- [40] Viano, David C., Ira R. Casson, and Elliot J. Pellman. "Concussion in Professional Football: Biomechanics of the Struck Player - Part 14." *Neurosurgery* 61, no. 2 (August 2007): 313-28. Digital file.
- [41] "Schutt DNA Youth Football Helmets." Real Stuff Sports. (2007). Retrieved from <http://LabVIEW.realstuffsports.com/schuttdnayouth.htm>
- [42] Barth, Jeffrey. "Child Brain Versus Adult Brain with Traumatic Brain Injury." Interview by Victoria Tilney McDonough and Brian King. Brainline.org. Last modified April 28, 2011. Accessed March 18, 2016. <http://LabVIEW.brainline.org/content/multimedia.php?id=3510>.
- [43] Broglio, S. P., Schnebel, B., Sosnoff, J. J., Shin, S., Feng, X., He, X., & Zimmerman, J. (2010). The Biomechanical Properties of Concussions in High School Football. *Medicine and Science in Sports and Exercise*, 42(11), 2064–2071. <http://doi.org/10.1249/MSS.0b013e3181dd9156>

## 7.0 Appendices

### Appendix A- Hanging String Method for Determining the Head's Center of Mass

First, attach a long piece of string to any point on the head. Then attach a second piece of string that is weighted with a nut on the end to the same point as the first string. It should span the head. Hold the first string and lift the head. Draw a straight line on the head where the weighted string falls (Figure 43). Repeat to find the intersection of the two lines. This intersection is the location of the center of mass. Repeat the entire process to determine the center of mass on the top, bottom, and sides of the head.



*Figure 43 Method to find the center of mass.*

### Appendix B – Determining the Bending Stiffness of the Neck

First, the length and diameter of the neck were measured as 0.164 m and 0.08255 m, respectively. Next, the supporting base platform for the neck was laid on its side and clamped to a table. A picture was taken to determine a baseline position for the neck (Figure 44).

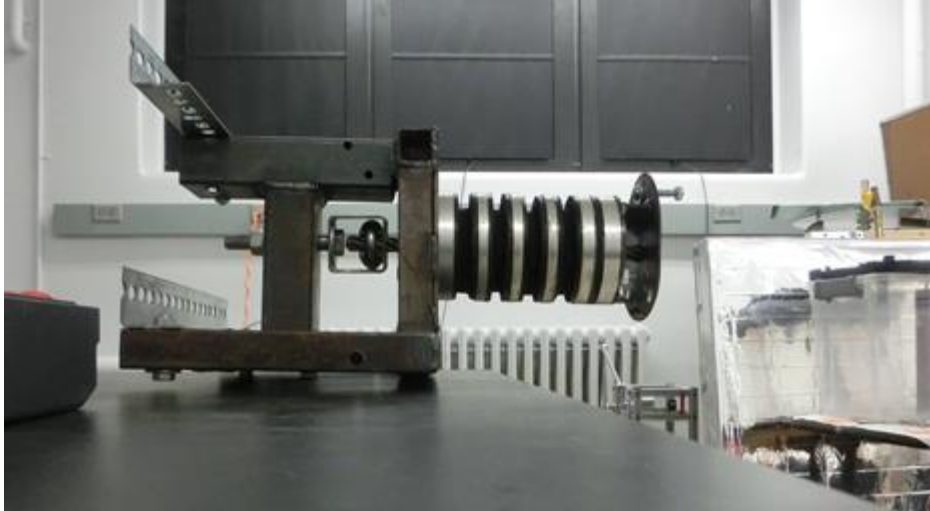


*Figure 44 Determining Baseline Position for Neck.*

A second picture was then taken after a 18.44 kg kettlebell was hung from a bolt at the far end of the neck (Figure 45).

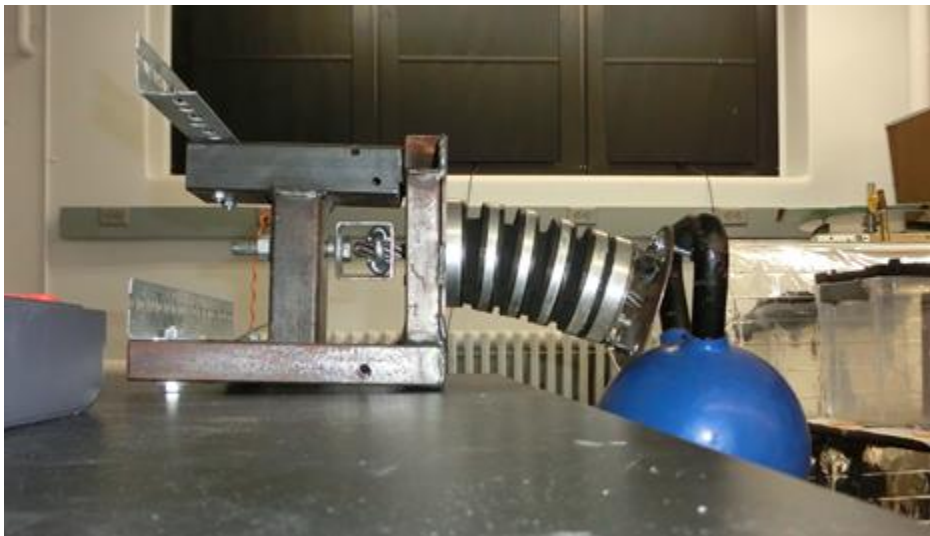


*Figure 45 Position after weight applied to neck.*

Using Adobe Photoshop, the change in angle of the neck from was determined to be  $11.4^\circ$ . The following equations were used to calculate the neck's displacement, area moment of inertia, elastic modulus, and bending stiffness.

$$\tan(11.4^\circ) = D/(0.164\text{m}) \rightarrow D(\text{displacement}) = 0.033 \text{ m}$$

$$I = \pi d^4/64 = \pi(.08255\text{m})^4/64 = 2.2795 \times 10^{-6} \text{ m}^4$$

$$F = mg = [(3EI)/L^3]D = (18.44\text{kg})(9.81\text{m/s}^2) = [3E(2.2795 \times 10^{-6} \text{ m}^4)/(0.164\text{m})^3](0.033\text{m}) \quad --$$

$$> E = 3535791.742 \text{ N/m}^2$$



$$k = (3EI)/L^3 = [3(3535791.742 \text{ N/m}^2)(2.2795 \times 10^{-6} \text{ m}^4)]/(0.164\text{m})^3 = 5481.7 \text{ N/m}$$

## Appendix C Pendulum Calculations

### Length of Pendulum

Desired impact velocity is  $9.3 \frac{m}{s}$

$$\frac{1}{2}mv^2 = mgh$$

$$ah = \frac{v^2}{2g}$$

$$h = \frac{v^2}{2g} = \frac{(9.3 \frac{m}{s})^2}{2 * 9.8 \frac{m}{s^2}} = 4.4m$$

Impact force capable of causing a concussion using the average mass and acceleration of a college football player:

$$m_{player} = 90kg$$

$$a_{player} = 34.4 \frac{m}{s^2}$$

$$F_{hit} = m_{player} * a_{player} = 90 * 34.4 = 3096N = 3.1kN$$

### Load supported by pendulum

$$F = mgh$$

$$m = \frac{F}{gh} = \frac{3096N}{9.8 \frac{m}{s^2} * 4.4m} = 71.8kg$$

The pendulum would have to be very large (4.4 meter long arm) and able to support a significant load of approximately 72 kg. We do not have lab space conducive for this type of set-up. It would also be more difficult (compared to the air cylinder) to change impact angles/locations and ensure accuracy. Therefore, the pendulum set up was not used.

## Appendix D

### Air Cylinder Calculations

#### Impact Calculations:

$$m_{player} = 90kg$$

$$a_{player} = 34.4 \frac{m}{s^2}$$

$$F_{hit} = m_{player} * a_{player}$$

$$F_{hit} = 3.096 kN$$

For these calculations, the team chose to assume the pressure within the cylinder as 80 psi (551.6 kPa). This assumption was made because this pressure corresponded to the maximum, safe pressure to use from the team’s air supply.

$$P = 551.6 kPa$$

$$A_{area} = \frac{F_{hit}}{P}$$

$$A_{area} = 5.61 * 10^{-3} m^2$$

$$D = 2 \left( \frac{A_{area}}{\pi} \right)^{0.5}$$

$$D = 0.089$$

Table 8 Variables Used in Determining Impact Force and Air Cylinder Requirements

Variables	
$m_{player}$	Average mass of an NFL Defensive Back
$a_{player}$	Acceleration of player while delivering concussion-inducing blow
P	Pressure from lab’s pressurized tanks

- Pneumatic cylinder will have a 250 mm stroke length
- Cost of 100 mm bore pneumatic cylinder with 250 mm stroke ~\$200
- Impacting cap will be fastened to end of pneumatic cylinder’s striking rod (cap, foam pad, backing plate to simulate helmet shell+liner of striking player)
- For our testing procedure, a 2000 N impact force is used. There is a wide range of impact forces that potentially cause brain damage; they can be as low as 500 N and as high as

3096 N as calculations show. 2000 N is used in order to not produce unfavorable reactions from the test rig (addressed in equations below).

- In order to simulate a 2000 N impact, a pressure of 254.8 kPa (~ 40 psi) will be used.

$$Force = Pressure * Area$$

$$Pressure = \frac{2000N}{\pi * (\frac{0.1}{2})^2} = 254777.07 Pa$$

### Impact Model

In order to determine the test rig's maximum velocity and movement in response to the impact force, the following calculations were made:

$$k_{neck} = 50N \frac{m}{rad}$$

$$r_{neck} = 0.1778m$$

$$m_{headneck} = 14kg$$

$$v_1 = 0 \frac{m}{s}$$

$$x_{contact} = 0.025m$$

$$F_{impact} = 2000N$$

$$V_{max} = \left[ \left[ (F_{impact} * x_{contact} - 0.5k_{neck} * (\frac{x_{contact}}{r_{neck}})^2) * (\frac{2}{m_{headneck}}) \right] \right]^{0.5}$$

$$V_{max} = 2.66 \frac{m}{s}$$

Conservation of Energy:

$$\frac{1}{2}mv_1^2 + \frac{1}{2}k\theta_1^2 = \frac{1}{2}mv_2^2 + \frac{1}{2}k\theta_2^2$$

Distance the Head will Rotate:

$$\theta_0 = \frac{x_{contact}}{r_{neck}}$$

$$\theta_0 = 0.141 \text{ radians}$$

Full Range of Motion:

$$\theta_{max} = \left[ \frac{(m_{headneck} * V_{max}^2 + k_{neck} * \theta_0^2 - m_{headneck} * v_1^2)}{k_{neck}} \right]^{0.5}$$

$$\theta_{max} = 1.22 \text{ radians}$$

Table 9 Variables Used in Determining Neck Motion and Rotation

Variables	
$m_{headneck}$	Mass of the head, neck, and helmet
$k_{neck}$	Stiffness of the neck rig
$r_{neck}$	Length of the neck rig
$v_1$	Initial Velocity
$x_{contact}$	Distance for which the pneumatic cylinder's impacting cap allies the force to the test rig
$F_{impact}$	Force applied by the pneumatic cylinder's impacting cap
$\theta_0$	Angle test rig rotates while making contact with impacting cap (8°)
$\theta_{max}$	Max angle test rig rotates after being struck by impacting cap (70°)

## Appendix E Force Sensor Calibration and LabVIEW

### Force Sensor Calibration

The team created a LabVIEW VI which could record data from the force sensor. The test was performed by a number of steps:

1. The force sensor was laid on a flat surface.
2. The user entered 0 into the LabVIEW input for the weight experienced by the sensor.
3. The user placed a ten pound weight on the force sensor.
4. The user entered the total weight on the force sensor into the LabVIEW input.
5. Steps 3-4 were repeated until a total weight of 100 lbs rested on the force sensor.
6. The excel file which the LabVIEW was writing to was opened.
7. The user made a chart that graphed user input weight vs voltage given by the force sensor.
8. The user made a trendline and obtained an equation from it.

Upon completion of these steps, the team could use the equation obtained from step 8 to determine any force experienced by the sensor.

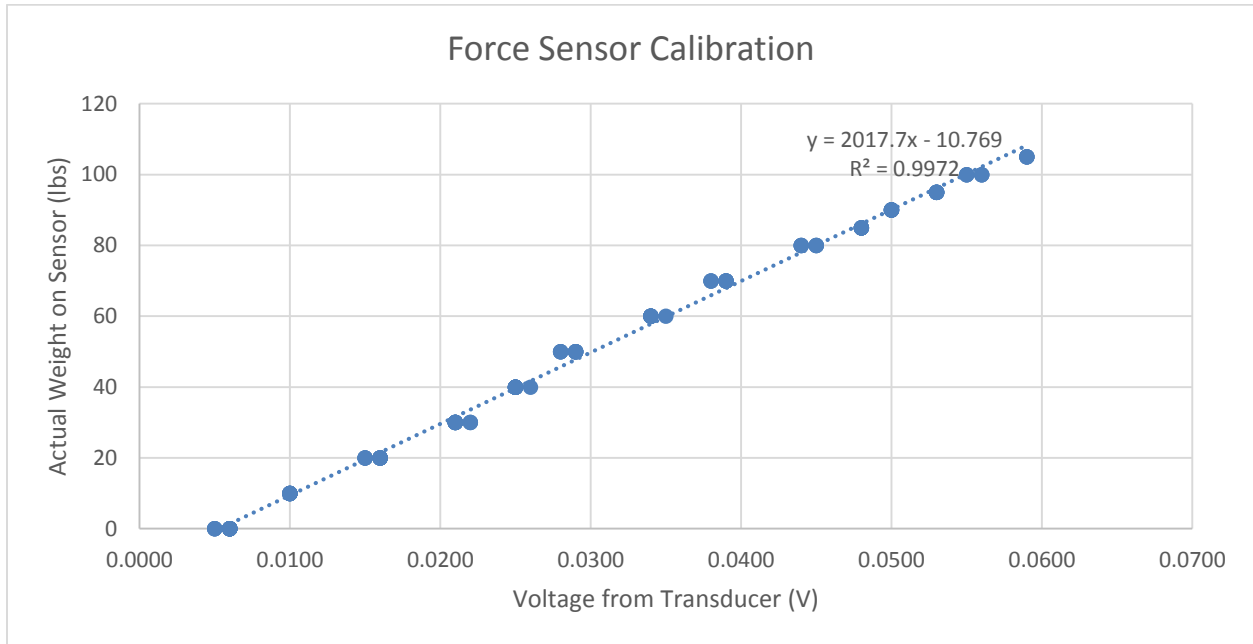


Figure 46 Force Sensor Calibration Graph.

The team determined the calibration values to be 2017.7 for a slope, and -10.769 for the intercept (Figure 46).

**LabVIEW for Force Sensor**

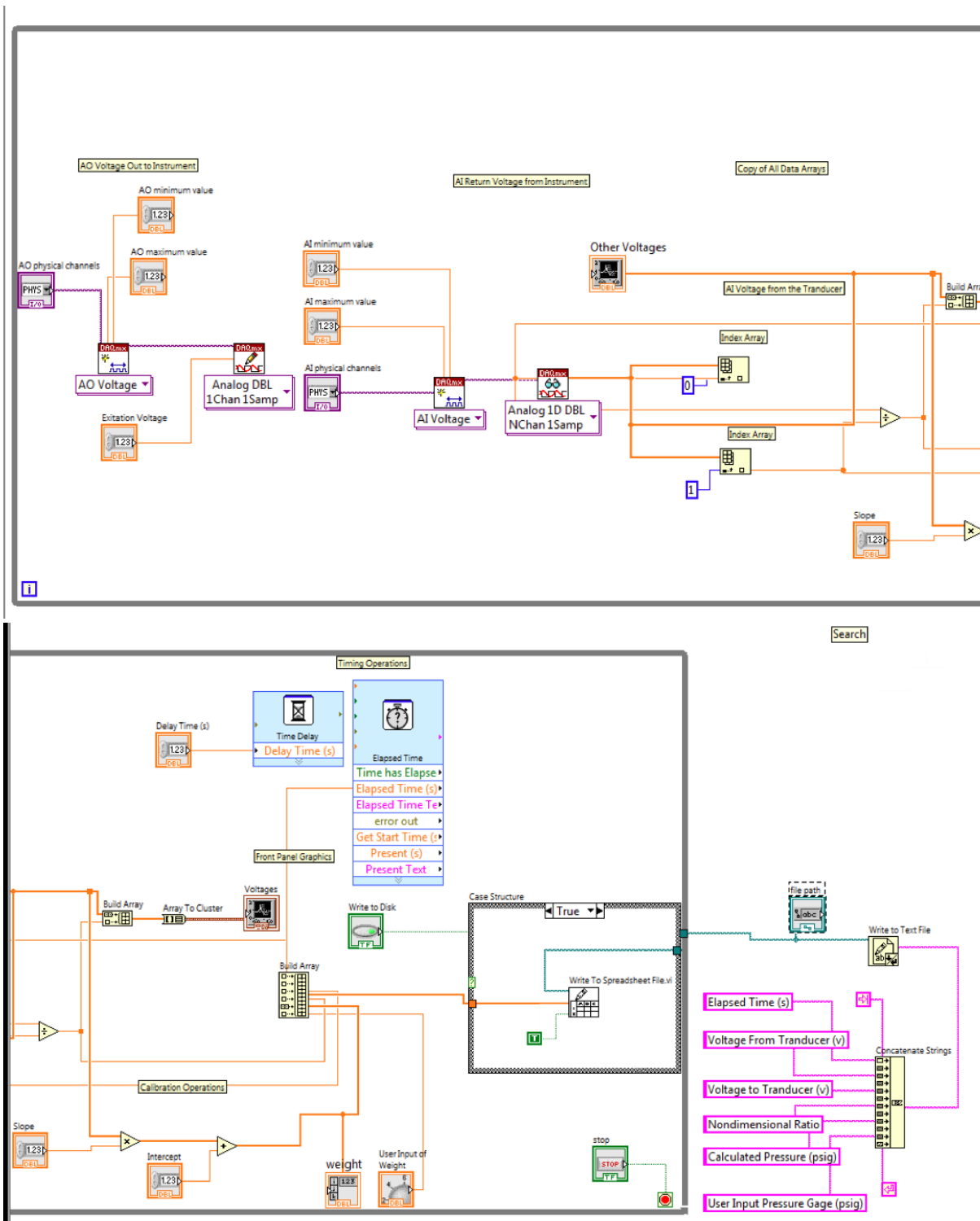


Figure 47 Force Sensor LabVIEW Program Block Diagram.

### Appendix F LabVIEW for Acceleration Testing

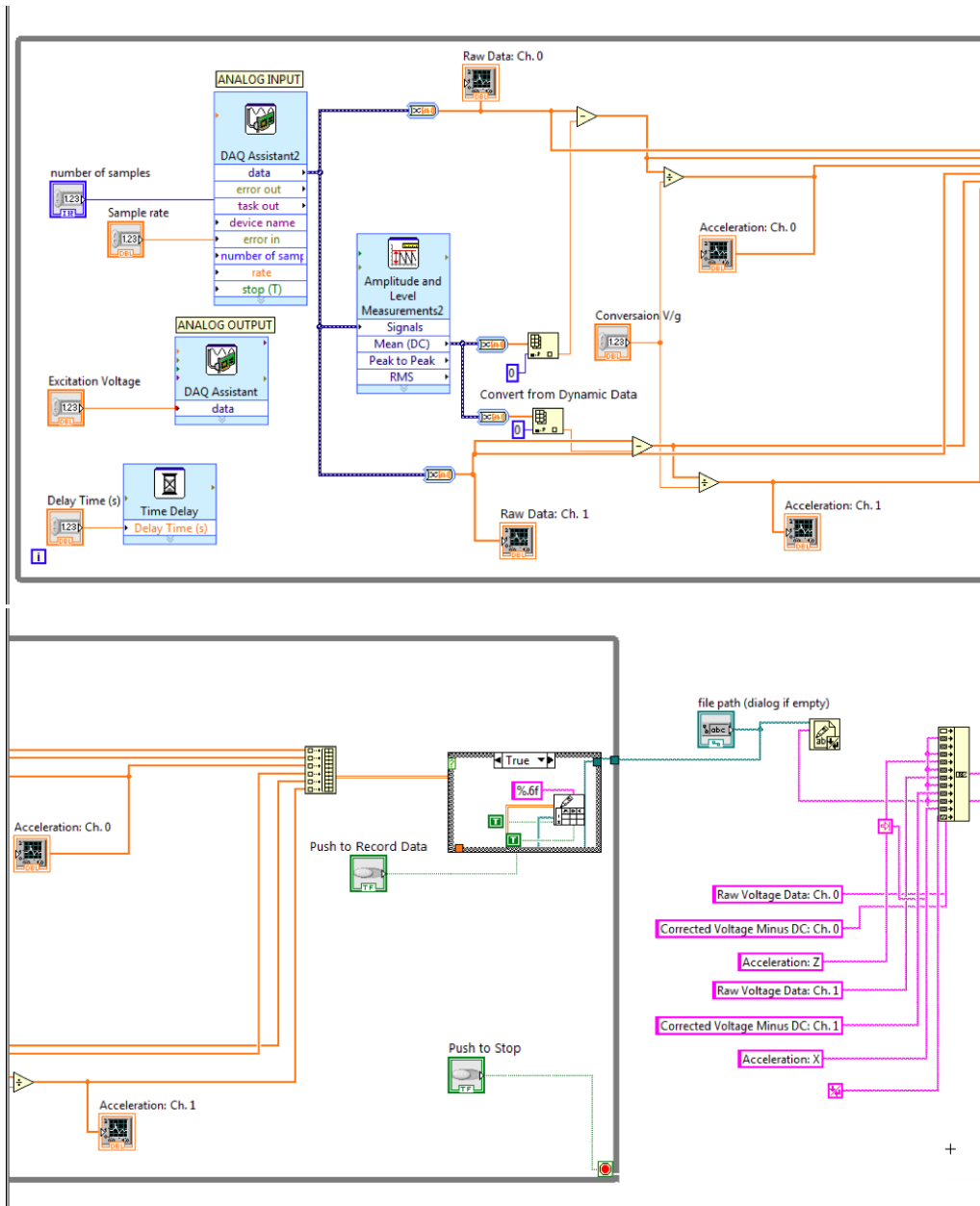


Figure 48 LabVIEW Accelerometer Program Block Diagram.

### Appendix G- System Model

As illustrated in Figure 40, this system’s state variables were  $p_h'$ ,  $p_m'$ ,  $x_p'$ , and  $x_n'$ . Each of these state variables were functions of the source of effort (in this case, F) and the derivative of each state variable.

$$\dot{x}_p = f(p_h, p_m, x_p, x_n, F)$$

$$\dot{x}_n = f(p_h, p_m, x_p, x_n, F)$$

$$\dot{p}_{\text{LabVIEW}} = f(p_h, p_m, x_p, x_n, F)$$

$$\dot{p}_m = f(p_h, p_m, x_p, x_n, F)$$

Using Figure 40, the derivative equation for each state variable was obtained.

$$\dot{x}_p = (p_h/M_h) - (p_m/M_m) = v_0 - v$$

$$\dot{x}_n = p_m / M_M = v$$

$$\dot{p}_{\text{LabVIEW}} = F - [K_p * x_p + D_p * ( (p_h/M_h) - (p_m/M_m) ) ]$$

$$\dot{p}_m = [K_p * x_p + D_p * ( (p_h/M_h) - (p_m/M_m) ) ] - K_n * x_n - D_n * (p_m/M_M)$$

X refers to displacement and p refers to momentum.

Since momentum is equal to mass multiplied by velocity, the integral of momentum ( $\dot{p}$ ) was written as  $M * \dot{x}$  or  $M * a$  (mass times acceleration). Thus, these state equations were re-written to obtain two equations of motion, one at the helmet and the other at the model head:

$$M_h * a_h = F - [K_p * x_p + D_p * (v_0 - v) ]$$

$$M_m * a_m = [K_p * x_p + D_p * (v_0 - v) ] - K_n * x_n - D_n * v$$

$$a_m = \{ [K_p * x_p + D_p * (v_0 - v) ] - K_n * x_n - D_n * v \} / (9.8 * M_m)$$

X is displacement. The excel sheet calculated values for the stiffness coefficients which varied depending on the applied force. As an example, the data from the excel sheet for the 9 lb/ft<sup>3</sup> density pad is shown in **Error! Reference source not found.**

These stiffness values were average to obtain a single stiffness coefficient for the pad.



The following equations were used to calculate damping for each PORON® sample:

### Appendix H – Preliminary Force Plate Test Results

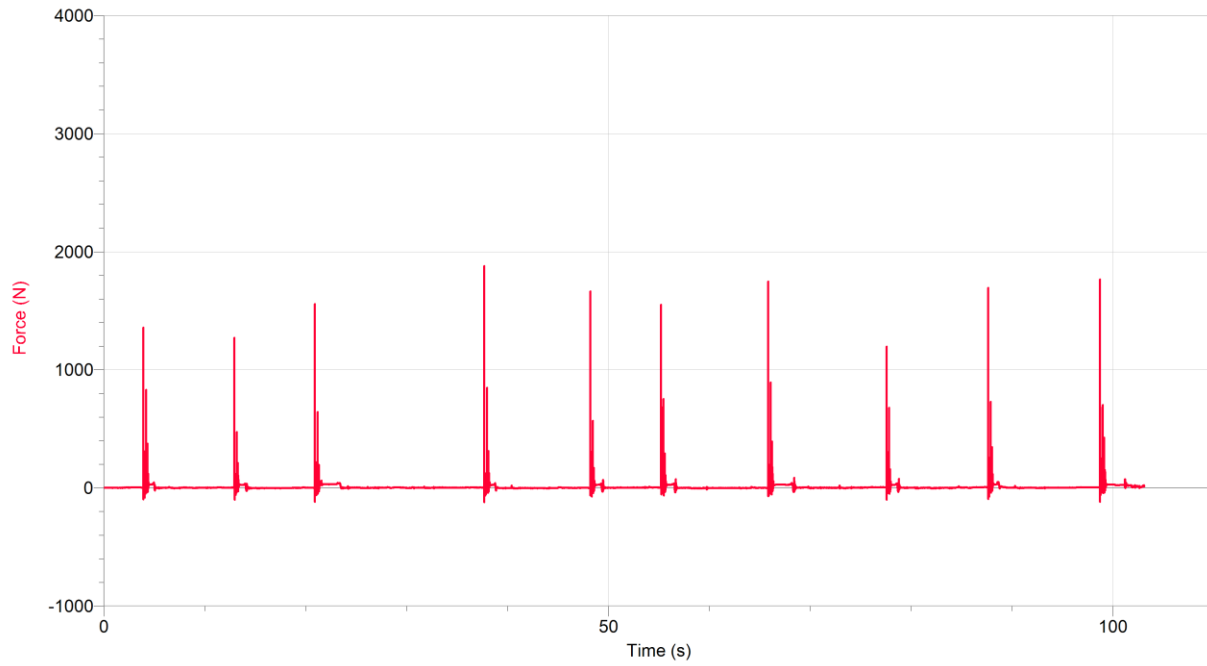


Figure 49 Sorbothane© Sample 2 1569 N average (17% improvement).

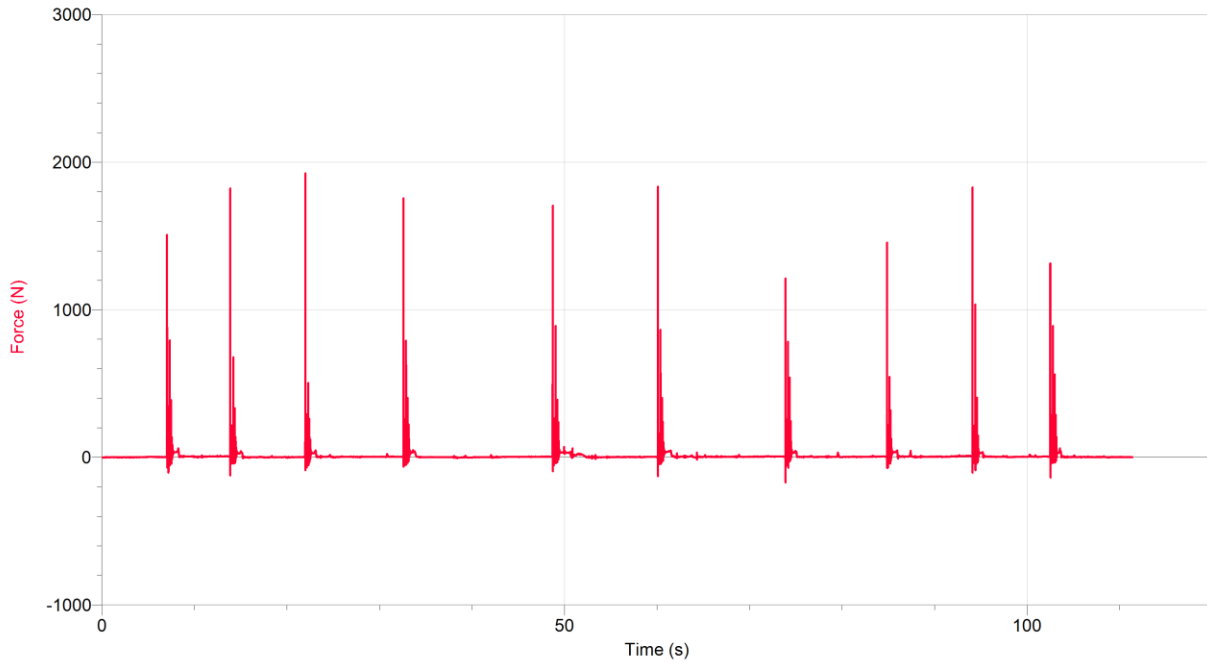


Figure 50 Sample 1 Sorbothane© 1637 N average (13% improvement).

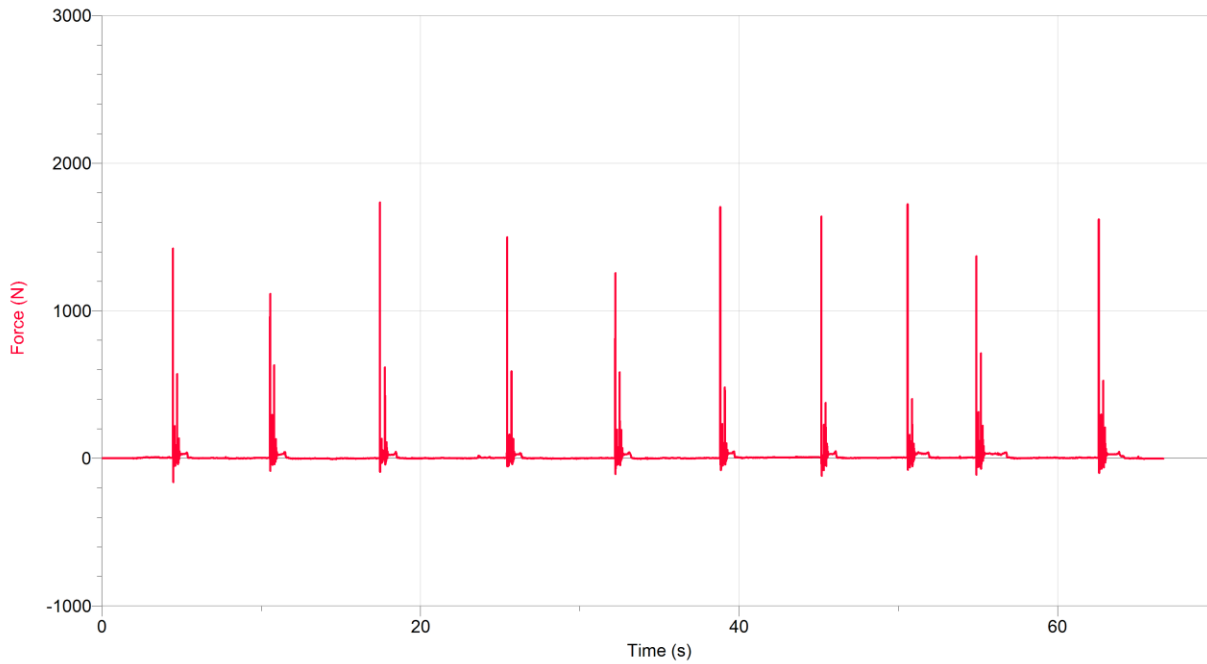


Figure 51 PORON© Sample A 1508 N average (20%).

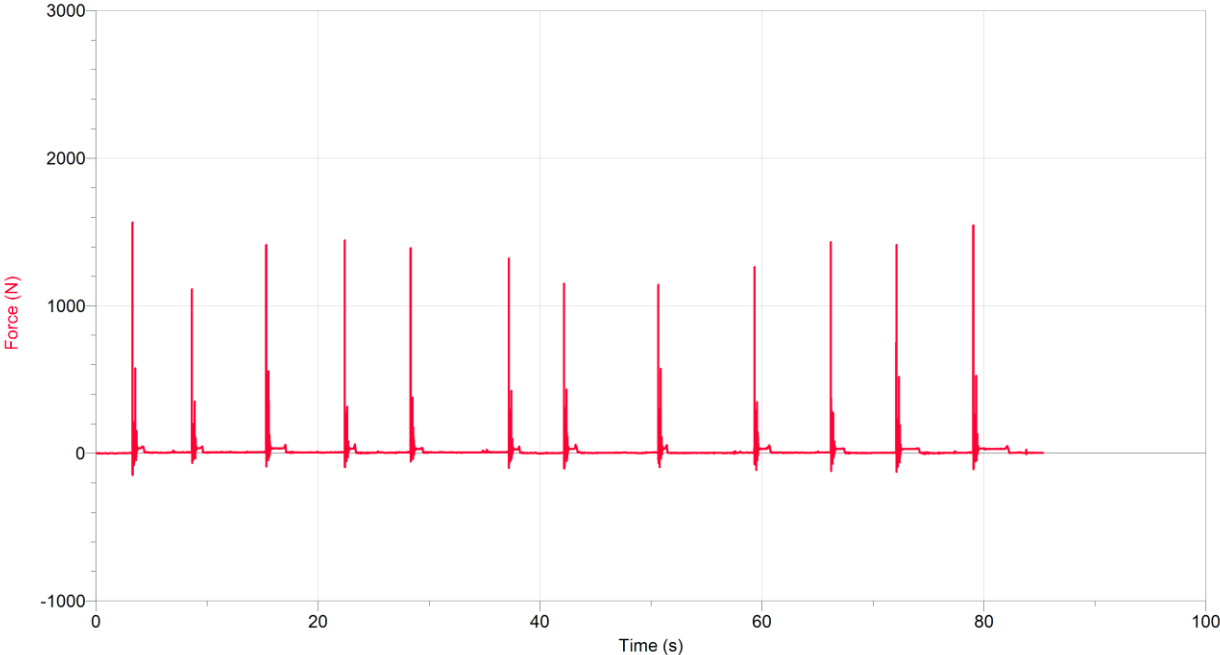


Figure 52 PORON© Sample B 1350 N average (29% improvement).

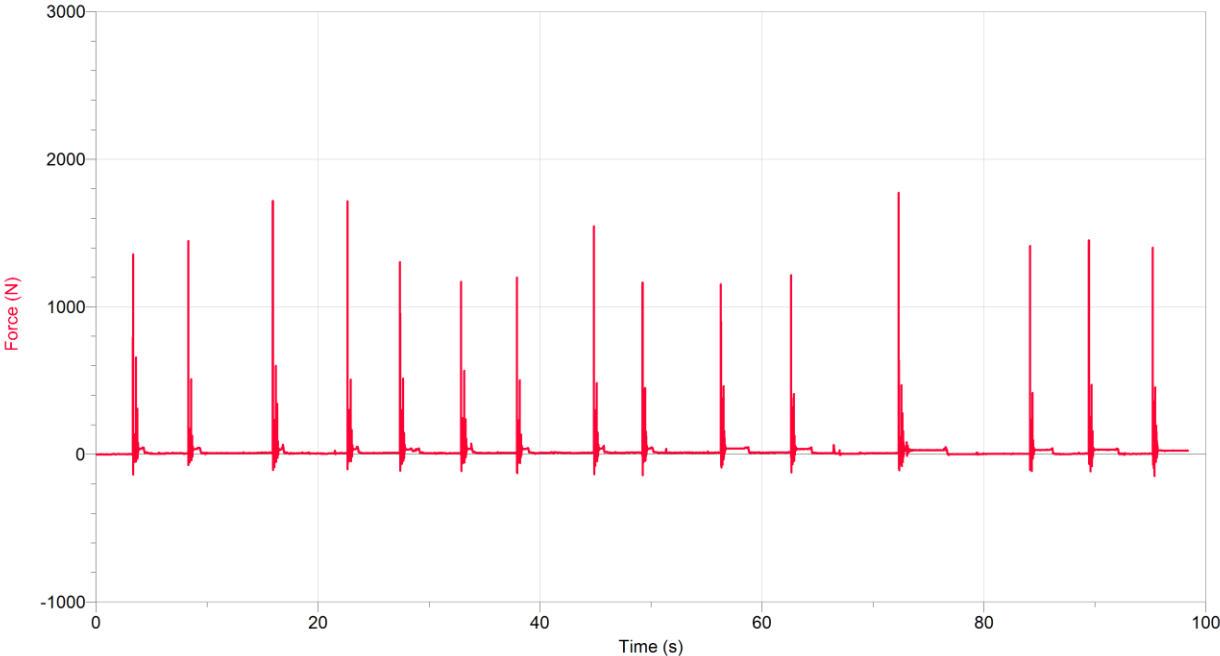


Figure 53 PORON© Sample C 1402 N average (26% improvement).

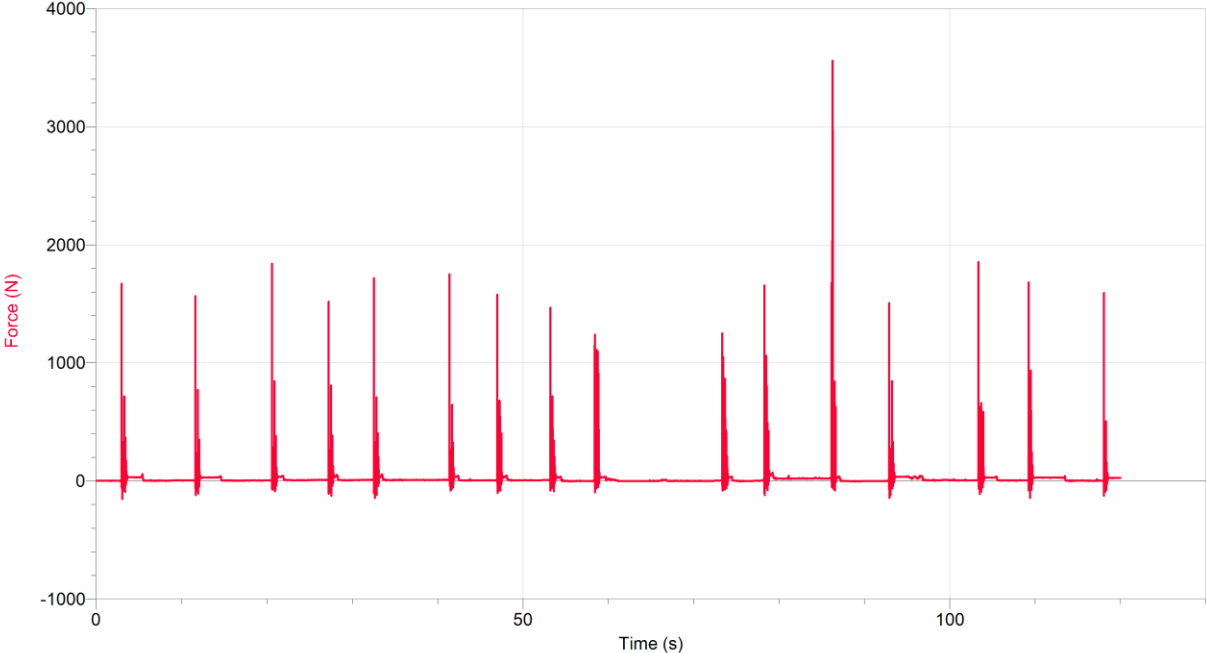


Figure 54 PORON© Sample D 1594 N average (16% improvement).

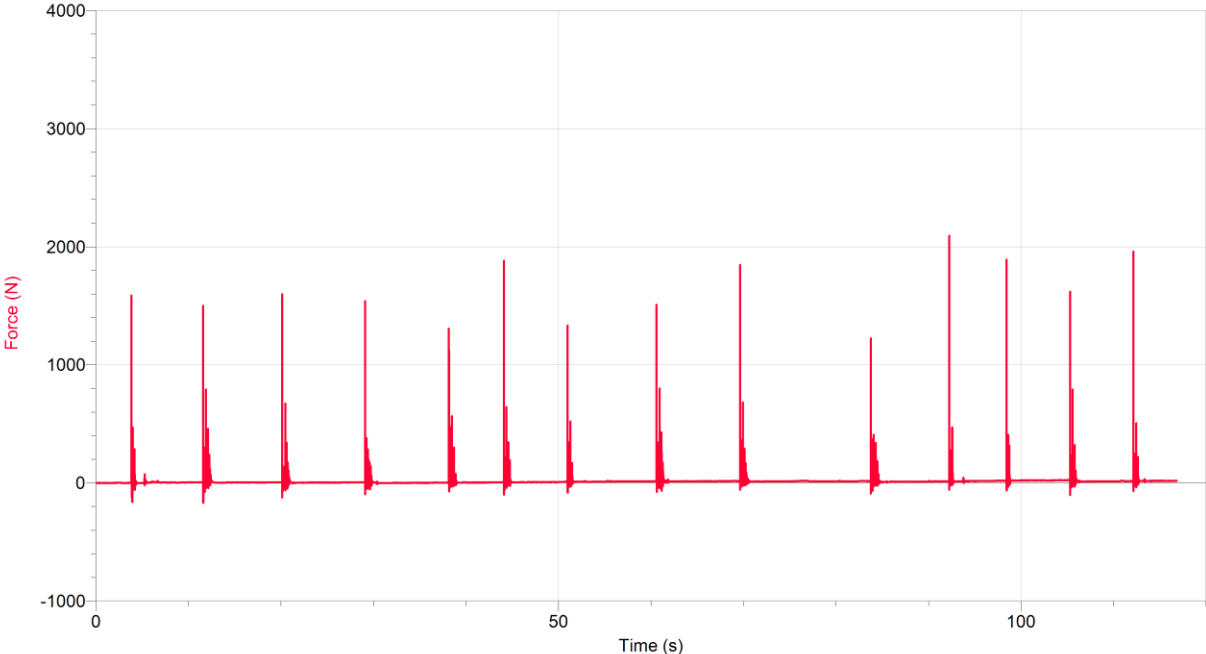
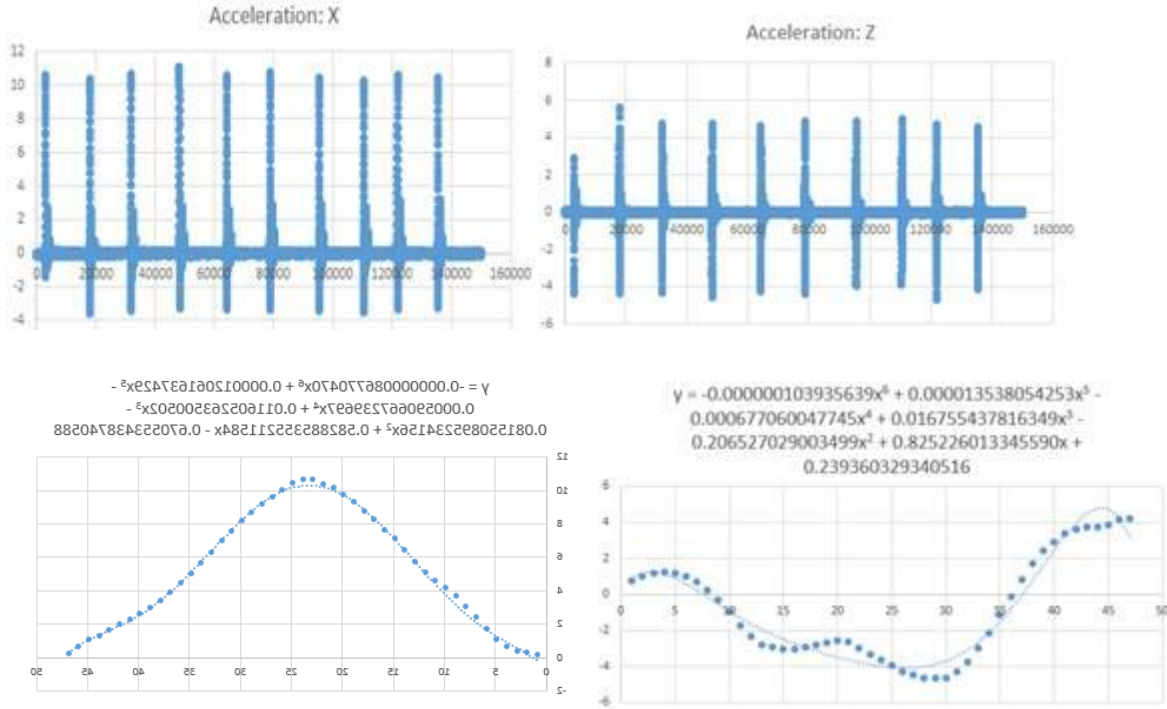


Figure 55 Neoprene 1664 N average (12% improvement).

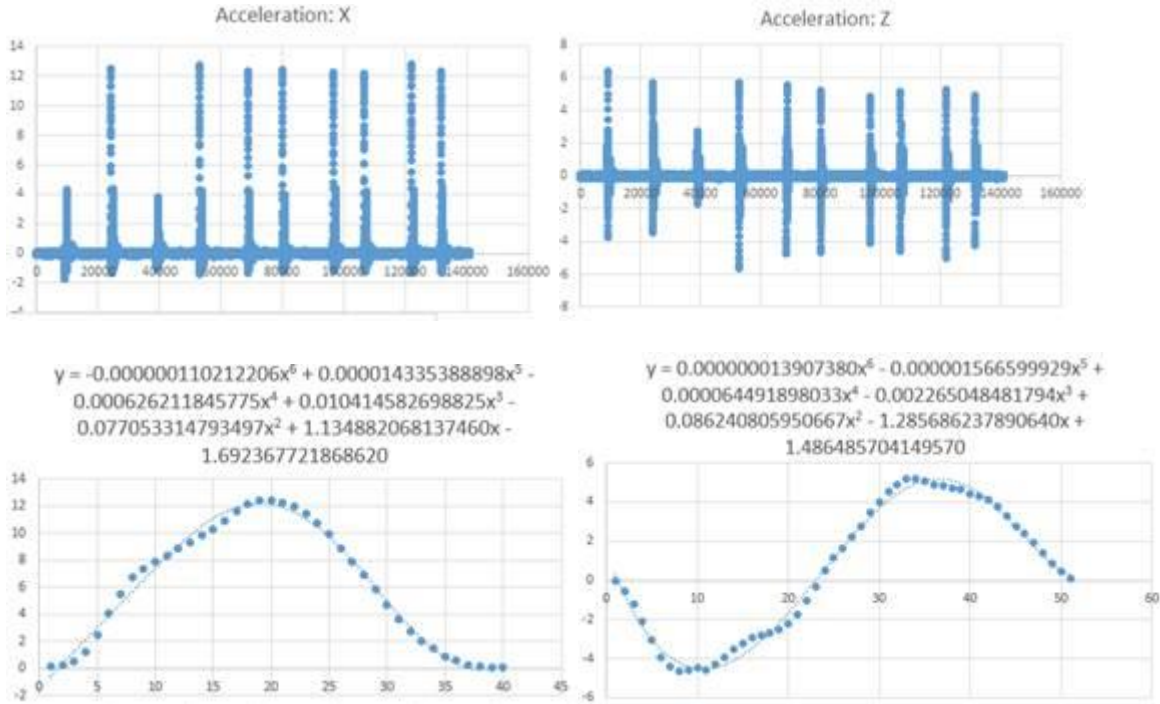
## Appendix I – Impacts to Front of Helmet

### Control



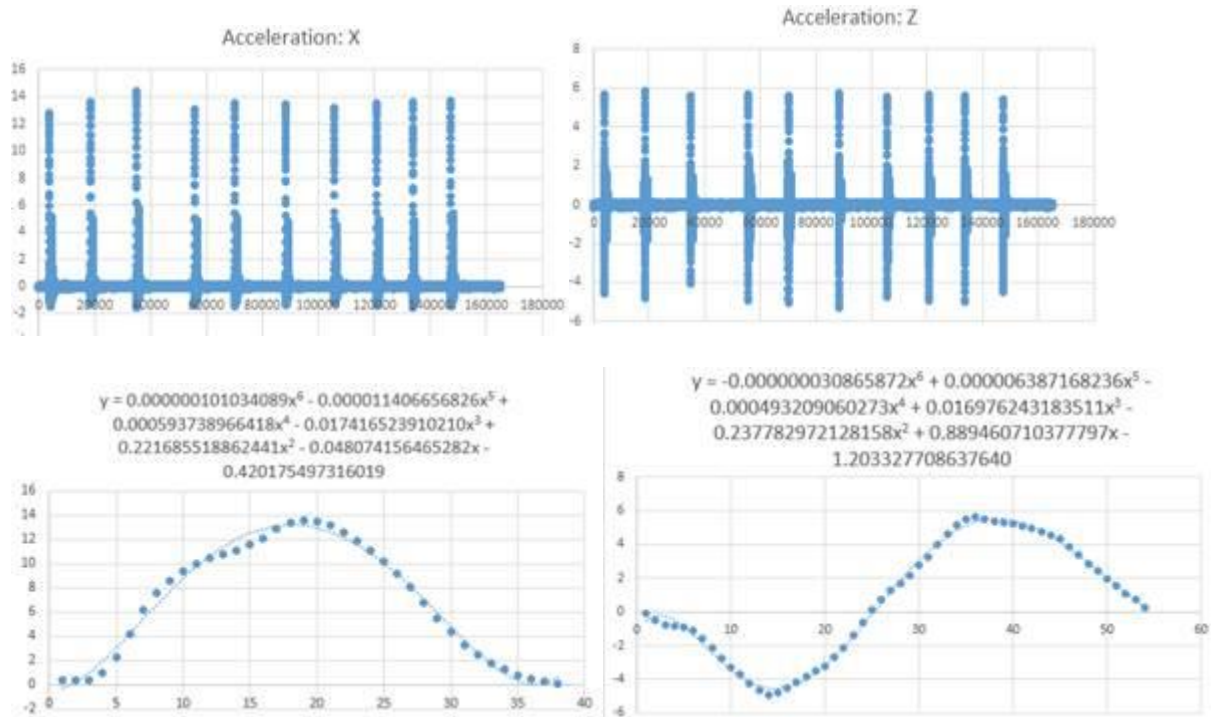
Hit #	Z Max	Z Min	X Max	X Min	Collision Time (ms)
1					
2	5.61918	-4.4058	10.38516	-3.57862	15
3	4.757682	-4.3201	10.68017	-3.38657	14.67
4	4.800965	-4.55627	11.06745	-3.22873	15.67
5	4.63141	-4.22869	10.55753	-3.29153	16
6	4.914036	-4.41084	10.78938	-3.33325	14.67
7	4.904186	-3.97357	10.46073	-3.39715	15
8	5.00707	-3.91187	10.23609	-3.50119	15.67
9	4.729347	-4.66907	10.61438	-3.30233	15
10	4.611253	-4.14589	10.45479	-3.20601	15
<b>Average</b>	4.886125	-4.29134	10.58285	-3.35837	15.19
<b>Std Dev</b>	0.304521	0.252768	0.244752	0.122201	0.4746051

Interior Front and Top Padding: 9 lbs/ft<sup>3</sup>



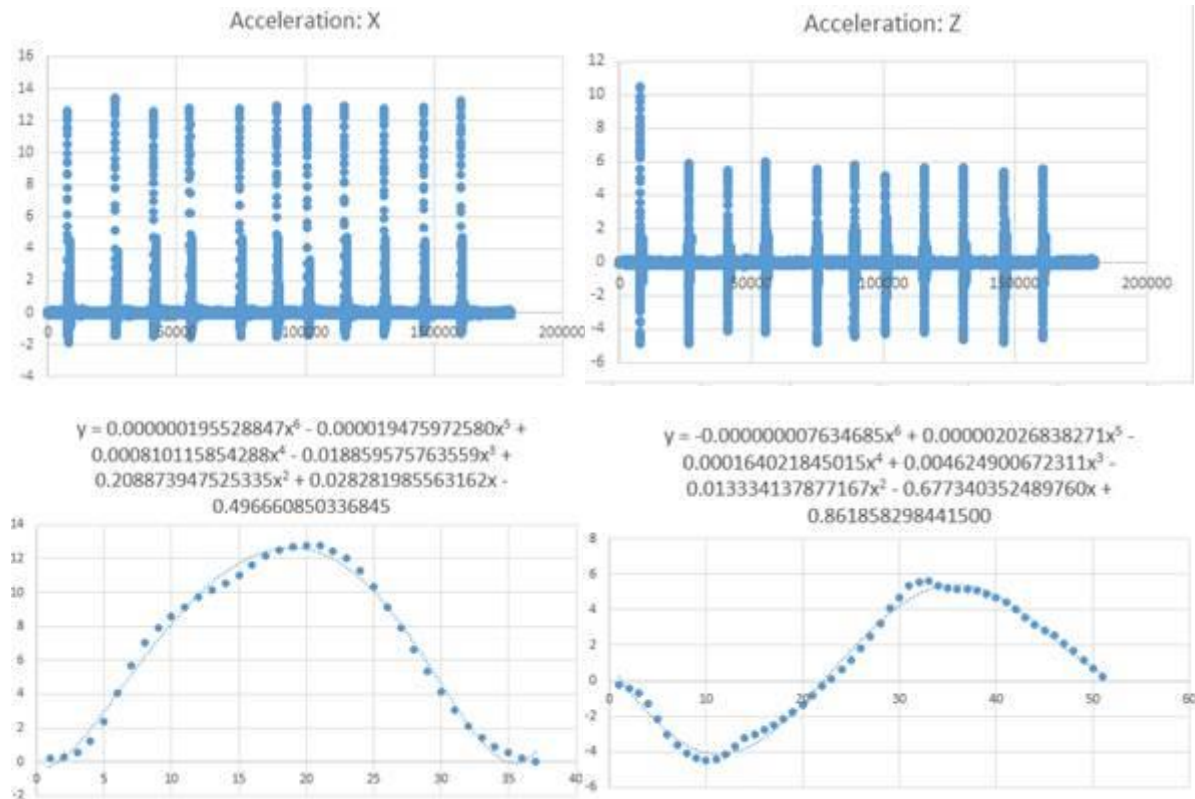
Hit #	Z Max	Z Min	X Max	X Min	Collision Time (ms)
2	5.676453	-3.46016	12.5293	-1.31388	11.67
3	5.692169	-5.64476	12.78749	-1.39398	11.33
4	5.565707	-4.75049	12.34459	-1.32209	11.33
5	5.194936	-4.63001	12.42574	-1.21153	11.67
6	4.851154	-4.07955	12.2582	-1.16727	12.33
7	5.172144	-4.57338	12.16211	-1.23394	12.33
8	5.310534	-5.03214	12.81284	-1.33038	11.33
9	4.934552	-4.21971	12.31806	-1.31039	12
<b>Average</b>	5.299706	-4.54877	12.45479	-1.28543	11.75
<b>Std Dev</b>	0.322629	0.654245	0.239173	0.07431	0.42716466

Interior Front and Top Padding: 12 lbs/ft<sup>3</sup>



Hit #	Z Max	Z Min	X Max	X Min	Collision Time (ms)
1	5.697712	-4.58613	12.83942	-1.50383	12
2	5.864128	-4.80212	13.6556	-1.29656	11.67
3	5.624411	-4.04169	14.40158	-1.59779	12
4	5.670502	-4.91044	13.05513	-1.35283	12.67
5	5.591097	-5.04573	13.56841	-1.4367	12
6	5.726811	-5.27772	13.45298	-1.34916	11.33
7	5.571286	-4.77433	13.18888	-1.22497	11.33
8	5.65486	-4.92314	13.5356	-1.41068	11.67
9	5.638767	-4.97453	13.61074	-1.55027	11.67
10	5.454341	-4.46768	13.6803	-1.4513	12
<b>Average</b>	5.649392	-4.78035	13.49886	-1.41741	11.83
<b>Std Dev</b>	0.107081	0.345516	0.424403	0.115321	0.3941009

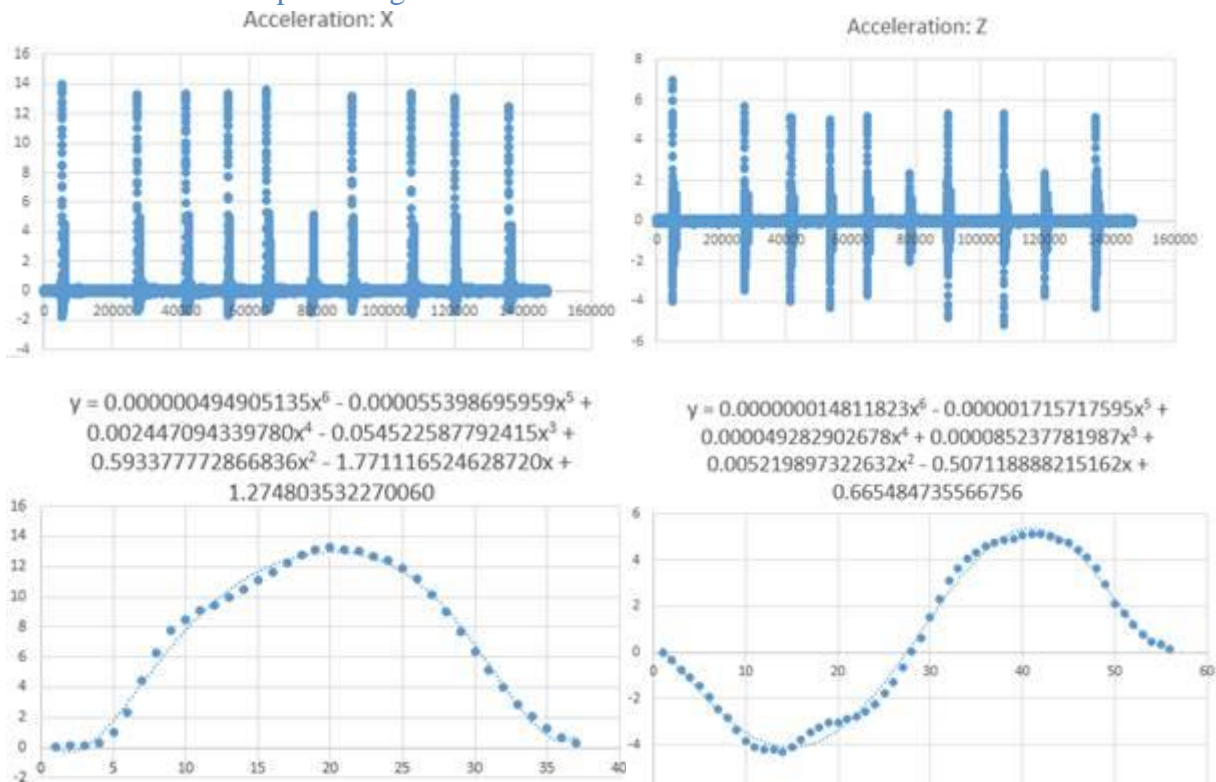
Interior Front and Top Padding: 15 lbs/ft<sup>3</sup>



Hit #	Z Max	Z Min	X Max	X Min	Collision Time (ms)
2	5.868661	-4.827	13.45324	-1.42244	12
3	5.476282	-4.06333	12.61143	-1.49943	11.33
4	6.011727	-4.18092	12.7954	-1.53608	11
5	5.543431	-4.72864	12.74187	-1.48077	11.67
6	5.837194	-4.43782	12.90342	-1.52808	11.33
7	5.156089	-4.28351	12.7801	-1.42195	12
8	5.640916	-4.21345	12.8999	-1.47865	11
9	5.646215	-4.61703	12.75983	-1.36869	11.67
10	5.385087	-4.78403	12.84783	-1.27774	12
11	5.607377	-4.50291	13.26252	-1.29841	11.67
<b>Average</b>	5.617298	-4.46386	12.90555	-1.43122	11.57
<b>Std Dev</b>	0.249573	0.272001	0.256724	0.09129	0.3673704

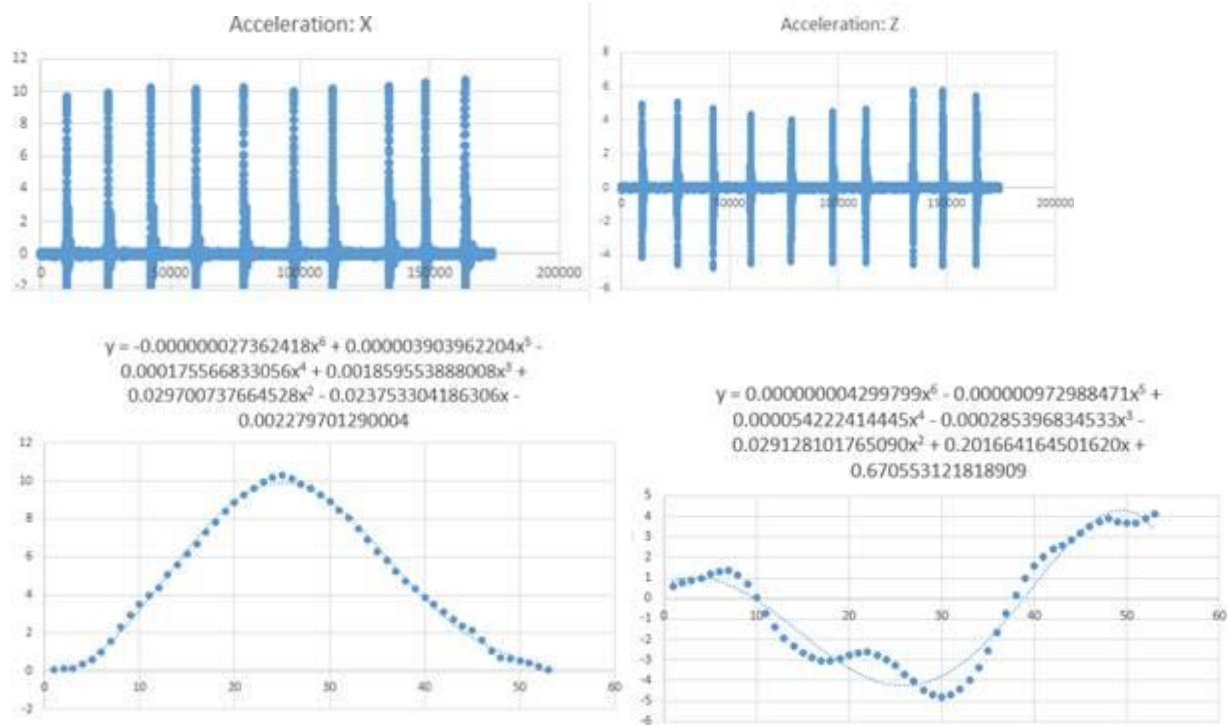


Interior Front and Top Padding: 20 lbs/ft<sup>3</sup>



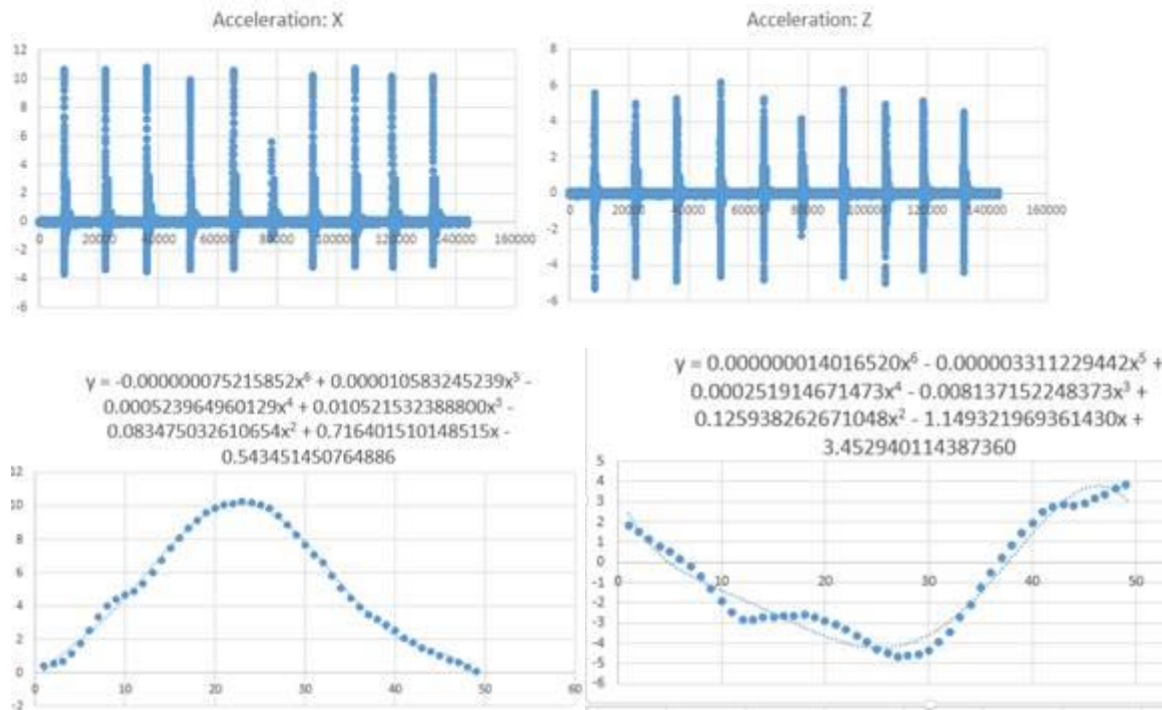
Hit #	Z Max	Z Min	X Max	X Min	Collision Time (ms)
1	6.987102	-4.02331	14.02067	-1.74926	11.33
2	5.712316	-3.45666	13.25865	-1.41995	12
3	5.169177	-3.98803	13.35871	-1.40813	11.67
4	4.998785	-4.29373	13.32223	-1.61523	11.33
5	5.17279	-3.6932	13.5884	-1.28434	11.67
7	5.348325	-4.82079	13.13836	-1.3755	11.33
8	5.326974	-5.19219	13.40485	-1.52083	11.33
10	5.142309	-4.32376	12.5001	-1.24895	11.67
<b>Average</b>	5.482222	-4.22396	13.324	-1.45277	11.54
<b>Std Dev</b>	0.643943	0.570075	0.42771	0.168134	0.25033906

Interior Back Padding: 9 lbs/ft<sup>3</sup>



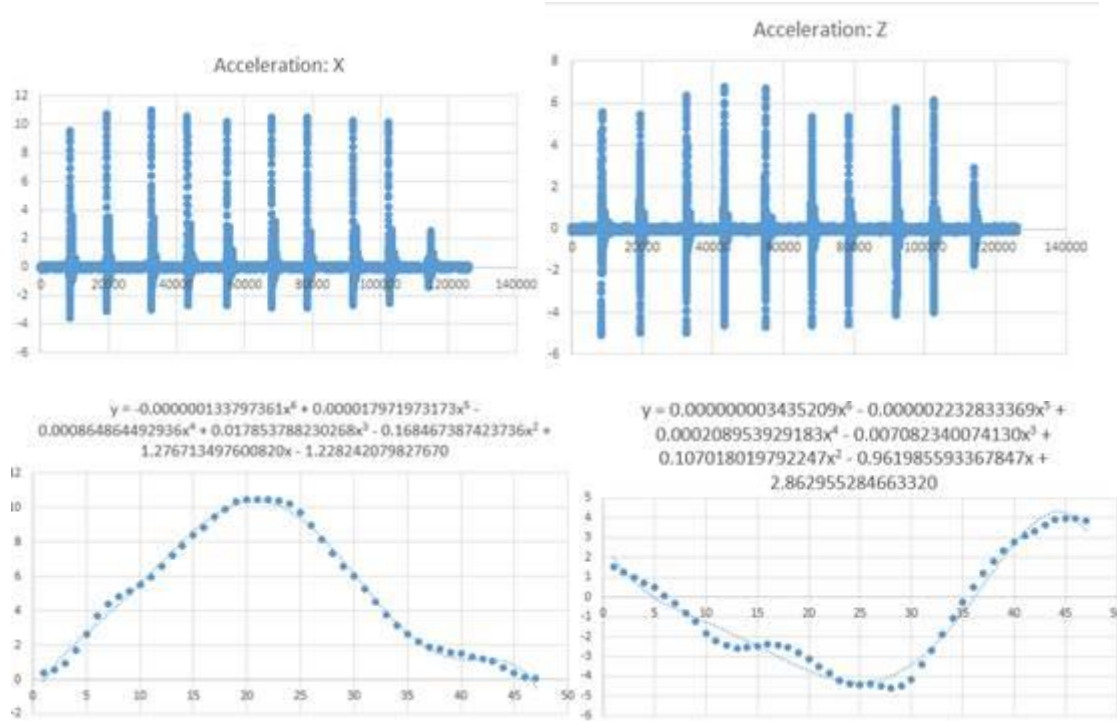
Hit #	Z Max (g)	Z Min (g)	X Max (g)	X Min (g)	Collision Time (ms)
1	4.942426	-4.17654	9.72989	-3.91914	16.0
2	5.083207	-4.58584	9.912551	-3.73942	16.3
3	4.741273	-4.78951	10.26283	-3.61565	16.3
4	4.33132	-4.51408	10.18102	-3.37976	16.0
5	4.055138	-4.39608	10.2831	-3.36299	16.0
6	4.512875	-4.44136	10.02301	-3.18773	18.67
7	4.679958	-4.44195	10.16092	-3.02628	17
8	5.767921	-4.57475	10.35077	-3.10117	16.33
9	5.749621	-4.61658	10.60648	-3.16316	16.33
10	5.437692	-4.56964	10.7511	-3.03325	16.33
<b>Average</b>	4.930143	-4.51063	10.22617	-3.35285	16.53
<b>Std Dev</b>	0.582256	0.16211	0.304141	0.311876	0.80556981

Interior Back Padding: 12 lbs/ft<sup>3</sup>



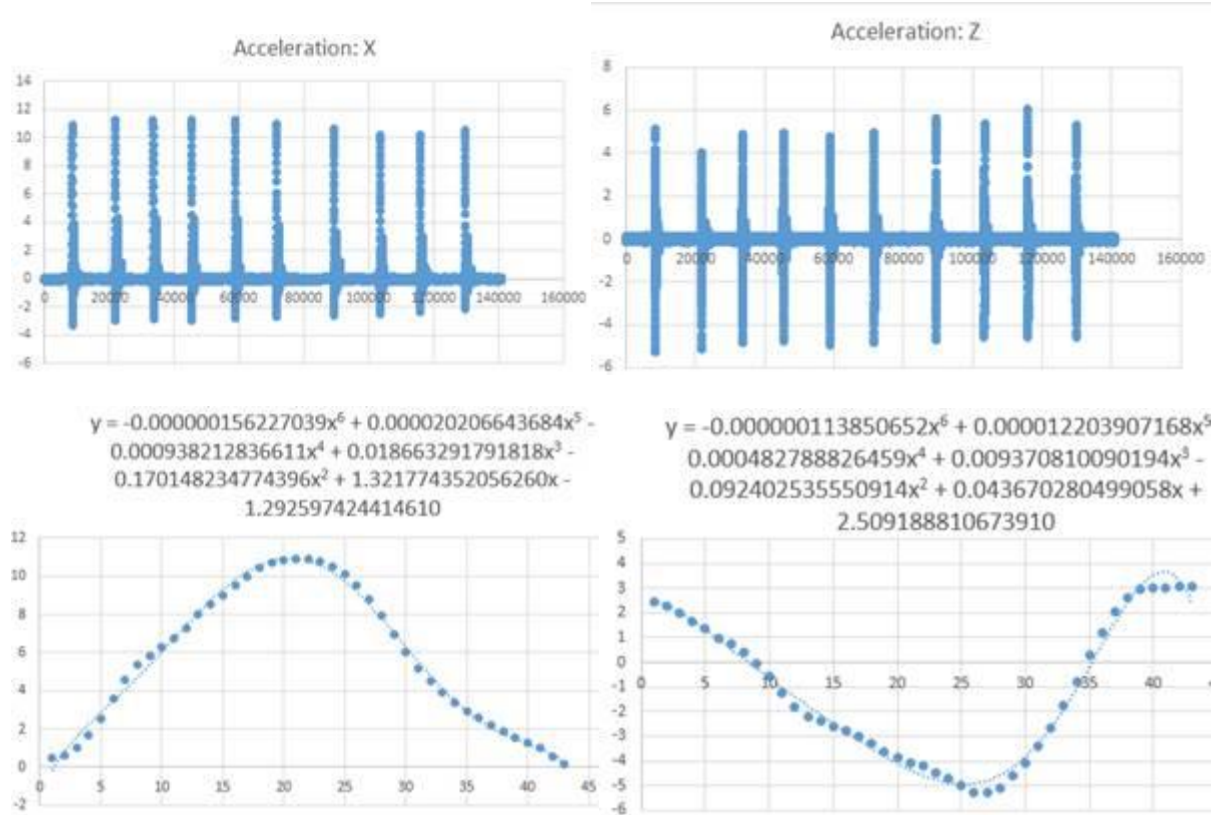
Hit #	Z Max (g)	Z Min (g)	X Max (g)	X Min (g)	Collision Time (ms)
1	5.593651	-5.29616	10.67462	-3.65098	15.33
2	5.036066	-4.6065	10.65784	-3.3383	15.00
3	5.266049	-4.8913	10.85507	-3.44994	14.67
4	6.178963	-4.65201	9.930888	-3.35633	14.33
5	5.242406	-4.78845	10.56938	-3.26203	16.00
6	5.735656	-4.65408	10.25492	-3.14996	16.00
7	4.92956	-5.01599	10.7182	-3.10733	16.00
8	5.161315	-4.23122	10.19881	-3.16195	15.67
9	4.514263	-4.37231	10.21659	-2.99414	17.00
10					
<b>Average</b>	5.295325	-4.72311	10.45292	-3.27455	15.56
<b>Std Dev</b>	0.486875	0.323101	0.31003	0.199425	0.81655404

Interior Back Padding: 15 lbs/ft<sup>3</sup>



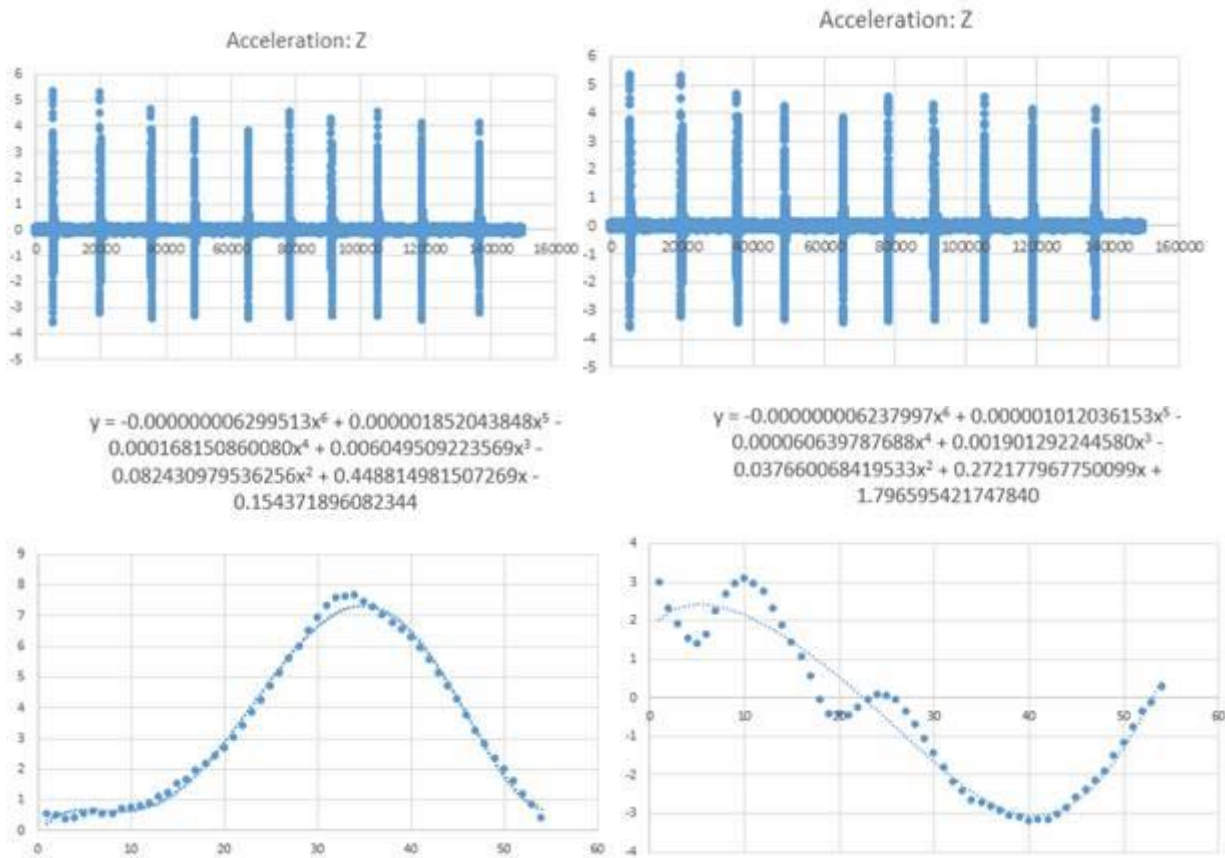
Hit #	Z Max (g)	Z Min (g)	X Max (g)	X Min (g)	Collision Time (ms)
1	5.575524	-5.05248	9.532698	-3.55743	15.67
2	5.487417	-4.96998	10.72332	-3.09632	14.67
3	6.384324	-4.95849	11.01114	-2.98794	15.33
4	6.785998	-4.60388	10.57113	-2.6749	15.67
5	6.701247	-4.69158	10.15748	-2.66202	15.33
6	5.332219	-4.61039	10.47333	-2.8433	15.00
7	5.373316	-4.57224	10.50469	-2.83253	16.67
8	5.743673	-4.11363	10.25251	-2.64348	13.67
9	6.173541	-4.01322	10.17027	-2.54333	14.67
10					
<b>Average</b>	5.950807	-4.62065	10.3774	-2.87125	15.19
<b>Std Dev</b>	0.571497	0.363393	0.41902	0.312077	0.834908

Interior Back Padding: 20 lbs/ft<sup>3</sup>



Hit #	Z Max	Z Min	X Max	X Min	Collision Time (ms)
1	5.163948	-5.24638	10.93153	-3.29994	14.00
2	4.043808	-5.15164	11.28903	-2.95714	16.67
3	4.917574	-4.86325	11.27348	-2.88445	14.33
4	4.944164	-4.79254	11.29335	-2.97931	14.00
5	4.758333	-4.95483	11.28045	-2.80688	14.33
6	4.95727	-4.83826	10.99438	-2.64288	14.00
7	5.654475	-4.73232	10.64454	-2.55442	14.67
8	5.371593	-4.56808	10.23212	-2.48148	14.00
9	6.093363	-4.56994	10.21078	-2.36457	14.00
10	5.302628	-4.57821	10.532	-2.1316	14.33
<b>Average</b>	5.120716	-4.82954	10.86817	-2.71027	14.43
<b>Std Dev</b>	0.549651	0.236679	0.436123	0.342581	0.81850881

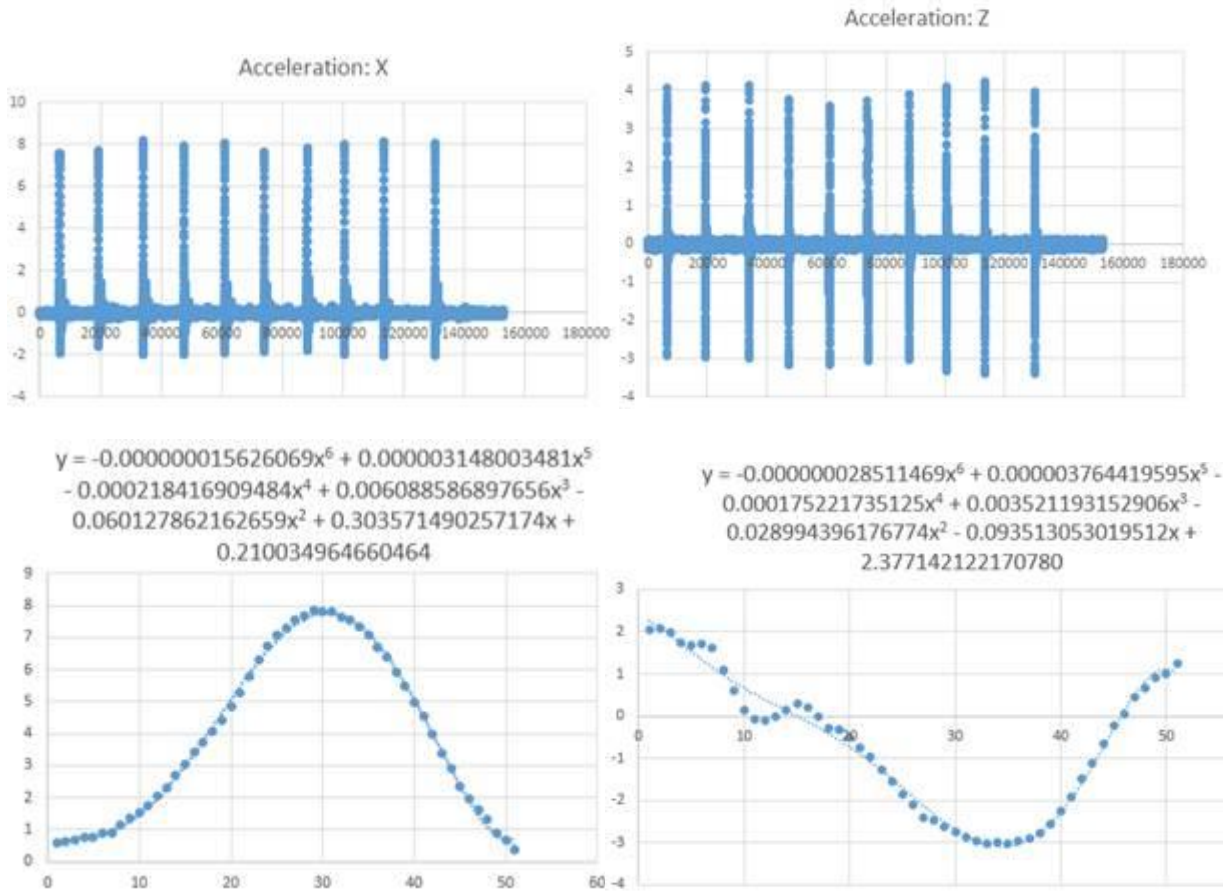
Exterior Padding: 9 lbs/ft<sup>3</sup>



Hit #	Z Max (g)	Z Min (g)	X Max (g)	X Min (g)	Collision Time (ms)
1	5.330003	-3.6007	7.981148	-2.19973	15.00
2	5.318758	-3.20306	7.661627	-1.8368	14.33
3	4.663739	-3.45508	7.009532	-1.79762	14.33
4	4.236893	-3.32596	7.199461	-1.69006	14.33
5	3.804735	-3.42866	7.564437	-1.77809	14.67
6	4.532455	-3.40693	8.946141	-2.28195	15.67
7	4.294773	-3.32692	7.3569	-1.56204	15.33
8	4.530937	-3.3555	6.934003	-1.50545	15.00
9	4.108226	-3.51346	7.557888	-1.80523	14.67
10	4.114186	-3.23099	8.061344	-1.72831	16.33
<b>Average</b>	4.493471	-3.38473	7.627248	-1.81853	14.97
<b>Std Dev</b>	0.515376	0.116521	0.609506	0.260305	0.655653

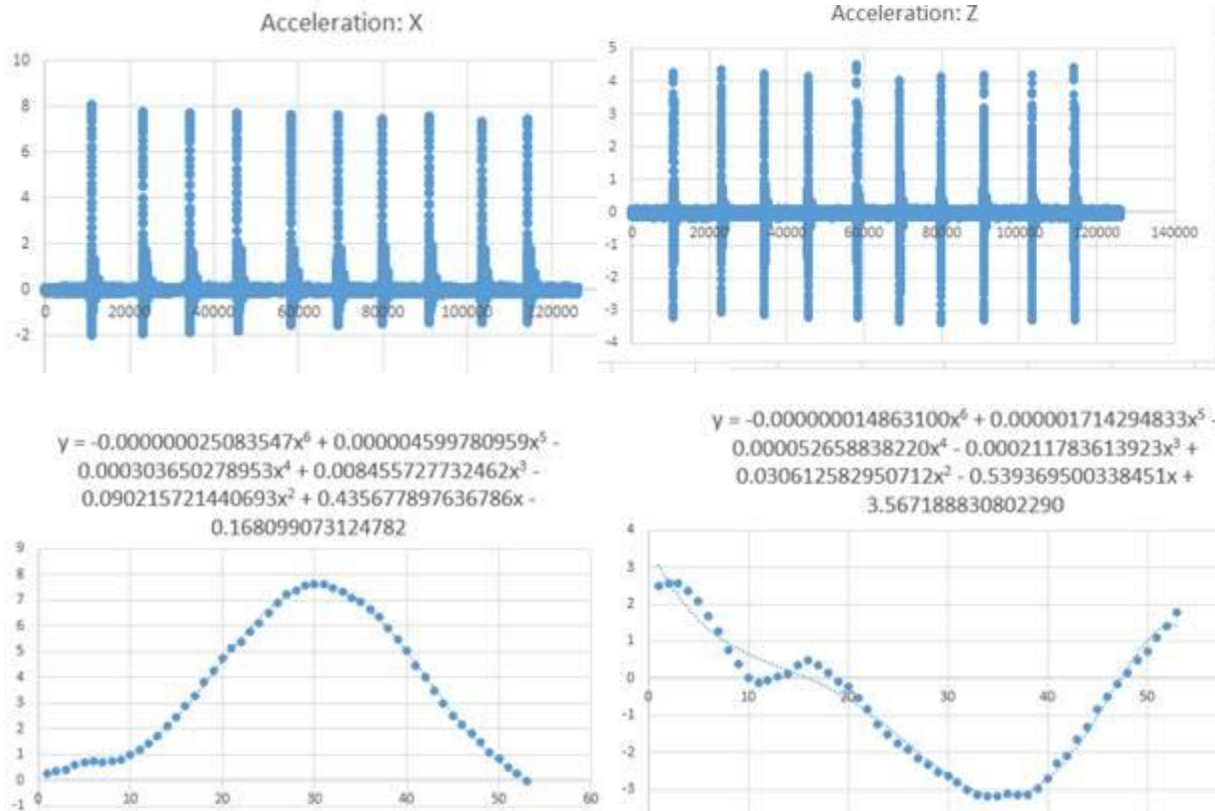


Exterior Padding: 12 lbs/ft<sup>3</sup>



Hit #	Z Max (g)	Z Min (g)	X Max (g)	X Min (g)	Collision Time (ms)
1	4.072534	-2.90494	7.561998	-1.936432	15.33
2	4.157233	-2.94379	7.742684	-1.623374	15.33
3	4.134961	-2.97195	8.192888	-1.964461	15.33
4	3.780046	-3.15919	7.981077	-1.988009	15.67
5	3.612856	-3.14989	8.092278	-1.894458	15.33
6	3.728119	-3.04051	7.661555	-1.848642	16.33
7	3.894776	-3.0121	7.862701	-1.806342	16.67
8	4.104103	-3.32638	8.03661	-2.003075	16.00
9	4.239802	-3.39954	8.160615	-2.040858	16.33
10	3.993049	-3.39037	8.062103	-2.045239	18.00
<b>Average</b>	3.971748	-3.12987	7.935451	-1.915089	16.03
<b>Std Dev</b>	0.208662	0.18633	0.217782	0.12930293	0.852754

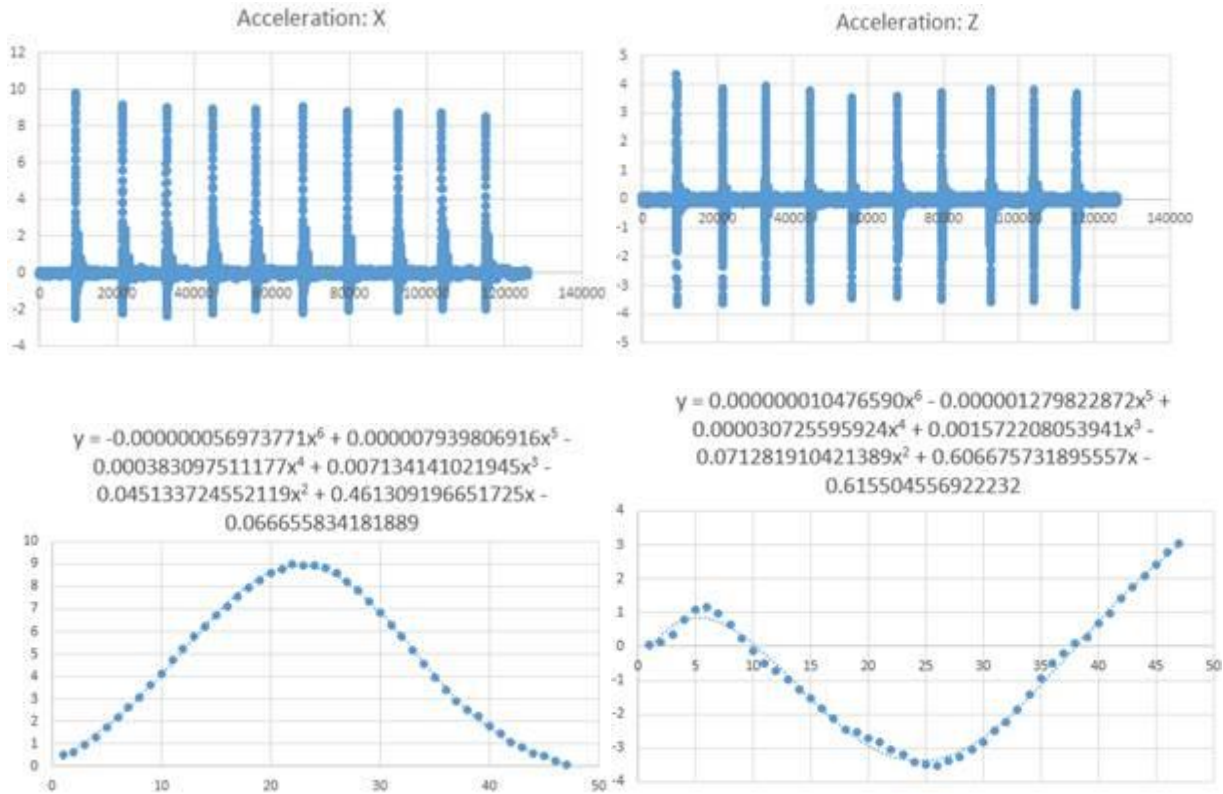
Exterior Padding: 15 lbs/ft<sup>3</sup>



Hit #	Z Max (g)	Z Min (g)	X Max (g)	X Min (g)	Collision Time (ms)
1	4.284971	-3.222	8.083983	-1.98512	16.33
2	4.375265	-3.03463	7.752937	-1.91611	17.33
3	4.251642	-3.1406	7.732196	-1.87213	18.33
4	4.145525	-3.2173	7.706403	-1.80968	17.67
5	4.528894	-3.19869	7.626328	-1.51323	17.33
6	4.049493	-3.32804	7.674569	-1.53264	15.33
7	4.151579	-3.38775	7.485686	-1.46561	18.33
8	4.217829	-3.29796	7.565095	-1.39502	17.67
9	4.199008	-3.28443	7.34194	-1.39756	15.67
10	4.427161	-3.27395	7.4702	-1.40461	18.33
<b>Average</b>	4.263137	-3.23853	7.643934	-1.62917	17.23
<b>Std Dev</b>	0.144837	0.100359	0.203062	0.237827	1.1000384



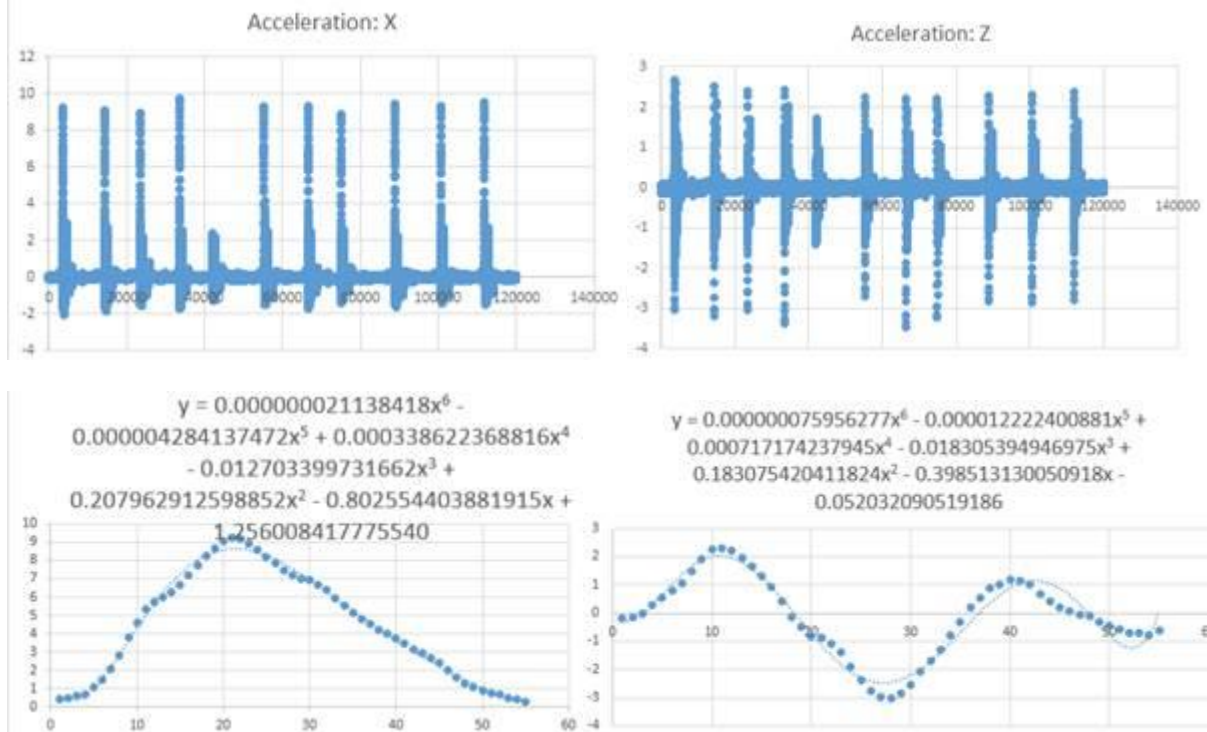
Exterior Padding: 20 lbs/ft<sup>3</sup>



Hit #	Z Max (g)	Z Min (g)	X Max (g)	X Min (g)	Collision Time (ms)
1	4.354382	-3.67325	9.836692	-2.45038	16.67
2	3.878444	-3.6197	9.177787	-2.17385	15.67
3	3.954728	-3.59342	9.033801	-2.34431	14.67
4	3.792284	-3.50877	8.976088	-2.17258	15.33
5	3.586676	-3.43787	8.937897	-1.99604	15.00
6	3.588211	-3.38044	9.084872	-2.15793	16.00
7	3.732301	-3.49227	8.844741	-2.04213	15.67
8	3.850699	-3.57684	8.740247	-2.07896	16.00
9	3.835939	-3.54748	8.779092	-1.94305	16.67
10	3.71966	-3.68729	8.509283	-1.95693	16.00
<b>Average</b>	3.829332	-3.55173	8.99205	-2.13162	15.77
<b>Std Dev</b>	0.219634	0.09879	0.353551	0.165408	0.64937235

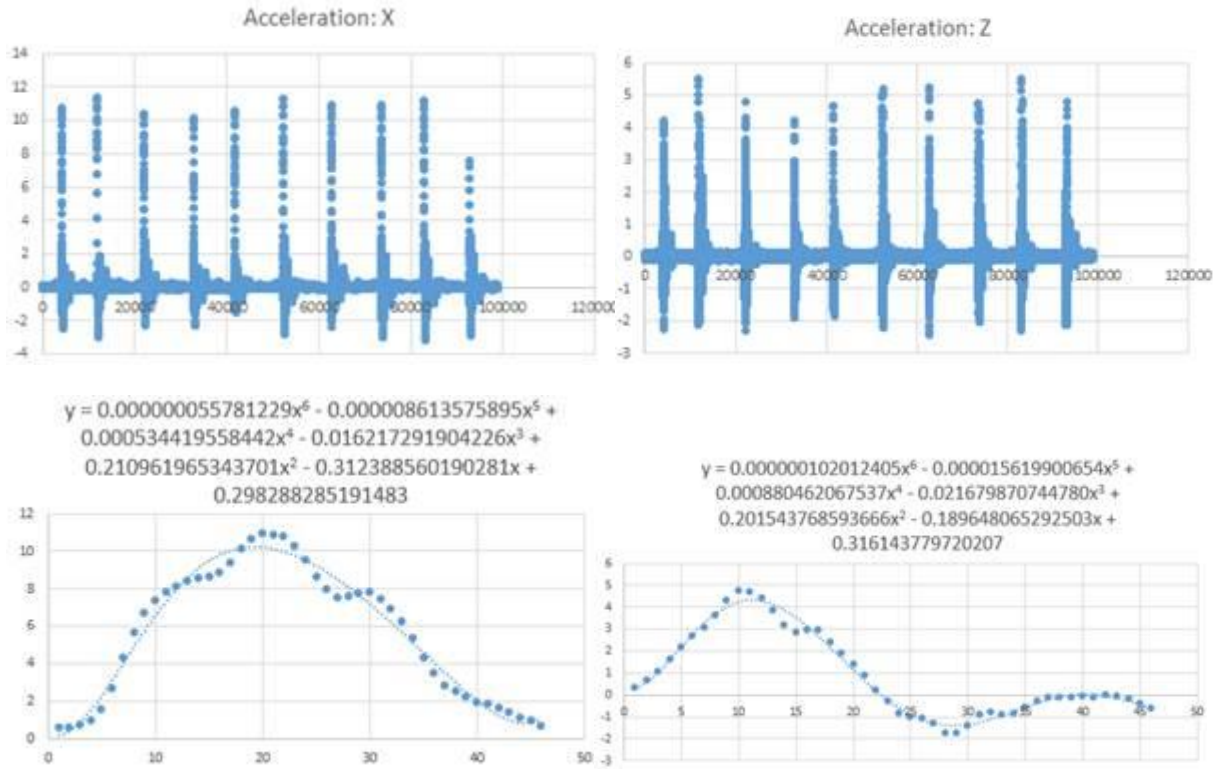
### Appendix J – Impacts to Facemask

#### Control



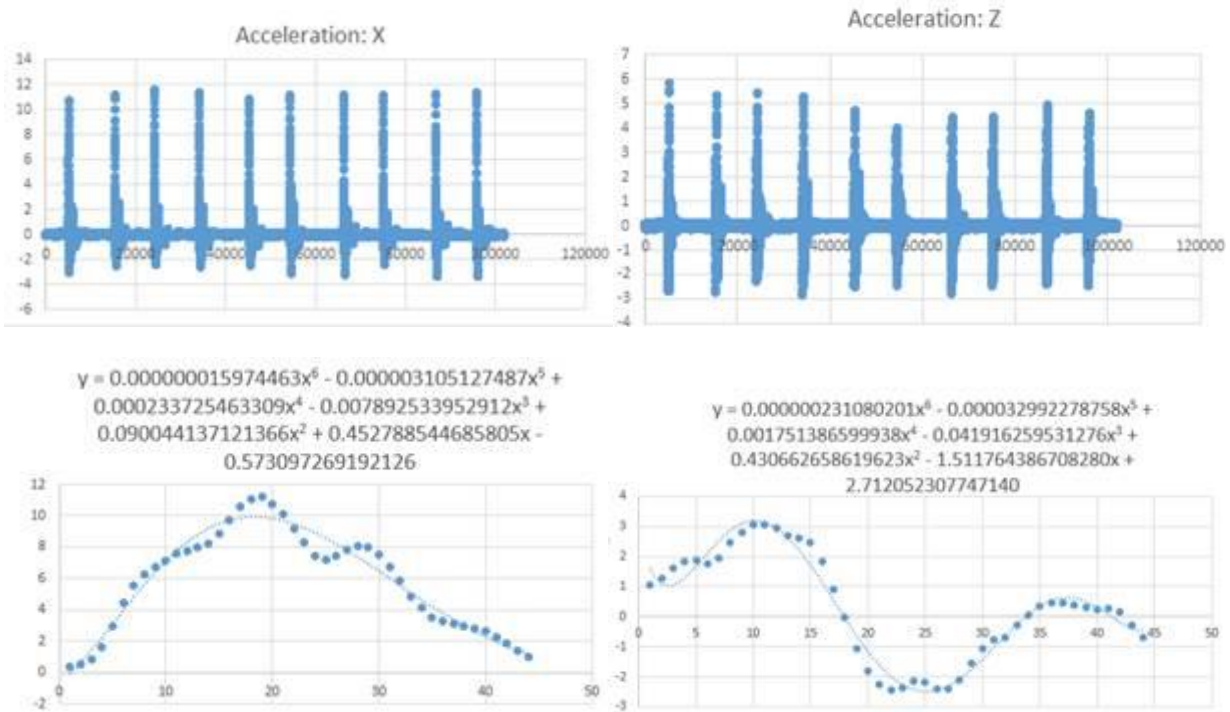
Hit #	Z Max (g)	Z Min (g)	X Max (g)	X Min (g)	Collision Time (ms)
1	2.669407	-3.03434	9.23323	-0.14134	16.67
2	2.51115	-3.19849	9.10399	0.174583	16.67
3	2.409029	-3.04456	8.972289	0.157663	16.67
4	2.415409	-3.37075	9.724937	0.330517	16.67
5					
6	2.241494	-2.70588	9.348903	0.231136	16.00
7	2.223897	-3.45631	9.33325	0.218427	16.67
8	2.228973	-3.21873	8.86134	0.067316	15.33
9	2.279856	-2.80878	9.433514	0.124444	15.67
10	2.292938	-2.84279	9.312399	0.129884	16.00
11	2.362838	-2.77878	9.527032	0.247394	16.33
<b>Average</b>	2.363573	-3.07562	9.258206	0.143626	16.26
<b>Std Dev</b>	0.159902	0.259505	0.274049	0.139749	0.52115731

Interior Front and Top Padding: 9 lbs/ft<sup>3</sup>



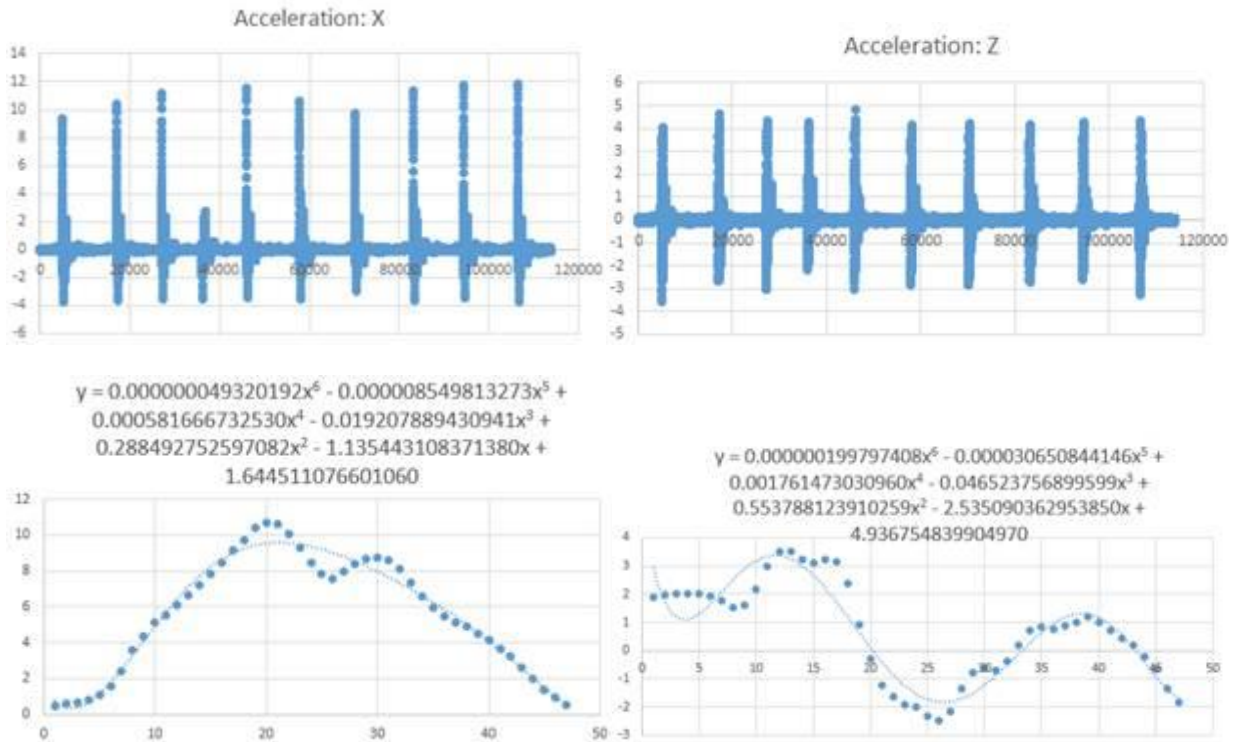
Hit #	Z Max (g)	Z Min (g)	X Max (g)	X Min (g)	Collision Time (ms)
1	4.191906	-2.28294	10.74825	-2.49282	18.33
2	5.481821	-2.12846	11.36898	-3.02989	8.33
3	4.767162	-2.30514	10.3651	-2.34032	19.00
4	4.190373	-1.89893	10.06976	-2.35606	10.00
5	4.637497	-1.86973	10.51736	-1.55932	15.00
6	5.195793	-2.21497	11.23986	-2.81351	16.33
7	5.225782	-2.47046	10.89474	-2.3803	15.00
8	4.723868	-2.06884	10.88926	-3.01989	15.00
9	5.499207	-2.30004	11.16711	-3.19234	15.67
<b>Average</b>	4.879268	-2.17105	10.80671	-2.57605	14.74
<b>Std Dev</b>	0.501232	0.19869	0.429166	0.502758	3.503341

Interior Front and Top Padding: 12 lbs/ft<sup>3</sup>



Hit #	Z Max (g)	Z Min (g)	X Max (g)	X Min (g)	Collision Time (ms)
1	2.746265	-2.66612	10.80265	-1.14934	15.00
2	5.365442	-2.71046	11.24685	-2.52987	14.67
3	5.449415	-2.30274	11.63038	-2.43182	14.67
4	5.321806	-2.82473	11.41941	-2.59864	14.33
5	4.748036	-2.50379	10.91652	-2.54822	15.33
6	4.01398	-2.42261	11.15579	-3.09477	15.00
7	4.435179	-2.76073	11.2415	-3.24156	15.00
8	4.467336	-2.43721	11.19697	-2.40022	14.33
9	4.937525	-2.40554	11.32889	-3.36313	14.00
10	4.618345	-2.46867	11.36168	-3.3892	13.67
<b>Average</b>	4.609443	-2.55933	11.21544	-2.59528	14.70
<b>Std Dev</b>	0.850585	0.184195	0.247982	0.65372	0.423143

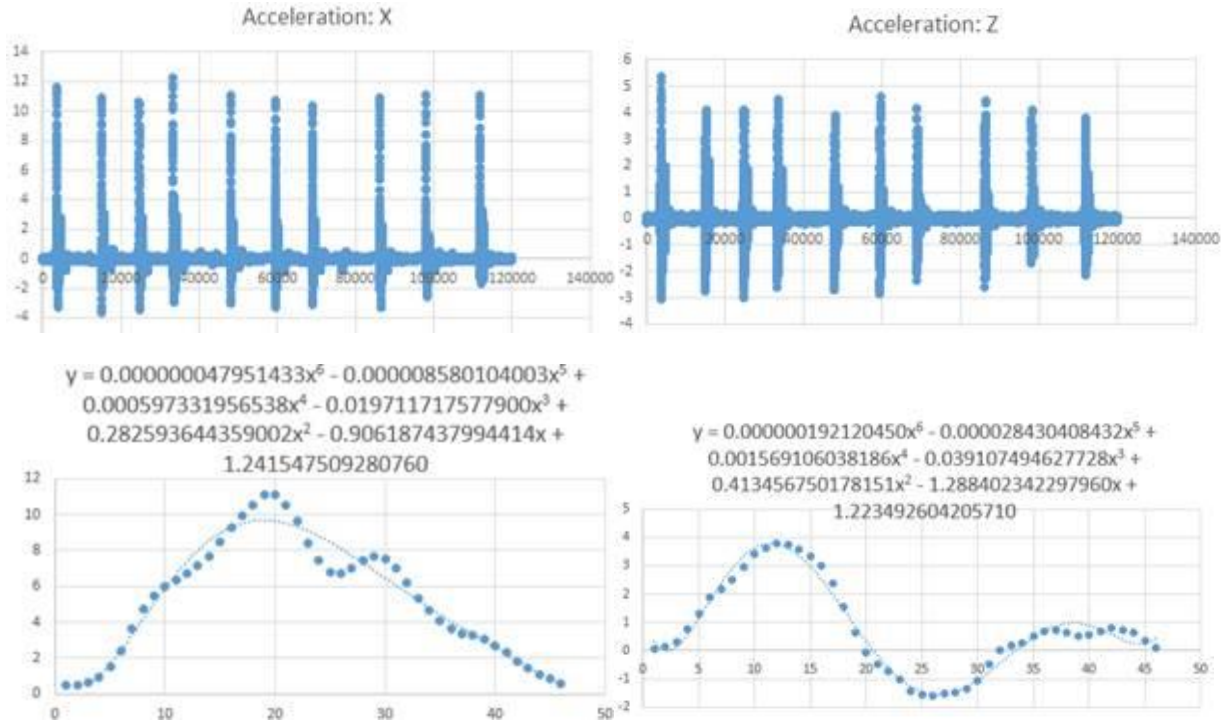
Interior Front and Top Padding: 15 lbs/ft<sup>3</sup>



Hit #	Z Max (g)	Z Min (g)	X Max (g)	X Min (g)	Collision Time (ms)
1	4.053939	-3.58932	9.414982	-3.70541	16.67
2	4.610241	-2.67691	10.39259	-3.649	14.67
3	4.318065	-3.01617	11.20969	-3.52353	15.00
5	4.798998	-3.01497	11.55719	-3.45268	14.67
6	4.163165	-2.82673	10.66764	-3.53582	15.33
7	4.195684	-2.83835	9.775924	-2.94127	15.33
8	4.163001	-2.69739	11.34572	-3.59352	14.33
9	4.26918	-2.56767	11.71654	-3.44343	14.33
10	4.325002	-3.24468	11.82964	-3.69234	13.67
<b>Average</b>	4.321534	-2.90344	10.76004	-3.48058	15.04
<b>Std Dev</b>	0.254035	0.318975	0.846571	0.235913	0.76613

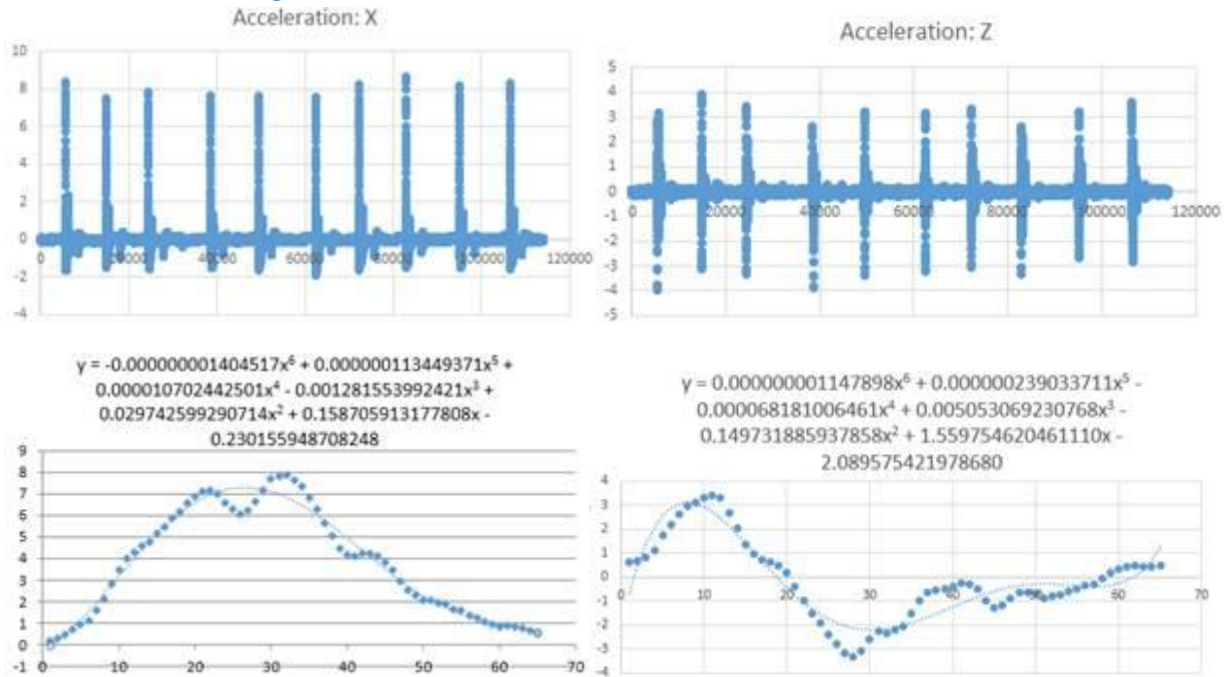


Interior Front and Top Padding: 20 lbs/ft<sup>3</sup>



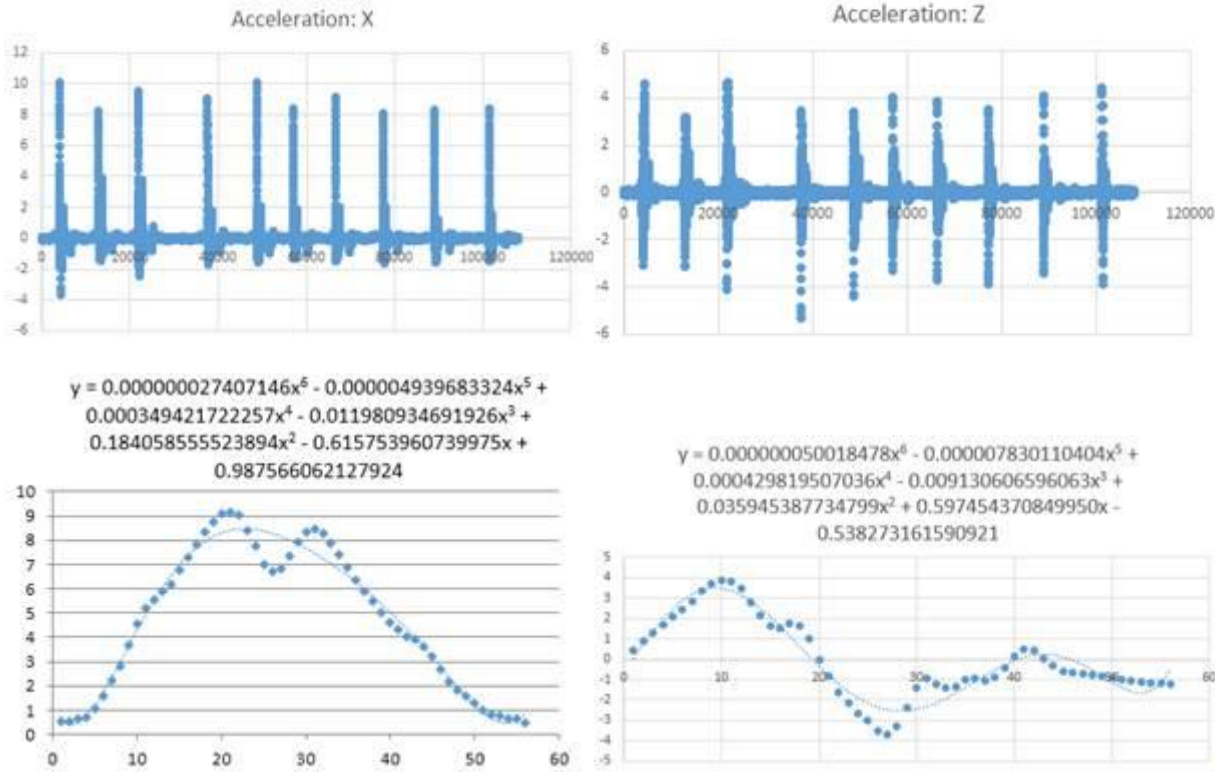
Hit #	Z Max (g)	Z Min (g)	X Max (g)	X Min (g)	Collision Time (ms)
1	5.346286	-3.04159	11.59271	-3.2759	15.33
2	4.092852	-2.76858	10.9267	-3.63275	14.33
3	4.09989	-2.98124	10.67148	-3.48195	15.67
4	4.487018	-2.60883	12.26787	-2.96275	14.67
5	3.906393	-2.6938	11.12046	-3.06468	14.33
6	4.63228	-2.855	10.74843	-3.27845	14.67
7	4.143114	-2.33173	10.34128	-3.07591	15.33
8	4.482627	-2.58673	10.88725	-3.2603	15.00
9	4.10529	-1.66615	11.0863	-2.55503	15.00
10	3.825089	-2.13471	11.09648	-1.65898	15.33
<b>Average</b>	4.366194	-2.61485	11.07139	-3.17641	14.93
<b>Std Dev</b>	0.437953	0.416066	0.565476	0.312909	0.465352

Interior Back Padding: 9 lbs/ft<sup>3</sup>



Hit #	Z Max (g)	Z Min (g)	X Max (g)	X Min (g)	Collision Time (ms)
1	3.178006	-3.95021	8.425489	-1.6635	18.67
2	3.929808	-3.12483	7.53707	-1.46885	20.67
3	3.419903	-3.33454	7.874565	-1.59048	21.67
4	2.629739	-3.84216	7.681432	-1.51579	22.00
5	3.205571	-3.36051	7.639632	-1.62823	22.33
6	3.152141	-3.18438	7.559986	-1.87563	21.33
7	3.342641	-3.03214	8.24335	-1.60725	22.33
8	2.600995	-3.29994	8.669894	-1.49856	22.33
9	3.206972	-2.64099	8.175952	-1.501	24.33
10	3.617566	-2.8043	8.313905	-1.59261	24.00
<b>Average</b>	3.228334	-3.2574	8.012128	-1.59419	21.97
<b>Std Dev</b>	0.402011	0.408143	0.404426	0.117871	1.604149

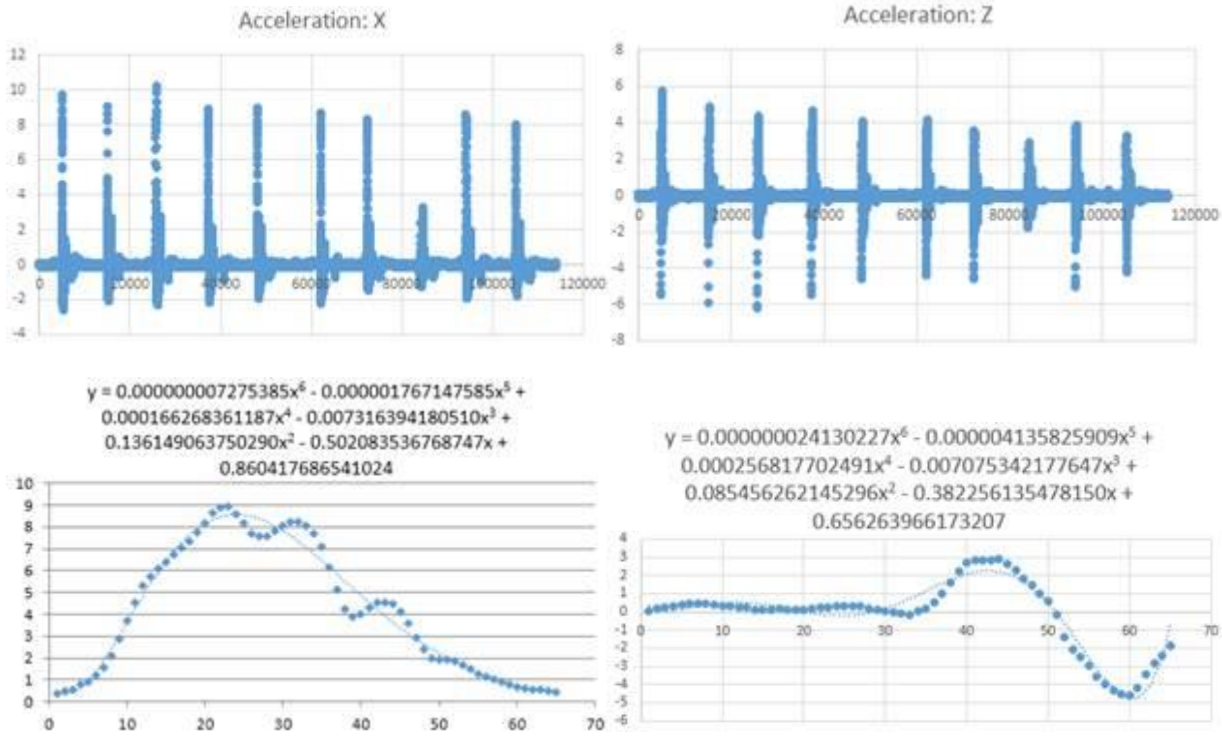
Interior Back Padding: 12 lbs/ft<sup>3</sup>



Hit #	Z Max (g)	Z Min (g)	X Max (g)	X Min (g)	Collision Time (ms)
1	4.591589	-3.06639	10.08653	-3.62543	16.00
2	3.199894	-3.13368	8.259348	-0.57882	19.67
3	4.638982	-4.09323	9.556355	-1.81583	19.00
4	3.453429	-5.29644	9.047395	-1.7038	18.00
5	3.418402	-4.42499	10.09808	-1.51544	17.67
6	4.017567	-3.31961	8.437245	-1.34272	21.33
7	3.896966	-3.69038	9.173643	-1.45688	18.33
8	3.505274	-3.91137	8.081592	-1.65128	22.67
9	4.126161	-3.43175	8.289755	-1.5785	20.67
10	4.454408	-3.90697	8.384667	-1.50125	21.00
<b>Average</b>	3.872029	-3.81865	9.003327	-1.69652	19.26
<b>Std Dev</b>	0.519573	0.714647	0.785919	0.807435	2.053807

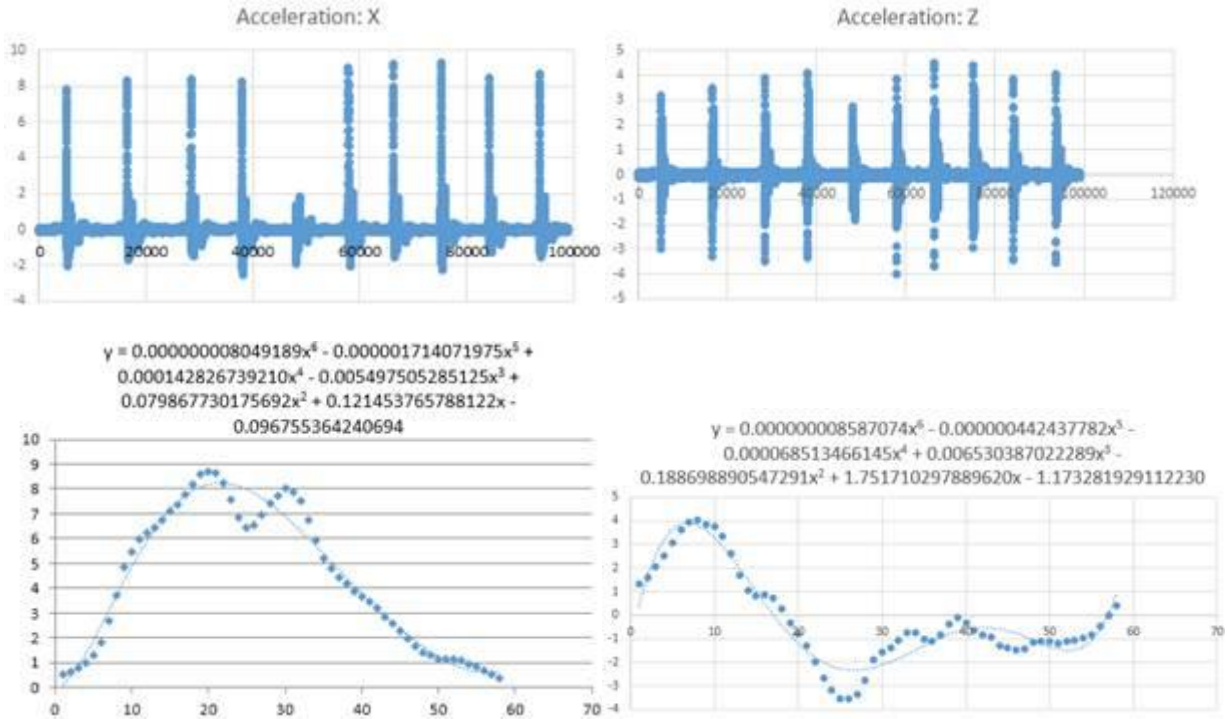


Interior Back Padding: 15 lbs/ft<sup>3</sup>



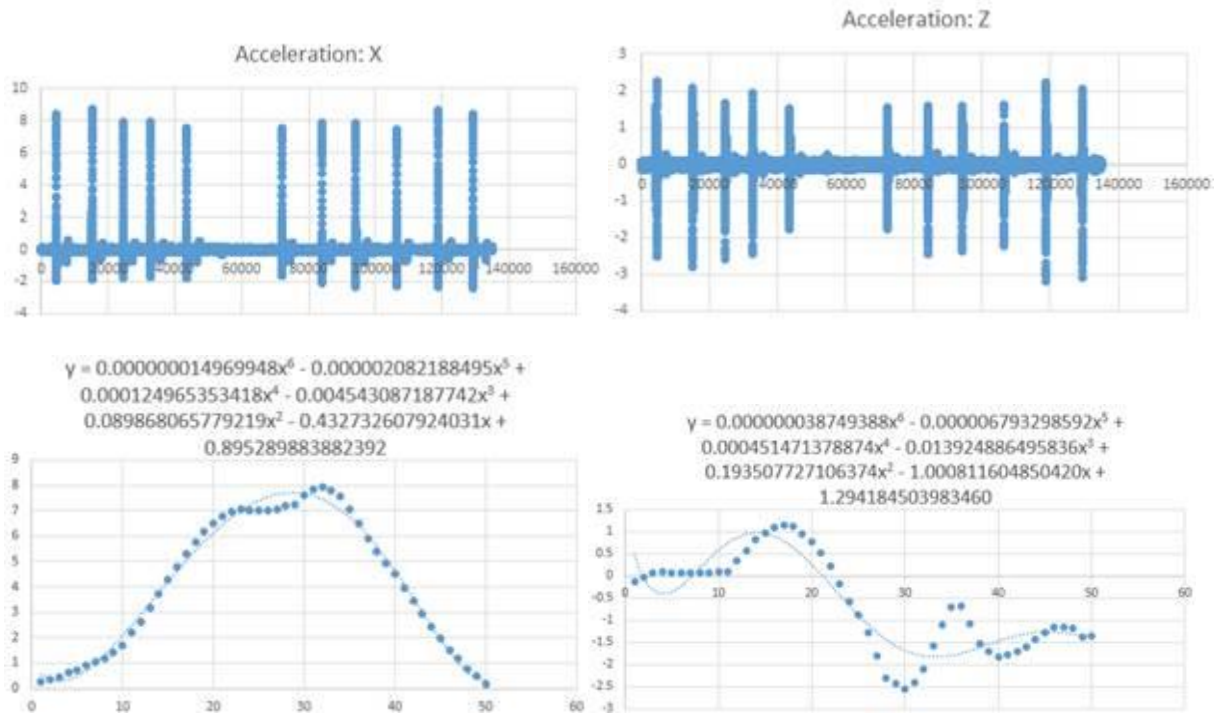
Hit #	Z Max (g)	Z Min (g)	X Max (g)	X Min (g)	Collision Time (ms)
1	5.787519	-5.43751	9.734969	-2.61433	17.33
2	4.876094	-5.90452	9.090946	-2.09877	9.67
3	4.353412	-6.17409	10.23857	-2.33735	15.67
4	4.658734	-5.43908	8.946796	-2.13991	18.67
5	4.092697	-4.58654	8.957673	-1.9083	21.33
6	4.179847	-4.39344	8.699975	-2.20131	20.00
7	3.582121	-4.56441	8.342659	-1.505	21.00
9	3.88729	-4.98619	8.610495	-1.91996	21.67
10	3.286534	-4.22134	8.039323	-1.8201	20.33
<b>Average</b>	4.300472	-5.07857	8.962378	-2.06056	18.41
<b>Std Dev</b>	0.745515	0.694659	0.677413	0.320209	3.827626

Interior Back Padding: 20 lbs/ft<sup>3</sup>



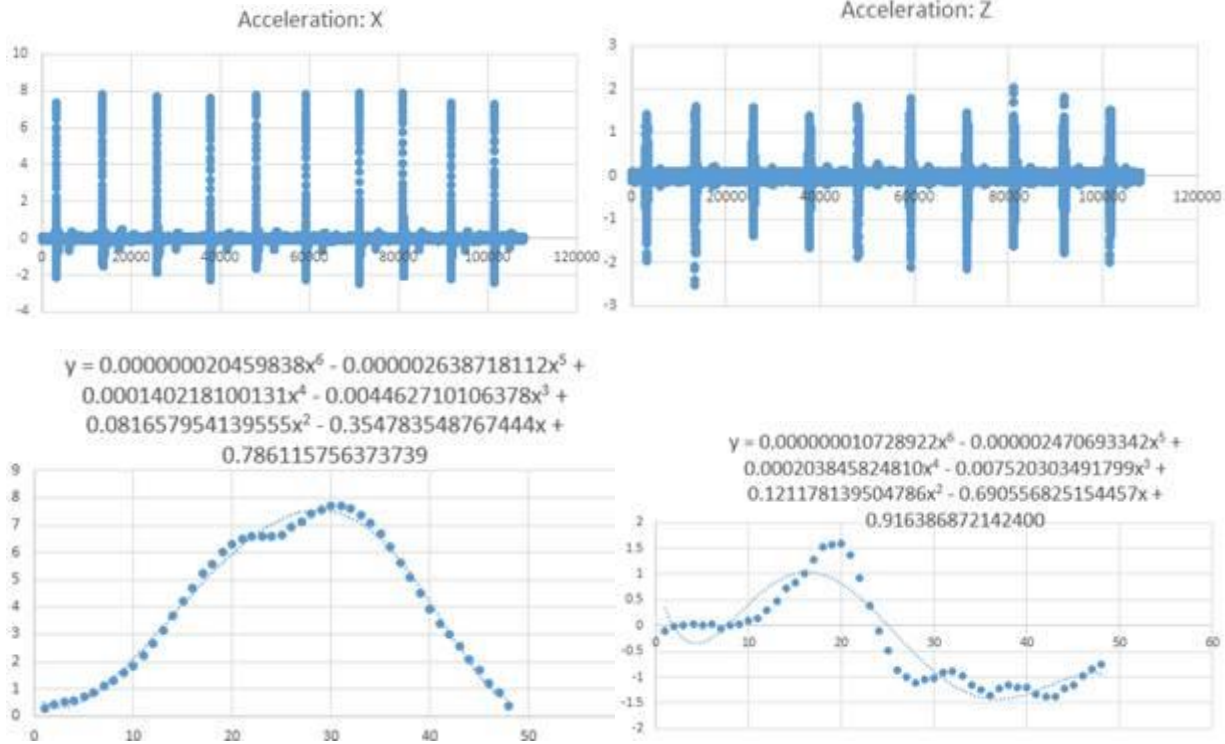
Hit #	Z Max (g)	Z Min (g)	X Max (g)	X Min (g)	Collision Time (ms)
1	3.19343	-2.97828	7.830224	-2.04686	19.33
2	3.510239	-3.30306	8.336822	-1.6521	21.00
3	3.907842	-3.47348	8.443388	-1.47196	22.67
4	4.110124	-3.34478	8.287443	-1.51312	22.67
6	3.859493	-4.00744	9.042011	-2.04764	23.33
7	4.541559	-3.69033	9.270974	-1.53025	23.00
8	4.411886	-2.93118	9.315043	-2.22784	20.00
9	3.845753	-3.45905	8.491117	-1.28002	20.00
10	4.045677	-3.55638	8.674513	-1.50866	19.00
<b>Average</b>	3.936223	-3.416	8.632393	-1.6976	21.22
<b>Std Dev</b>	0.415781	0.334366	0.493567	0.326107	1.708477

Exterior Padding: 9 lbs/ft<sup>3</sup>



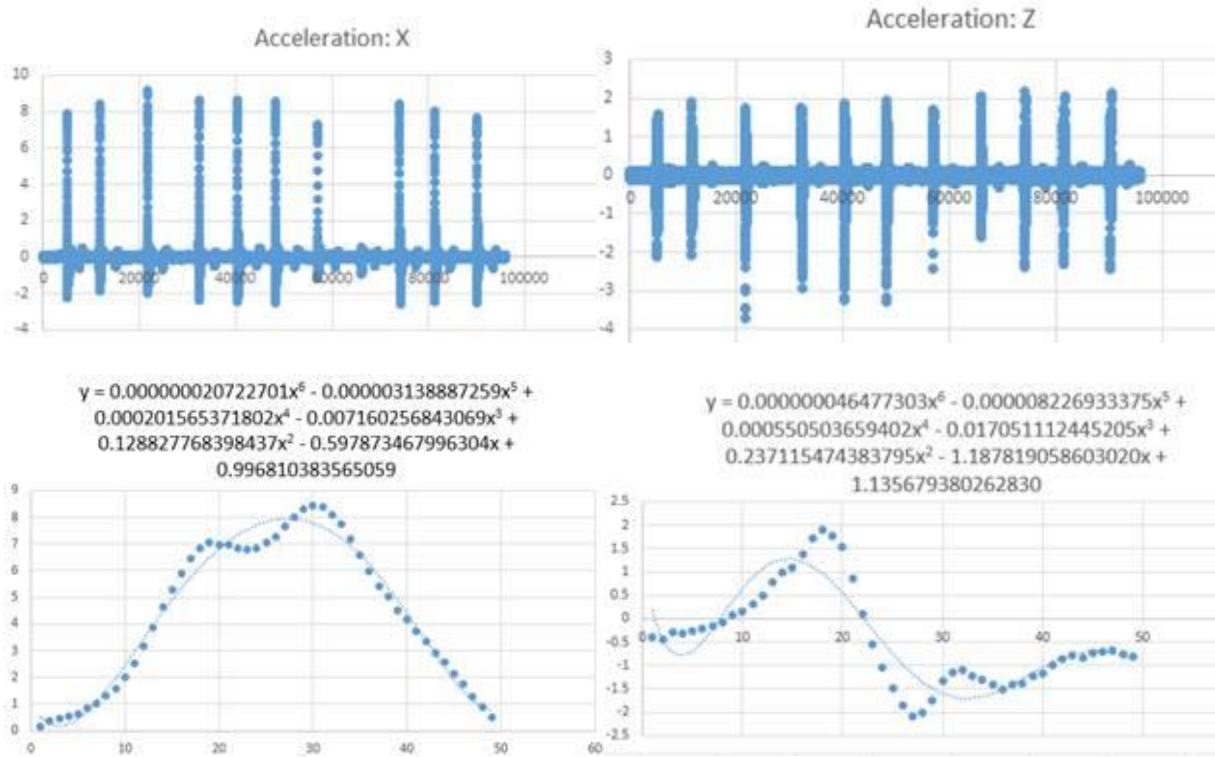
Hit #	Z Max (g)	Z Min (g)	X Max (g)	X Min (g)	Collision Time (ms)
1	2.273175	-2.5241	8.396577	-1.90432	15.33
2	2.094312	-2.78831	8.750641	-1.86222	15.00
3	1.67356	-2.56452	7.913322	-1.76952	16.00
4	1.9369	-2.43068	7.967366	-1.68899	16.33
5	1.524494	-1.76591	7.578273	-1.76905	15.67
6	1.543322	-1.74413	7.56749	-1.64151	17.00
7	1.581337	-2.42718	7.907957	-2.05153	10.00
8	1.60518	-2.37979	7.862248	-2.29149	14.33
9	1.614103	-2.20606	7.441563	-2.25305	14.33
10	2.222735	-3.17199	8.650115	-2.28943	14.00
11	2.050848	-3.07017	8.420915	-2.38914	14.67
<b>Average</b>	1.829088	-2.46117	8.041497	-1.99184	14.79
<b>Std Dev</b>	0.289772	0.454876	0.448822	0.273124	1.839446

Exterior Padding: 12 lbs/ft<sup>3</sup>



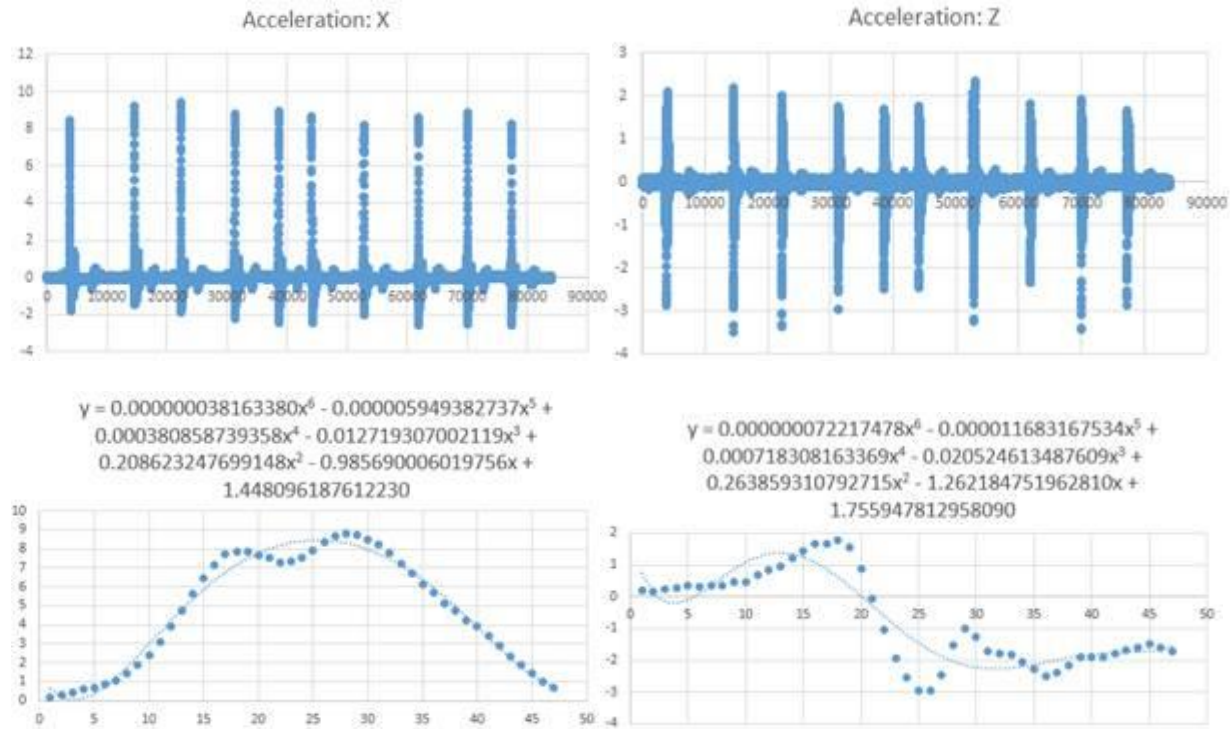
Hit #	Z Max (g)	Z Min (g)	X Max (g)	X Min (g)	Collision Time (ms)
1	1.441312	-1.96681	7.37535	-2.11324	15.67
2	1.616758	-2.50948	7.827464	-1.50809	17.00
3	1.578672	-1.3821	7.715808	-1.87579	15.67
4	1.385423	-1.65775	7.607756	-2.2811	15.00
5	1.617639	-1.87583	7.780944	-1.63996	16.33
6	1.784283	-2.10062	7.835343	-2.26836	14.33
7	1.472993	-2.1382	7.922142	-2.46704	14.33
8	2.050426	-1.62258	7.891953	-2.09108	14.67
9	1.843116	-1.78868	7.34176	-2.23513	14.67
10	1.518405	-1.98978	7.324114	-2.4117	15.67
<b>Average</b>	1.630903	-1.90319	7.662263	-2.08915	15.33
<b>Std Dev</b>	0.205875	0.315828	0.234959	0.320177	0.889172

Exterior Padding: 15 lbs/ft<sup>3</sup>



Hit #	Z Max (g)	Z Min (g)	X Max (g)	X Min (g)	Collision Time (ms)
1	1.594334	-2.11399	7.930853	-2.21994	15.33
2	1.904847	-2.07718	8.416026	-1.85249	16.00
3	1.746056	-3.73107	9.147993	-1.98875	15.67
4	1.754918	-2.92169	8.633298	-2.3504	14.67
5	1.853341	-3.23824	8.638943	-2.41833	15.00
6	1.928593	-3.28954	8.590094	-2.49367	15.00
7	1.72637	-2.44108	7.26535	-1.19832	7.67
8	2.17741	-2.37264	8.431629	-2.55795	14.67
9	2.07397	-2.3201	8.068262	-2.4357	14.33
10	2.122519	-2.4393	7.682932	-2.4914	14.00
<b>Average</b>	1.888236	-2.69448	8.280538	-2.20069	14.23
<b>Std Dev</b>	0.190525	0.56441	0.547465	0.420882	2.382479

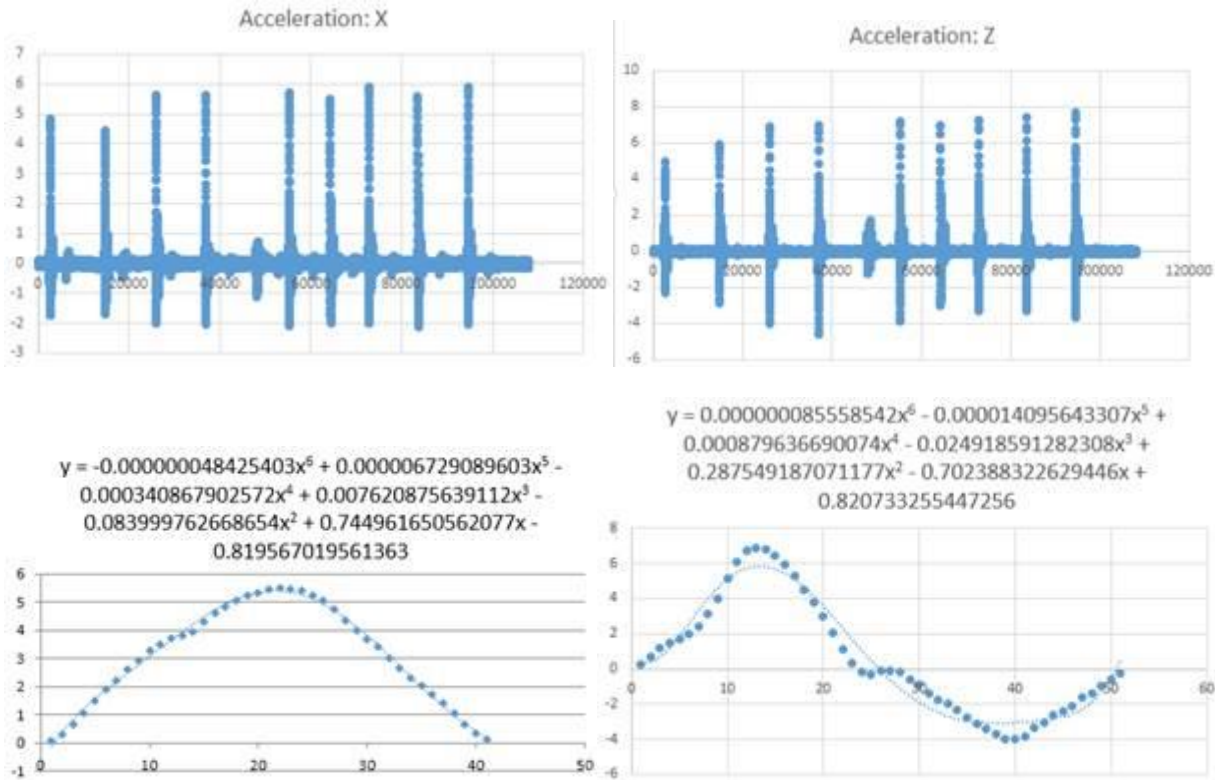
Exterior Padding: 20 lbs/ft<sup>3</sup>



Hit #	Z Max (g)	Z Min (g)	X Max (g)	X Min (g)	Collision Time (ms)
1	2.097717	-2.8526	8.482017	-1.83948	18.33
2	2.213633	-3.49306	9.235012	-1.48381	15.67
3	2.0261	-3.36862	9.429875	-1.87462	15.33
4	1.756785	-2.95808	8.799884	-2.2103	15.33
5	1.70954	-2.49911	8.929793	-2.41885	14.67
6	1.773345	-2.47062	8.694794	-2.41251	14.33
7	2.370099	-3.23358	8.217017	-2.03973	14.33
8	1.838457	-2.33193	8.617469	-2.55164	14.00
9	1.929591	-3.42687	8.885987	-2.49209	14.33
10	1.656033	-2.86164	8.289467	-2.56179	14.33
<b>Average</b>	1.93713	-2.94961	8.758132	-2.18848	15.07
<b>Std Dev</b>	0.23513	0.423013	0.385674	0.366084	1.274443



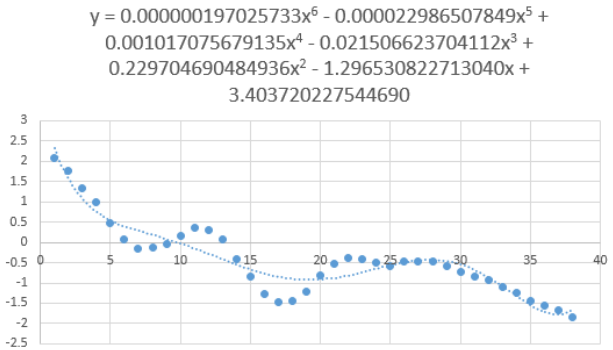
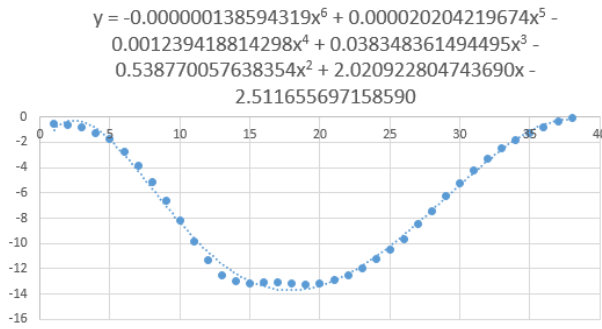
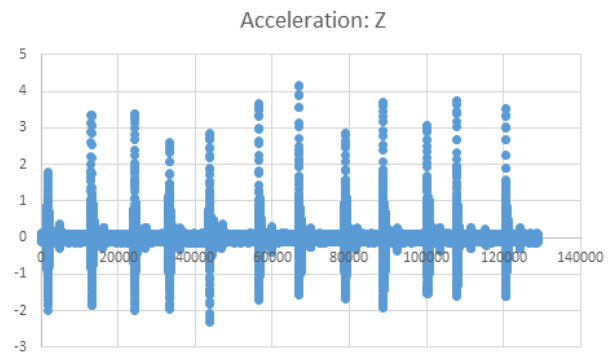
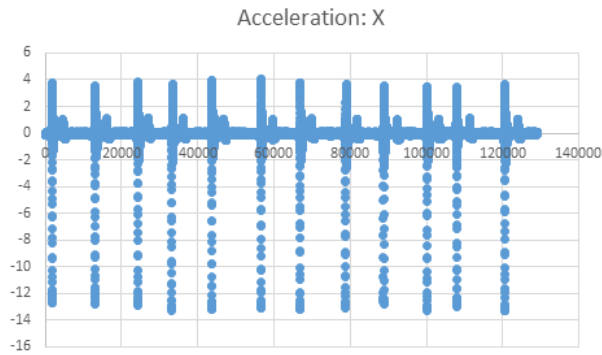
Exterior Padding: 9 and 12 lbs/ft<sup>3</sup>



Hit #	Z Max (g)	Z Min (g)	X Max (g)	X Min (g)	Collision Time (ms)
1	5.019029	-2.30932	4.830275	-1.72698	19.67
2	5.924919	-2.86616	4.434629	-1.68704	19.33
3	6.906147	-4.00692	5.653781	-1.99242	14.00
4	7.004384	-4.60325	5.616649	-2.02955	14.67
6	7.206533	-3.88312	5.704336	-2.09196	14.00
7	6.962477	-3.00585	5.501606	-1.99744	13.67
8	7.292058	-3.32375	5.915657	-2.00425	14.00
9	7.407973	-3.26964	5.906526	-2.04576	14.00
10	7.690851	-3.6784	5.906526	-2.04576	14.00
<b>Average</b>	6.823819	-3.43849	5.496665	-1.95791	15.26
<b>Std Dev</b>	0.835359	0.686155	0.520307	0.145834	2.41938

## Appendix K – Impacts to Side of Helmet

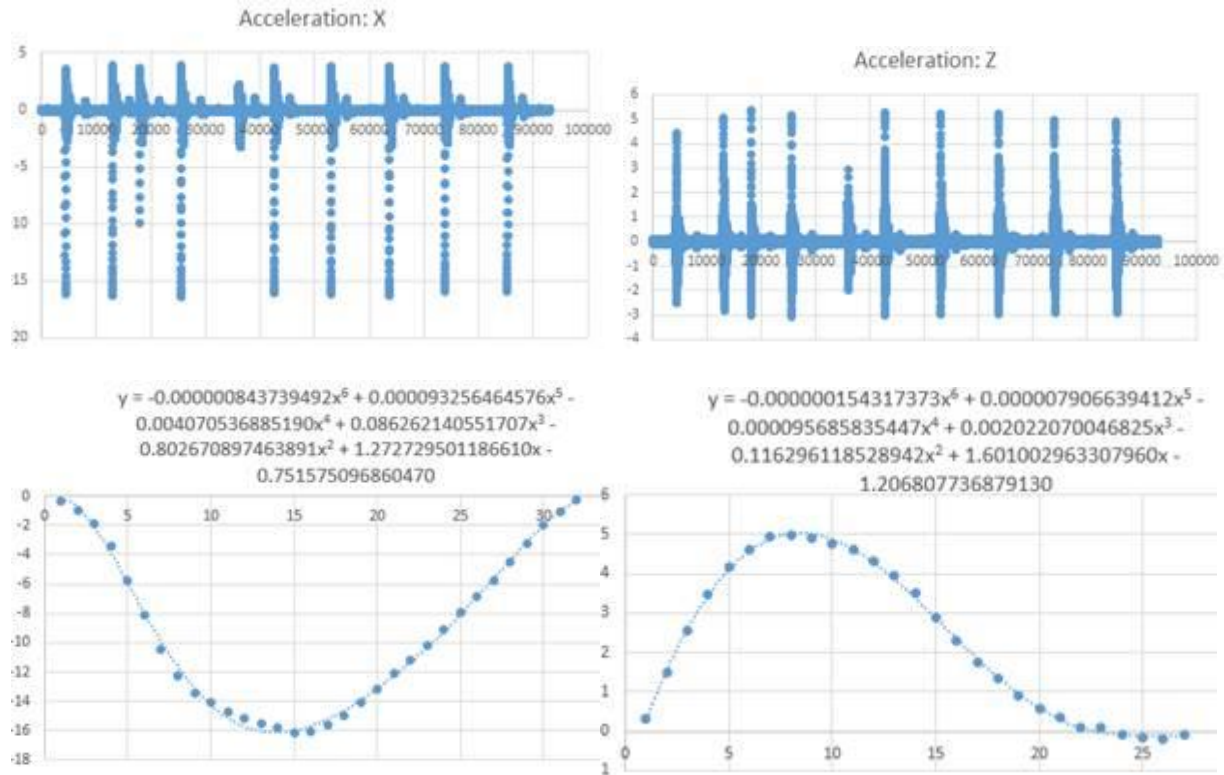
### Control



Hit #	Z Max (g)	Z Min (g)	X Max (g)	X Min (g)	Collision Time (ms)
1	1.780485	-2.0073	3.734274	-12.7059	12.33
2	3.364296	-1.86267	3.517272	-12.7934	12.33
3	3.389892	-1.98423	3.830336	-12.8512	12.67
4	2.604543	-1.95434	3.667001	-13.2765	12.33
5	2.866883	-2.32182	3.970089	-13.2382	12.00
6	3.66962	-1.69567	4.063988	-13.0796	13.67
7	4.166845	-1.5634	3.798586	-13.2096	12.33
8	2.848801	-1.69536	3.656627	-13.0573	13.33
9	3.693847	-1.91278	3.535667	-12.7927	15.00
10	3.081258	-1.53354	3.500464	-13.3164	11.67
11	3.749902	-1.59185	3.466992	-12.9585	11.67
12	3.53331	-1.61714	3.653568	-13.3134	14.00
<b>Average</b>	3.22914	-1.81167	3.699572	-13.0494	12.78
<b>Std Dev</b>	0.638433	0.236186	0.189003	0.223984	1.018288

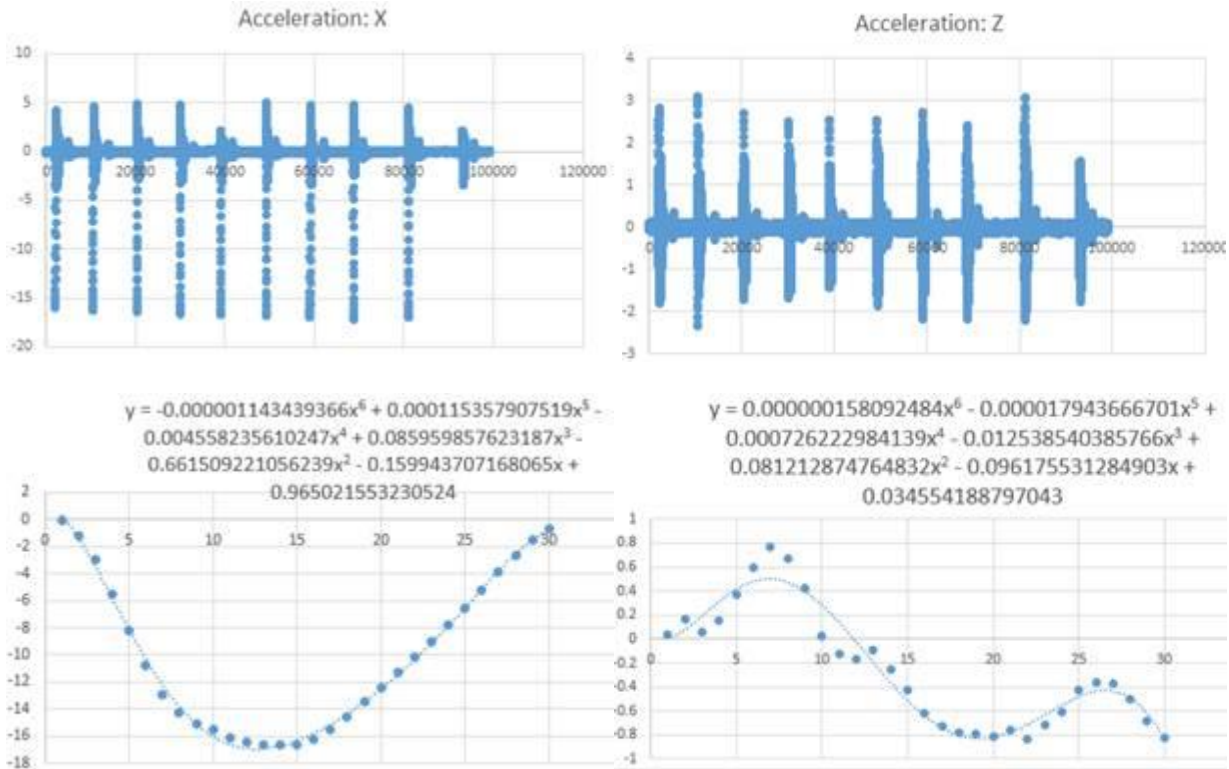


Interior Padding: 9 lbs/ft<sup>3</sup>



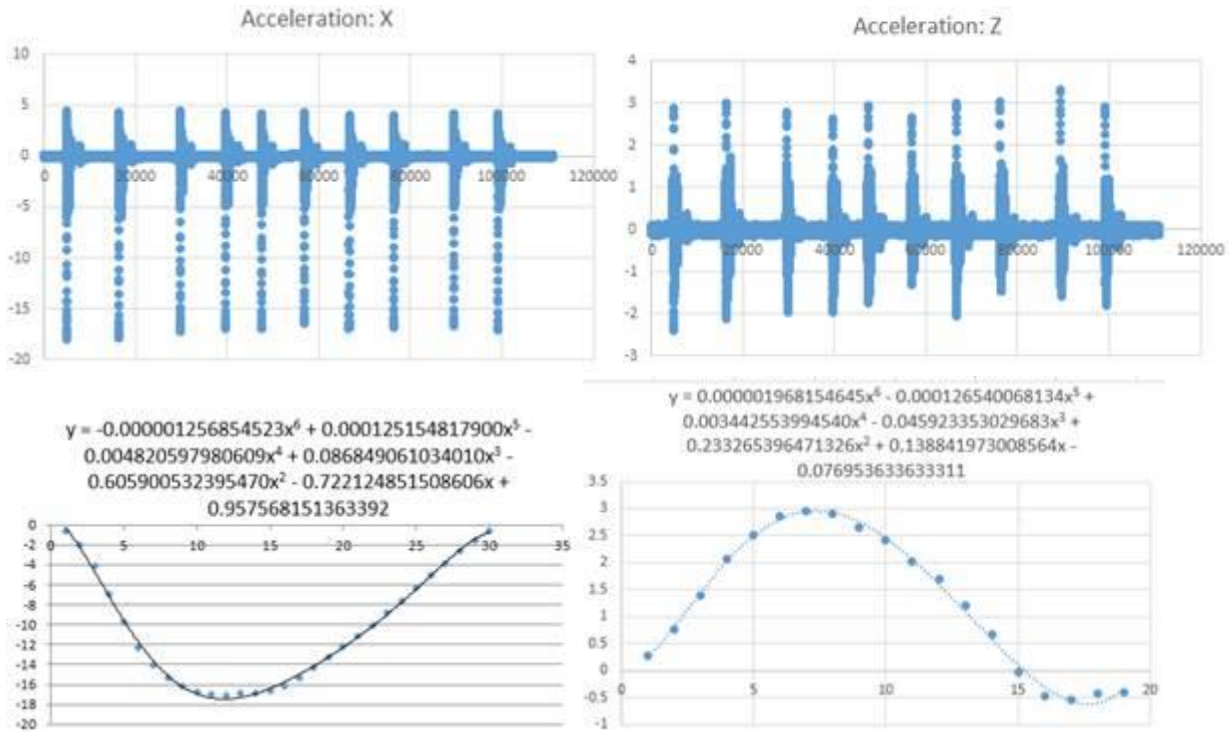
Hit #	Z Max (g)	Z Min (g)	X Max (g)	X Min (g)	Collision Time (ms)
1	4.425193	-2.51761	3.556219	-16.2008	10.00
2	5.056635	-2.83974	3.917831	-16.2513	10.33
3	5.387628	-3.00613			
4	5.16935	-3.05959	3.962937	-16.4122	10.33
6	5.290179	-3.01529	3.705814	-16.0895	10.33
7	5.198918	-2.98588	3.773729	-16.1158	10.67
8	5.200272	-2.95804	3.817816	-16.2512	10.00
9	4.979304	-2.89646	3.844517	-15.9243	10.33
10	4.91825	-2.91337	3.813429	-15.9907	10.67
<b>Average</b>	5.069525	-2.91023	3.799037	-16.1545	10.33
<b>Std Dev</b>	0.28285	0.161968	0.126432	0.157114	0.251976315

Interior Padding: 12 lbs/ft<sup>3</sup>



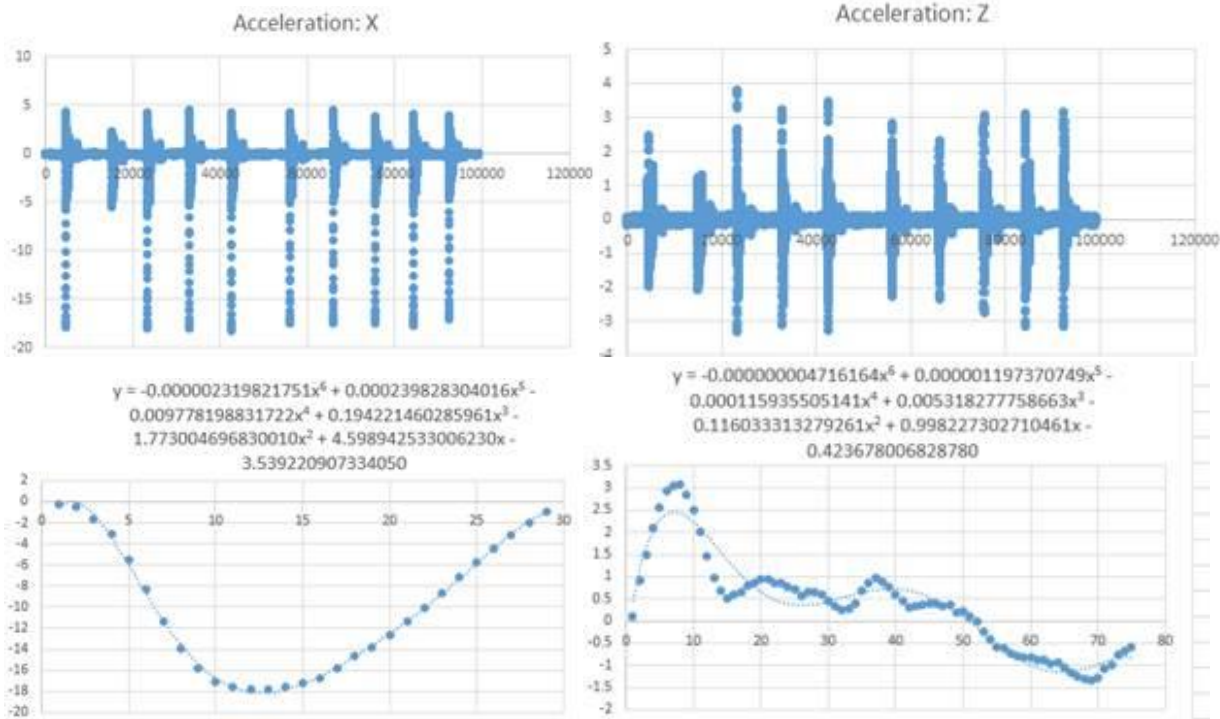
Hit #	Z Max (g)	Z Min (g)	X Max (g)	X Min (g)	Collision Time (ms)
1	2.833073	-1.7935	4.201275	-15.9678	10.33
2	3.112266	-2.34721	4.568321	-16.3101	10.67
3	2.707206	-1.70746	4.959368	-16.4547	10.33
4	2.49928	-1.67994	4.806984	-16.6777	10.33
5	2.549065	-1.43369	2.128383	-16.6719	10.00
6	2.559912	-1.87536	5.034423	-16.8682	10.33
7	2.744752	-2.17025	4.731705	-16.9089	10.33
8	2.404686	-2.18363	4.790073	-17.1625	10.00
9	3.088153	-2.20651	4.554645	-16.9124	10.00
<b>Average</b>	2.722044	-1.93306	4.419464	-16.6593	10.26
<b>Std Dev</b>	0.251476	0.30669	0.893853	0.364986	0.2222222

Interior Padding: 15 lbs/ft<sup>3</sup>



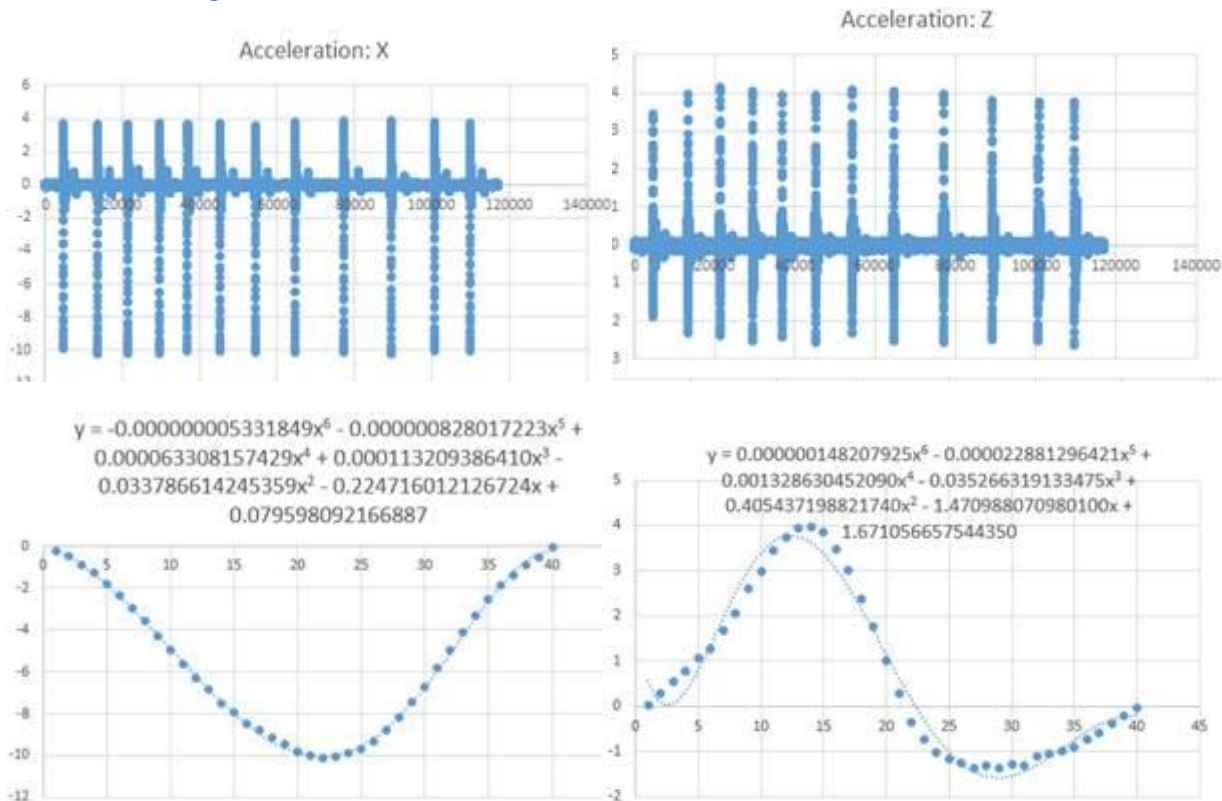
Hit #	Z Max (g)	Z Min (g)	X Max (g)	X Min (g)	Collision Time (ms)
1	2.88445	-2.38372	4.439364	-17.94	9.33
2	3.016175	-2.1225	4.342848	-17.8511	9.67
3	2.80202	-1.96582	4.466311	-17.2038	9.67
4	2.630053	-1.94943	4.32469	-16.9275	10.00
5	2.944655	-1.72901	4.183394	-16.9481	10.00
6	2.665545	-1.31649	4.31035	-16.3738	10.33
7	3.022548	-2.05432	4.070207	-16.8965	10.00
8	3.036994	-1.45125	3.973515	-16.7489	9.67
9	3.319747	-1.58054	4.126988	-16.6248	9.67
10	2.905657	-1.8151	4.167438	-17.0494	10.00
<b>Average</b>	2.922784	-1.83682	4.240511	-17.0564	9.83
<b>Std Dev</b>	0.19944	0.325666	0.161501	0.498304	0.282418

Interior Padding: 20 lbs/ft<sup>3</sup>



Hit #	Z Max (g)	Z Min (g)	X Max (g)	X Min (g)	Collision Time (ms)
1	2.487488	-1.97721	4.335694	-17.8494	17.66
3	3.829961	-3.31003	4.275802	-17.9358	17.00
4	3.240829	-3.09275	4.58	-18.0466	17.00
5	3.470735	-3.2631	4.308271	-18.1917	17.60
6	2.844656	-2.24104	4.31196	-17.4464	17.30
7	2.329766	-2.35272	4.59256	-17.4483	17.00
8	3.069528	-2.74312	3.915251	-17.5017	16.70
9	3.142872	-3.1289	4.072195	-17.7656	16.00
10	3.156353	-3.13896	3.965017	-17.037	16.60
<b>Average</b>	3.063576	-2.80531	4.261861	-17.6914	16.98
<b>Std Dev</b>	0.463378	0.496968	0.24112	0.362298	0.516409

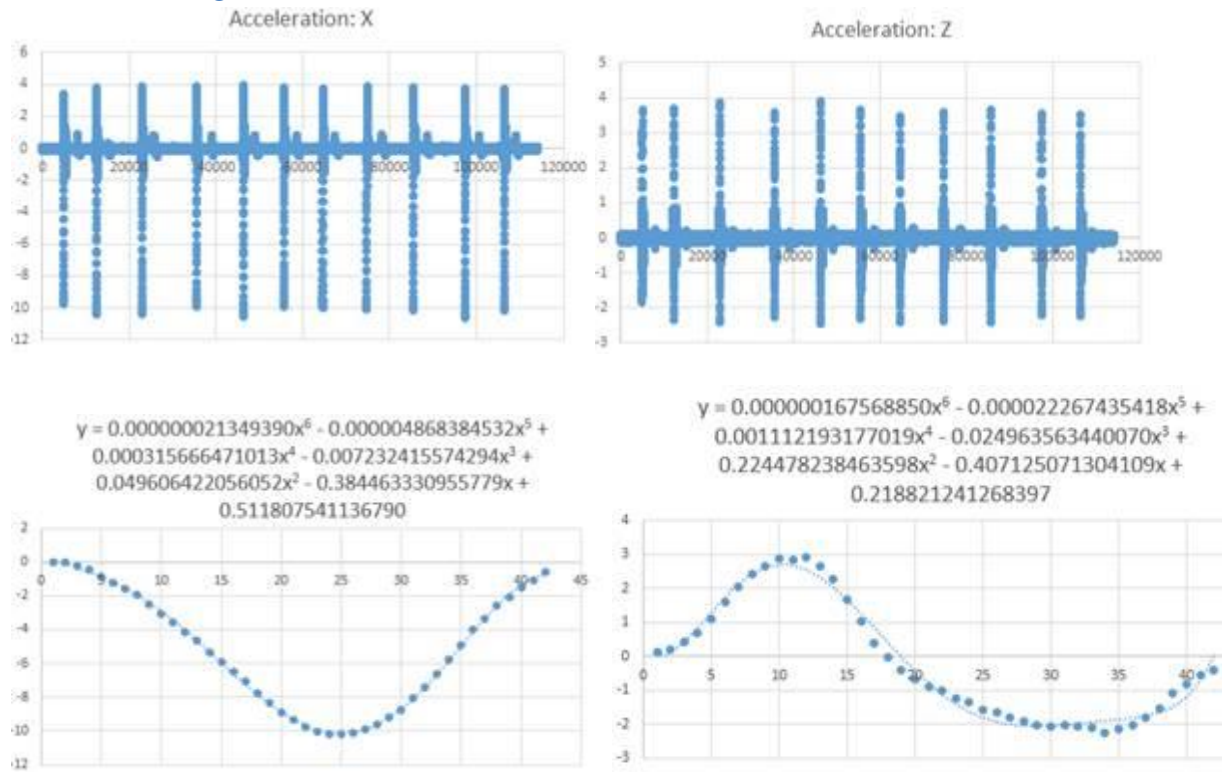
Exterior Padding: 9 lbs/ft<sup>3</sup>



Hit #	Z Max (g)	Z Min (g)	X Max (g)	X Min (g)	Collision Time (ms)
1	3.451465	-1.89911	3.741668	-9.932	12.67
2	3.988906	-2.30935	3.649635	-10.2565	13.00
3	4.170962	-2.36863	3.670619	-10.2179	12.67
4	4.074241	-2.54482	3.759267	-10.1852	12.33
5	3.965352	-2.42709	3.655753	-10.0738	12.67
6	3.964661	-2.56905	3.713114	-10.0959	12.67
7	4.11269	-2.30624	3.598931	-10.1248	13.33
8	4.076348	-2.51328	3.768368	-10.1408	12.67
9	3.982954	-2.56253	3.857482	-10.1105	12.67
10	3.802221	-2.4931	3.898159	-10.2287	13.00
11	3.787053	-2.51121	3.788211	-10.0238	13.00
12	3.784493	-2.64326	3.722193	-10.0368	13.00
<b>Average</b>	3.930112	-2.42897	3.735283	-10.1189	12.81
<b>Std Dev</b>	0.197557	0.19738	0.086901	0.094896	0.263312

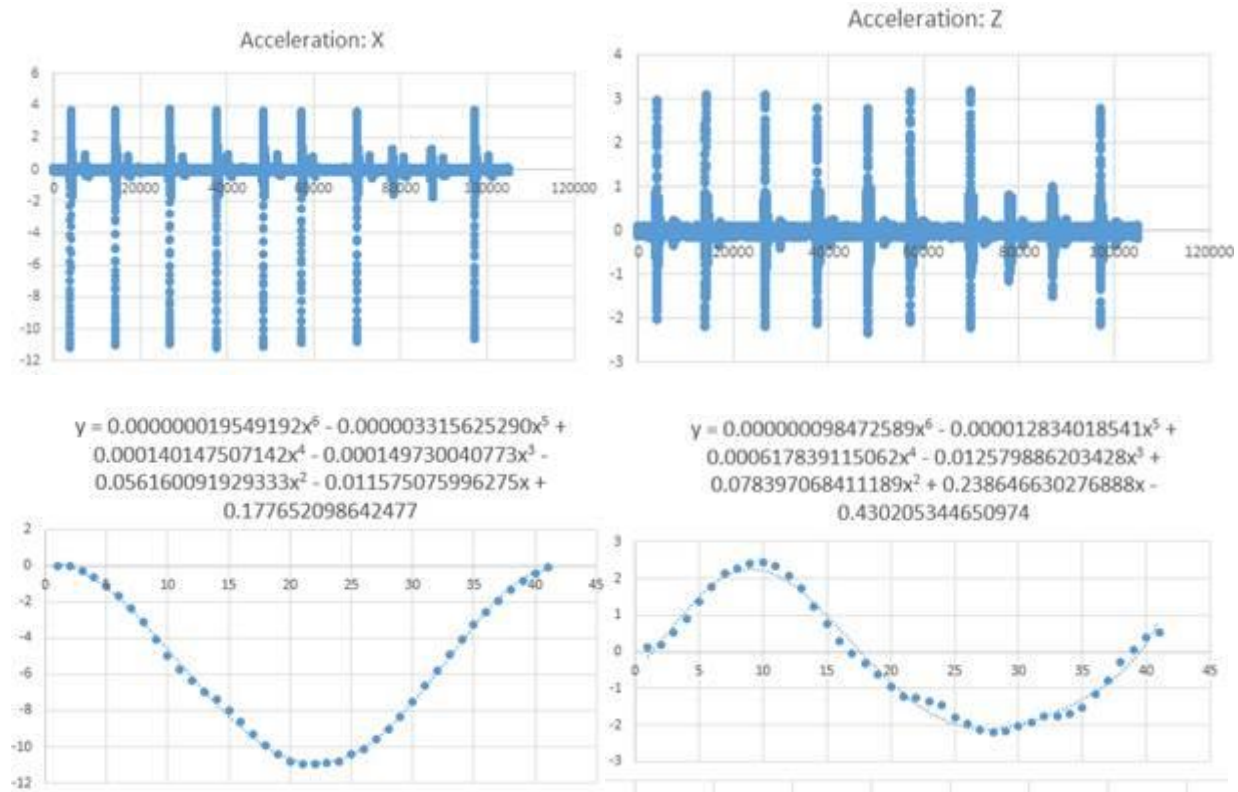


Exterior Padding: 12 lbs/ft<sup>3</sup>



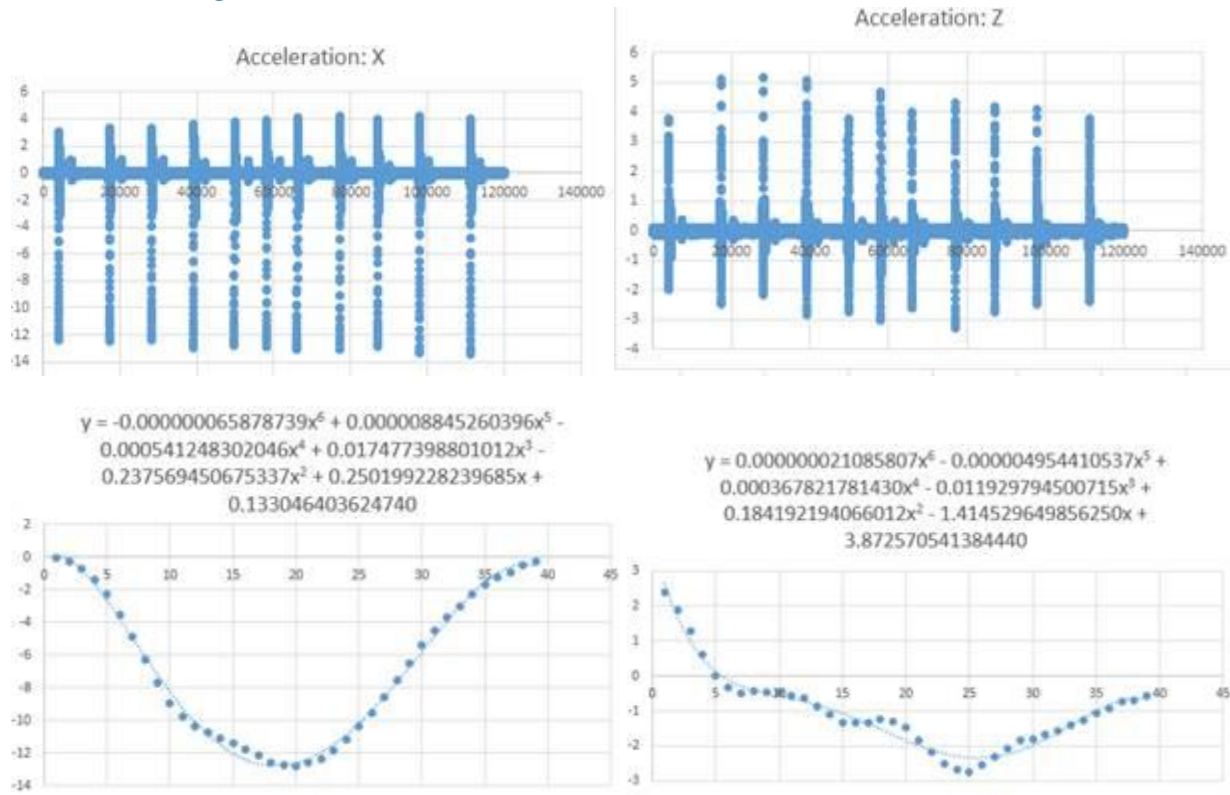
Hit #	Z Max (g)	Z Min (g)	X Max (g)	X Min (g)	Collision Time (ms)
1	3.667459	-1.85382	3.40124	-9.72207	13.67
2	3.695918	-2.36395	3.789585	-10.4168	13.00
3	3.867696	-2.41585	3.890628	-10.3481	13.00
4	3.57599	-2.28963	3.857268	-9.87526	13.00
5	3.927407	-2.46503	3.971234	-10.5118	13.33
6	3.660356	-2.32593	3.822046	-9.91049	13.33
7	3.47835	-2.43436	3.746696	-9.97112	13.00
8	3.577695	-2.38211	3.904551	-10.1076	13.67
9	3.651638	-2.42295	3.805735	-10.177	14.00
10	3.541426	-2.21825	3.7353	-10.6271	13.33
11	3.510479	-2.24036	3.697536	-10.1645	13.67
<b>Average</b>	3.650401	-2.3102	3.783802	-10.1665	13.36
<b>Std Dev</b>	0.140816	0.17135	0.15034	0.285763	0.349121

Exterior Padding: 15 lbs/ft<sup>3</sup>



Hit #	Z Max (g)	Z Min (g)	X Max (g)	X Min (g)	Collision Time (ms)
1	2.996319	-2.02757	3.706446	-11.2063	13.00
2	3.109209	-2.18545	3.724959	-10.9847	13.33
3	3.10066	-2.18811	3.793522	-10.9161	12.67
4	2.807185	-2.10193	3.720232	-11.1542	12.67
5	2.789143	-2.32599	3.694601	-11.1063	13.00
6	3.164642	-2.08587	3.62189	-10.8611	13.33
7	3.202532	-2.19808	3.625251	-10.8166	13.67
10	2.780158	-2.1319	3.716877	-10.6337	13.00
<b>Average</b>	2.993731	-2.15561	3.700472	-10.9599	13.08
<b>Std Dev</b>	0.177222	0.090617	0.055833	0.192398	0.344007

Exterior Padding: 20 lbs/ft<sup>3</sup>



Hit #	Z Max (g)	Z Min (g)	X Max (g)	X Min (g)	Collision Time (ms)
1	3.781665	-1.97801	3.081654	-12.4226	15.67
2	5.134354	-2.45299	3.326225	-12.4694	15.33
3	5.18231	-2.14016	3.338466	-12.3924	15.00
4	5.065656	-2.83072	3.620099	-12.9143	13.33
5	3.803595	-2.72128	3.79271	-12.7534	13.00
6	4.706822	-3.01591	3.901189	-12.9098	12.33
7	4.021859	-2.60014	4.100643	-13.0518	12.67
8	4.334666	-3.27328	4.217912	-13.0611	12.00
9	4.212152	-3.27328	4.217912	-12.8544	12.67
10	4.10218	-2.45213	4.174371	-13.3812	13.00
11	3.804891	-2.3933	3.999855	-13.4351	12.67
<b>Average</b>	4.377286	-2.64829	3.797367	-12.8769	13.42
<b>Std Dev</b>	0.551931	0.425018	0.401978	0.354373	1.282953



**Appendix L- MATLAB Code Example:**

```
% COMBINED side_exterior20 HIC
```

```
% acceleration in x direction for exterior 20 pad for side hit
```

```
sideexterior20axh = @(t)-0.000000065878739*(3000*t).^6 + 0.000008845260396*(3000*t).^5 -  
0.000541248302046*(3000*t).^4 + 0.017477398801012*(3000*t).^3 - 0.237569450675337*(3000*t).^2  
+ 0.250199228239685*(3000*t) + 0.133046403624740;
```

```
% acceleration in z direction for exterior 20 pad for side hit
```

```
sideexterior20azh = @(t) 0.000000021085807*(3000*t).^6 - 0.000004954410537*(3000*t).^5 +  
0.000367821781430*(3000*t).^4 - 0.011929794500715*(3000*t).^3 + 0.184192194066012*(3000*t).^2  
- 1.414529649856250*(3000*t) + 3.872570541384440
```

```
% accelerations x and z combined per HIC equation
```

```
sideexterior20axzh = @(t)sqrt((-0.000000065878739*(3000*t).^6 + 0.000008845260396*(3000*t).^5 -  
0.000541248302046*(3000*t).^4 + 0.017477398801012*(3000*t).^3 - 0.237569450675337*(3000*t).^2  
+ 0.250199228239685*(3000*t) + 0.133046403624740).^2+(0.000000021085807*(3000*t).^6 -  
0.000004954410537*(3000*t).^5 + 0.000367821781430*(3000*t).^4 - 0.011929794500715*(3000*t).^3  
+ 0.184192194066012*(3000*t).^2 - 1.414529649856250*(3000*t) + 3.872570541384440).^2);
```

```
% equation for the integral needed to calculate HIC
```

```
sideexterior20hint=integral(sideexterior20axzh,0,0.0127)
```

```
% COMBINED side_exterior20 GSI
```

```
% accelerations x and z combined per GSI equation
```

```
sideexterior20axzs=@(t)(sqrt((-0.000000065878739*(3000*t).^6 + 0.000008845260396*(3000*t).^5 -  
0.000541248302046*(3000*t).^4 + 0.017477398801012*(3000*t).^3 - 0.237569450675337*(3000*t).^2  
+ 0.250199228239685*(3000*t) + 0.133046403624740).^2+(0.000000021085807*(3000*t).^6 -  
0.000004954410537*(3000*t).^5 + 0.000367821781430*(3000*t).^4 - 0.011929794500715*(3000*t).^3  
+ 0.184192194066012*(3000*t).^2 - 1.414529649856250*(3000*t) + 3.872570541384440).^2).^2.5;
```

```
% equation for GSI
```

```
sideexterior20sint=integral(sideexterior20axzs,0,0.0127)
```